

NASA CR 120838
CW-WR-71-091.F

NASA

INTEGRAL LIFT ENGINE PRELIMINARY DESIGN

by

W. Pratt, A. Leto, R. Schaefer

CURTISS-WRIGHT CORPORATION

Prepared For

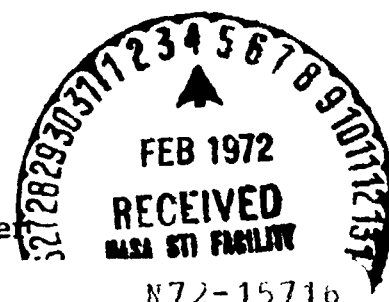
NATIONAL AERONAUTICS AND SPACE ADMINISTRATION

NASA LEWIS RESEARCH CENTER

CONTRACT NAS 3-14327

Richard J. Roelke, Project Manager

(NASA-CR-120838) INTEGRAL LIFT ENGINE
PRELIMINARY DESIGN W. Pratt, et al
(Curtiss-Wright Corp.) Nov. 1971 119 p
CSCL 21E



Unclass

G3/28 13332

FACIL

(NASA CR OR TMX OR AD NUMBER)

(CATEGORY)

NOTICE

This report was prepared as an account of Government-sponsored work. Neither the United States, nor the National Aeronautics and Space Administration (NASA), nor any person acting on behalf of NASA:

- A.) Makes any warranty or representation, expressed or implied, with respect to the accuracy, completeness, or usefulness of the information contained in this report, or that the use of any information, apparatus, method, or process disclosed in this report may not infringe privately-owned rights; or**
- B.) Assumes any liabilities with respect to the use of, or for damages resulting from the use of, any information, apparatus, method or process disclosed in this report.**

As used above, "person acting on behalf of NASA" includes any employee or contractor of NASA, or employee of such contractor, to the extent that such employee or contractor of NASA or employee of such contractor prepares, disseminates, or provides access to any information pursuant to his employment or contract with NASA, or his employment with such contractor.

Requests for copies of this report should be referred to

**National Aeronautics and Space Administration
Scientific and Technical Information Facility
P. O. Box 33
College Park, Md. 20740**

1. Report No. NASA CR 120838		2. Government Accession No.		3. Recipient's Catalog No.	
4. Title and Subtitle INTEGRAL LIFT ENGINE PRELIMINARY DESIGN				5. Report Date November, 1971	
				6. Performing Organization Code	
7. Author(s) W. Pratt, A. Leto and R. Schaefer				8. Performing Organization Report No. CW-WR-71-091F	
9. Performing Organization Name and Address Curtiss-Wright Corporation Wood-Ridge, New Jersey				10. Work Unit No.	
				11. Contract or Grant No. NAS 3-14327	
12. Sponsoring Agency Name and Address National Aeronautics and Space Administration Washington, D.C. 20546				13. Type of Report and Period Covered Contractor Report	
				14. Sponsoring Agency Code	
15. Supplementary Notes Project Manager, Richard J. Roelke, Fluid System Component Division NASA Lewis Research Center, Cleveland, Ohio					
16. Abstract A preliminary mechanical design of a complete Lift Fan Engine System is reported. A description of the Lift Fan Engine, layout drawings of the components and complete engine, and a discussion of the design analyses and results are presented. The design features and areas of analysis include fan and compressor rotor blades of composite construction, a combustor folded over the compressor, relatively high-temperature blades in the high-pressure turbine, the first stage of the low-pressure turbine used for bearing support and ducting of lubricant to the bearings, a complete lubrication system, critical speeds of the shafting, and vibration and flutter of the blading.					
17. Key Words (Suggested by Author(s)) Integral Lift Engine Lift Engine Design of Lift Engine			18. Distribution Statement Unclassified - Unlimited		
19. Security Classif. (of this report) Unclassified		20. Security Classif. (of this page) Unclassified		21. No. of Pages 107	
				22. Price* \$3.00	

* For sale by the National Technical Information Service, Springfield, Virginia 22151

PRECEDING PAGE BLANK NOT FILMED

FOREWORD

The technical and administrative guidance contributed on this design task by personnel of the Lewis Research Center of the NASA, including Messrs. Richard J. Roelke, William H. Rowe and some aerodynamic and thermodynamic specialists is gratefully acknowledged.

In addition to the authors cited, Curtiss-Wright personnel in the technical disciplines of stress, Vibrations, Heat Transfer, Aerodynamics, Metallurgy, Bearings and Seals, and Controls also contributed to this design effort.

TABLE OF CONTENTS

	<u>Page</u>
<u>I. SUMMARY</u>	1
<u>II. INTRODUCTION</u>	2
<u>III. ENGINE DESIGN SPECIFICATIONS</u>	3
<u>IV. ENGINE DESCRIPTION</u>	4
<u>V. COMPONENT DESCRIPTION</u>	6
A. Fan	6
1. Fan Rotor	6
2. Fan Stator Housing	7
3. Fan Exhaust Duct	8
B. Compressor	8
1. Compressor Rotor	8
2. Compressor Stator Housing	9
C. Combustor	9
D. High Pressure Turbine	10
E. Low Pressure Turbine	11
F. Bearings and Lubrication	12
G. Accessories	14
1. Turbine Impingement Starter	15
2. External Oil System	15
3. Fuel and Control System	16
<u>VI. DESIGN ANALYSIS AND DISCUSSION</u>	17
A. Fan	17
1. Fan Rotor Blade Stresses	18
2. Fan Rotor Blade Overspeed Strength	18
3. Fan Rotor Blade Vibratory Strength	19
4. Fan Rotor Blade Attachment Strength	20
5. Fan Rotor Blade Natural Frequencies	21
6. Fan Rotor Blade Flutter Margin	21
7. Fan Rotor Disk Strength	22

TABLE OF CONTENTS - Continued

	<u>Page</u>
B. Compressor	22
1. Compressor Rotor Blade Stresses	23
2. Compressor Rotor Blade Vibratory Strength	23
3. Compressor Rotor Blade Natural Frequencies	23
4. Compressor Rotor Blade Flutter Margin	24
5. Compressor Stator Vane Vibratory Strength	25
6. Compressor Stator Vane Natural Frequencies	25
C. Combustor	25
D. High Pressure Turbine	26
1. HP Turbine Rotor Blade Stress Rupture Life	26
2. HP Turbine Rotor Blade Fatigue Strength	28
3. HP Turbine Rotor Blade Attachment Fatigue Strength	29
4. HP Turbine Rotor Blade Frequencies	29
5. HP Turbine Stator Vane Stress Rupture Life	30
6. HP Turbine Rotor Disk Stress	31
E. Low Pressure Turbine	32
1. LP Turbine Blade Strength	32
2. LP Turbine Blade Attachment Fatigue Strength	33
3. LP Turbine Blade Natural Frequencies	33
4. LP Turbine First Stator Vane Strength	34
5. LP Turbine Rotor Disk Strength	36
F. Bearings and Lubrication	37
1. Bearing Thrust Loads	37
2. Bearing Selection and Lubrication	38
G. Critical Speeds	39
H. Impingement Starter	40
I. Engine Weight	41
<u>VII. CONCLUSIONS</u>	43
<u>VIII. REFERENCES</u>	45

LIST OF FIGURES

Figure

1	Engine Assembly Drawing
2	Component Performance
3	Engine Specifications Provided by NASA
4	Engine Service Time Requirements
5	Engine Thrust Variation Characteristics
6	Fan Rotor
7	Fan Stator Housing
8	Fan Exhaust Duct
9	Compressor Rotor
10	Compressor Stator Housing
11	Combustor
12	High Pressure Turbine
13	Low Pressure Turbine
14	Single Engine Lubrication Schematic
15	Three Engine Lubrication Schematic
16	Fuel Control Block Diagram
17	Ignition System Diagram
18	Fan Rotor Blade Centrifugal Stresses
19	Fan Rotor Blade Lean to Cancel Gas Bending Moments
20	Fan Rotor Blade Fatigue Strength
21	Fan Rotor Blade Vibratory Strength
22	Fan Rotor Blade Interference Diagram - By-Pass Portion
23	Fan Rotor Blade Interference Diagram - Core Portion
24	Fan and Compressor Rotor Blade Bending Flutter Parameter
25	Fan and Compressor Rotor Blade Torsional Flutter Parameter
26	Rotor Blade Root Thickness-to-Chord Requirements
27	Compressor Rotor Blade Vibratory Strength
28	First Stage Compressor Rotor Blade Interference Diagram
29	Fifth Stage Compressor Rotor Blade Interference Diagram
30	Ninth Stage Compressor Rotor Blade Interference Diagram
31	Compressor Stator Vane Vibratory Strength
32	Compressor Stator Vane Bending Interference Diagram

LIST OF FIGURES - Continued

Figure

33	Compressor Stator Vane Torsional Interference Diagram
34	High Pressure Turbine Rotor Blade Stresses
35	Engine Duty Cycle
36	High Pressure Turbine Rotor Blade Material Stress Rupture Properties
37	High Pressure Turbine Rotor
38	High Pressure Turbine Rotor Blade Interference Diagrams
39	High Pressure Turbine Rotor Disk Stresses
40	Low Pressure Turbine Third Stage Rotor Blade
41	Low Pressure Turbine First Stage Rotor Blade Interference Diagram
42	Low Pressure Turbine Third Stage Rotor Blade Interference Diagram
43	Rotor Thrust Loads
44	Rotor Shaft Bearing Characteristics
45	Oil Tube In Low Pressure Turbine Stator
46	Rear Bearing Oil Tube Calculated Temperatures
47	Critical Speeds - Turbine Mode Frequency
48	Critical Speeds - Fan Mode Frequency
49	Critical Speeds - Compressor Mode Frequency
50	Critical Speed Map
51	Engine Resistance Torque
52	Engine Starting Acceleration Characteristics
53	Starter Nozzle Sizing
54	Engine Weight

1. SUMMARY

A preliminary mechanical design of a complete Lift Fan Engine system was conducted by the Curtiss-Wright Corporation for the NASA Lewis Research Center, and the design accomplishments are reported herein. Design features and areas of analysis included the fan and compressor rotor blades of composite construction, a combustor folded over the compressor, the relatively high-temperature uncooled blades of the high-pressure turbine, the first stage of the low-pressure turbine as used for the turbine bearing support and ducting of lubricant to the bearings, the critical speeds of the shaft, vibration and flutter of all blading and the complete lubrication system. The flow path geometry and the aerodynamic design of this engine were provided by NASA. The layout drawings, a description of the engine components and complete engine system, and a detailed discussion of the design analyses are presented herein.

The completed preliminary design is considered mechanically feasible and suitable for starting a final design. Adequate strength and vibratory margins can be achieved to satisfy the required 2000-hour engine operating life and the 670-hour TBO for the specified duty cycle conditions, but to achieve this, some of the blade geometry as supplied by NASA will require modification and blade detuning measures. The estimated engine weight is 1012 lbs. Composite material construction was used in areas of the fan and compressor rotor blades, and weight savings and favorable blade vibratory characteristics were obtained.

The combustor was located outboard of the compressor which presents accessibility problems and beneficial effects on rotor critical speed as a result of the shorter rotor shaft.

The design incorporates the required noise-reduction measures of proper spacing between the fan rotor and stator blades and of acoustical material in the fan duct, but there is some accompanying penalty in overall engine weight.

To assure success of the engine, additional effort should be directed toward the composite construction of the fan and compressor blades and toward the welded Rene' 41 sheet metal construction of the low pressure turbine rotor blades.

II. INTRODUCTION

Interest in lift fan engines for Vertical and Short Take-Off and Landing (VSTOL) Aircraft for commercial applications has grown considerably during recent years. The NASA Lewis Research Center is currently studying VSTOL engines and endeavoring to establish technology goals.

As a part of this effort, NASA has assigned the Curtiss-Wright Corporation the task of jointly designing some of the more-promising lift fan systems. Examples of this type of joint effort are reported in References 1 and 2.

More recently, Curtiss-Wright conducted for the Lewis Research Center a preliminary flight-weight layout design of an Integral Lift Engine system. The aerodynamic designs of the fan, compressor, combustor and turbines were provided by NASA. Mechanical studies were conducted by Curtiss-Wright of such things as stresses, critical speeds, heat transfer and temperature distributions, bearings and lubrication, engine vibrations, and fuel and control systems with an objective of providing assurance concerning the feasibility of the design.

This Curtiss-Wright effort was performed under NASA Contracts NAS 3-12423 and NAS 3-14327, and this report presents the design features and analyses performed on this task to produce the engine design shown in Figure 1.

III. ENGINE DESIGN SPECIFICATIONS

A complete definition of all engine flow path geometry, diffuser and combustor shapes, blade geometry, component performance and interstage conditions was provided by NASA.

The engine component performance for the normal all-engines-operating condition and for an emergency engine-out condition is presented in Figure 2.

The performance, blade section coordinates and flow path information of the fan, compressor, combustor and turbine components were furnished by NASA in the form of computer print outs, layout sketches and tables as identified in Figure 3. All NASA turbine and combustor information, except where otherwise specified, required scaling to account for an increase in engine thrust of 25 percent.

Engine Service time requirements as well as thrust variation characteristics for normal and emergency operating conditions, as supplied by NASA, are shown in Figures 4 and 5.

IV. ENGINE DESCRIPTION

An assembly drawing of the engine is shown in Figure 1.

The engine is a two-spool turbo fan with a one-stage fan, nine-stage axial compressor, one-stage high pressure turbine, and a three-stage low pressure turbine.

Normal engine thrust is 10,000 pounds with variations to a maximum of 12,500 pounds as required for aircraft stability and control.

The engine incorporates the following features:

1. Graphite-epoxy composite rotor blades in the fan and the first three compressor stages.
2. Sound treatment honeycomb surfaces in the fan exhaust duct.
3. Two-position adjustment of compressor inlet guide vanes and of six stages of compressor stators for the purpose of facilitating engine acceleration.
4. Combustor flow path folded over the compressor to minimize engine length and weight.
5. Recirculating type of lubricating system to avoid the exhausting of contaminants.

The estimated weight of the engine is 1012 pounds.

The fan stator housing serves as the thrust bearing support for the core engine. The outer rim of this housing is used for engine-to-airframe mounting. The first stators of the low pressure turbine are used for turbine bearing support, and the fan exhaust housing stabilizes the core engine by transmitting turbine overhang loads to the mount rim of the fan stator housing.

There is no mechanical drive connection with either rotor. Starting is accomplished with air-impingement nozzles directed at high pressure turbine blades. Drives for the oil and fuel pumps are provided by an external motor.

IV. ENGINE DESCRIPTION (CONTINUED)

Speed sensing and engine control is accomplished electrically.

The variable position compressor stators are synchronized by a system of levers and rings located between the combustion chamber shell and the compressor case. Actuation is by hydraulic cylinders.

V. COMPONENT DESCRIPTION

A. Fan

The fan is composed of a single-stage rotor with composite blades, a titanium stator housing that is used as a main structural frame, and a fan exhaust housing designed to provide sound absorption.

1. Fan Rotor

The fan rotor is illustrated in Figure 6. Thirty-two composite blades are dovetailed in a titanium hoop. The blades incorporate a splitter shroud between the by-pass annulus and the core engine inlet annulus.

The blades are made of a graphite-epoxy composite. Graphite fibers run the full radial length of the twisted airfoil shape and are bonded together with an epoxy compound. These fibers continue into the attachment and are splayed by titanium wedges to form a dovetail. The attachment bearing surfaces are protected by metal shims bonded to the blade.

An applicable method of blade construction is described in Reference 3. Preimpregnated tapes of parallel graphite fibers bonded with epoxy are cut to form plies which are stacked, twisted, cambered and bonded to form the blade.

Metal fan blades normally require an interblade snubber at approximately 70 percent of the blade span in order to avoid blade flutter. The low density and high modulus of the graphite-epoxy composite blades result in flutter-free operation without snubbers.

Torsional rigidity may be enhanced by incorporating some plies of graphite fibers oriented to non-radial positions. However, the fan blade is a significantly twisted blade and consequently has considerable torsional rigidity.

V. COMPONENT DESCRIPTION (CONTINUED)

The blades are retained in a titanium hoop. Because the composite blades are relatively light, the required cross-section area of the hoop is small.

The blades are to be leaned so as to minimize bending moments in the blade. Since this engine is intended for operation over a very limited range of thrust, rotor speed and altitude, the cancellation of gas bending moments by centrifugal lean moments will be effective.

The splitter shrouds are to be interlocked and preloaded in torsion so that they form a continuous ring under operating conditions. Consequently, the blade attachments and core roots are protected from large vibratory moments.

2. Fan Stator Housing

Figure 7 shows the design of the fan stator housing. This fabricated titanium housing supports the fan and compressor thrust bearings and transmits various loads to the engine mounts. Oil and vent lines are incorporated as an integral part of the assembly.

In this construction, an annular mount ring, 38 by-pass fan stator vanes and a core engine spoked housing are welded together to form a large double-annulus spoked housing assembly. The conical arrangement of the stators gives a maximum rotor-to-stator spacing at the tip where peripheral speed is a maximum. This is required to minimize noise. This design is also advantageous for carrying thrust loads since the conical arrangement uses tension rather than bending to transmit the loads. The core engine spoked housing is formed by a hub and a rim connected by the core fan stator vanes. These vanes are set radially to minimize engine length.

Since strength and especially rigidity are important, the by-pass fan stators and the core fan stators are connected to the three annular components by piercing the sections almost completely. After the welds

V. COMPONENT DESCRIPTION (CONTINUED)

are made, each vane-to-ring connection will serve as a diaphragm that eliminates distortion of the annular sections.

3. Fan Exhaust Duct

The fan exhaust duct is illustrated in Figure 8. It is composed of four concentric cylinders connected with three struts. The cylinders are made of aluminum honeycomb and present a maximum amount of surface to the fan exhaust flow. Face sheets are perforated so that the honeycomb serves as a sound absorber (Reference 4).

The fan exhaust duct is used to structurally connect the engine mount ring to the turbine section. This relieves the fan stator housing of overhang loads. The turbine is connected to the fan exhaust housing with radial lugs that enforce concentricity yet permit radial and axial thermal expansion.

B. Compressor

The compressor is composed of a drum type of rotor and a stator assembly. Mechanism is provided to enable varying the setting angles of the inlet guide vanes and six of the stator stages.

1. Compressor Rotor

The compressor rotor layout is shown in Figure 9. The rotor drum is titanium and incorporates staggered dovetail slots for the first three stages. Composite blades of graphite-epoxy are used in these stages. The remaining stages have titanium blades and the rotor includes circumferential dovetail grooves for retention of these blades.

The composite blades and their attachments are identical in principle to the fan blade design. Graphite filaments in the blade extend radially into the attachment dovetail. Titanium wedges are molded into the attachment to splay the fibers and provide the "axe handle".

V. COMPONENT DESCRIPTION (CONTINUED)

Metal surfaces are bonded to the load surfaces of the blade dovetail to provide wear resistance between blade and rotor drum.

The higher stages use circumferential dovetails. Blades are provided with dovetails of one-half a pitch of tangential width. Loading slots are provided in the drum groove. Retainer blocks are inserted and keyed to transmit torque and to position the blades.

2. Compressor Stator Housing

The compressor stator housing is shown in Figure 10. The casing and blades are all titanium. The casing is welded of forged rings and sheet stock. It is an engine design requirement that the compressor incorporate variable geometry. The inlet guide vanes and stators 1, 2, and 3 must close and stators 7, 8 and 9 must open for low speed operation. The scheme to accomplish this is also shown in Figure 10.

The blades in each variable stator stage have lever arms connected to a synchronizing ring. By matching the length of the arms to the required turning angle for each stator stage, the angle of rotation of each synchronizing ring about the engine axis was made equal. Each ring was then keyed or linked to its neighbors so that all will turn together. Tangential hydraulic cylinders connected to one ring were selected to actuate the entire mechanism. Note that the levers for the high pressure stages were reversed so that they will open when the early stages close.

C. Combustor

Figure 11 illustrates the combustor and casing. The annular combustor is mounted to the casing by means of radial pins projecting from the headplate. The 24 atomizer nozzles are separately mounted on an annular fuel manifold which is then mounted on the casing with radial freedom. Relative radial displacement between nozzles and headplate, caused by temperature differences between the hot combustor and the relatively cool fuel manifold, is accommodated by local sliding seals.

V. COMPONENT DESCRIPTION (CONTINUED)

Inlet air scoops are directly mounted on the inner liner insuring alignment with the liner ports.

Engine disassembly sequence to remove the combustor and expose the compressor requires removal of both turbines and the combustion chamber housing. After this is done, access to the compressor exit diffuser mounting bolts permits removal of the HP stator and diffuser assembly and then permits disassembly of the combustor.

D. High Pressure Turbine

The high pressure turbine and compressor exit diffuser are shown in Figure 12. Air leaving the compressor enters a split diffuser and is routed to the combustor liner and to the HP stators. The diffuser is an annular fabrication of sheet metal and carries a shroud for the labyrinth seal with the rotor disk. The seal radius was chosen to reduce the load on the HP thrust bearing.

The HP stator vanes are hollow castings of MAR-M 246. They are loose at both their outer and inner shrouds, which makes them simply-supported beams. This mounting is favorable for low bending moments and permits accommodation of tolerances and thermal growths.

The outer shroud is radially splined to the casing flange to permit relative radial growth while maintaining concentricity with the turbine rotor.

The hollow stators are used to pass 20 percent of the compressor airflow to the outer surface of the combustion chamber. As a consequence, the stator blades are cooled by this forced convection flow.

The turbine rotor blades are solid and unshrouded and incorporate a conventional three-tooth firtree attachment. MAR-M 246 material was selected for maximum stress rupture life.

The rotor disk material is Udimet 700.

V. COMPONENT DESCRIPTION (CONTINUED)

E. Low Pressure Turbine

Figure 13 shows the LP turbine arrangement. The first stage stator vanes are hollow and are used as bearing supports. Oil supply and return lines are passed through specially thickened vanes. The inner shroud is split so that temperature differences between the inner shroud, the blades and the outer shroud will not result in loads. The rim of the bearing support cone is isolated from the inner shroud with radial splines. Again the objective was to minimize thermal loading since the bearing area will be kept relatively cool. The splines permit radial freedom but insure concentricity.

The outer shroud is of double construction and all but three of the stators pierce through and connect to both walls. Thus, these vanes are being used as cantilevers built in at the outer shroud and loaded at their hub ends. The three stator vanes that were specially thickened for oil tubes do not penetrate the outer shell. Consequently, they are structurally disconnected. Otherwise their deeper section would result in excessive stresses since all blades share the same hub deflection.

The effect of the three thick vanes on blade vibration has been checked. Turbine rotor blade natural frequencies are high enough to avoid excitation by third engine order and its first harmonic.

The second and third stage stator vanes are also hollow and are cantilevered from rails in the outer casing. They pilot their inner shrouds by radial slip fits at the hub connection. The exit stator vane is similar except that the outer connection is a brazed double-wall construction.

The rotor blades are hollow and shrouded. Each is attached to a rudimentary disk by means of a firtree connection. The tip shrouds are interlocked and preloaded in torsion. Consequently, blade frequencies and vibratory strength are increased.

V. COMPONENT DESCRIPTION (CONTINUED)

The rotor blade construction selected for the specified 97 blade configuration uses a Rene 41 sheet metal airfoil welded to a forged Rene 41 tip shroud and butt. This construction was dictated by the high number of blades and the small hub radius at the third stage. Blades are closely spaced and the blade attachments are small.

Thickening the disk rim to 1.20 inches results in satisfactory vibratory strength in the third stage attachment. Less thickening will be needed in the earlier stages since they have larger attachment radii.

Full advantage of the interlocked tip shrouds in reducing vibratory moment was taken. If it is desirable to introduce cast blades, their lower fatigue strength will require a larger attachment and a consequent reduction in the number of blades.

The first stage rotor is supported on the rotor shaft, and the remaining rotors are mounted on the first. Thus, during assembly, each rotor can have its tip clearance measured. Note also that the LP turbine rotor can be removed without exposing the lubrication system.

F. Bearings and Lubrication

Each rotor shaft is mounted on two bearings. The fan shaft has a ball bearing aft of the fan for both radial and thrust support. The rear bearing is forward of the turbine and is a roller bearing.

Similar bearings are used for the compressor shaft. The thrust bearing is forward of the compressor and the roller bearing is aft of the turbine.

All bearings are pressure-jet lubricated. Two jets are used for each bearing except for the LP roller bearing. This was done for reasons of redundancy; if one jet should become clogged, the bearing will continue to operate with a higher temperature rise of the oil from the one remaining jet. In the case of the LP roller bearing, the heat generated in the bearing is so low that if the one jet that is supplying it with oil should

V. COMPONENT DESCRIPTION (CONTINUED)

clog, the bearing would continue to operate on oil that comes down from the HP roller bearing placed just above it.

Both thrust bearings are split-inner-ring ball bearings with integral puller provision on the inner race. This assures that the bearings can be removed without damage to the races or to the balls.

All oil jets were so placed as to direct the oil at the inner diameter of the bearing cage to give the best possible penetration of the oil through the bearing.

The thrust bearing cavity has a single return and sump at the bottom point of the cavity. This sump was placed outside the lower shaft seal such that there will be no puddling or oil loading of the sealing face that might cause external leakage. This return system has three times the capacity of the pressure oil flow. This is sufficient for the intended application of this engine as it will not operate at altitude and will have an operating cycle that is limited to five minutes duration. A by-pass passage is provided around the HP thrust bearing so that oil from the LP bearing will not go through this HP bearing and cause oil churning.

A vent connection is placed between the two thrust bearings. This vent is separately connected to the oil supply tank. The area between the LP shaft and the HP shaft is used as a vent passage to the hot end roller bearing cavity. A tube through the compressor rotor will constrain any oil that gets into this vent transfer and will guide it into the roller bearing return system.

The hot end roller bearing support has the roller bearings for both the LP and the HP shafts. This bearing support is mounted to the first-stage LP turbine stator vanes. Oil supply and return lines pass through these vanes whereas the vent connection is to the thrust bearing cavity as described above. This was done for two reasons. First, running a vent connection through the hot stator vane is not recommended because low vapor velocity

V. COMPONENT DESCRIPTION (CONTINUED)

will encourage coking of the oil on the inner vent wall with the possibility of complete clogging of the vent line. Secondly, the required line size is too large to be placed within the vane.

The construction of the pressure jets, the return system and the shaft seals for the roller bearing cavity is essentially the same as in the thrust bearing setup.

All rotating shaft seals are a carbon-face type with a bellows acting as the secondary seal and as the seal face loading spring.

Since the oil supply for the rear bearings is conducted in tubes through the LP first stator blades, special measures are taken to insure that tubing walls remain cool enough to avoid coking of the lubricant.

A flattened tube was used to maximize the insulating air space between blade and tube. Adequate oil flow will be maintained to keep the tubing wall temperature below a coking value. Each oil tube is doubled and conducts both cool oil in and scavenge oil out. A small by-pass port can be provided between the two at the radially inward end of the stator so that continuous recirculation is assured in spite of aircraft maneuver accelerations.

G. Accessories

The engine is provided with the following equipment:

Impingement Starter

External Oil System

Fuel and Control System

Fuel Control and Fuel Pump

Ignition System

Sensors for HP Speed, Compressor Discharge Pressure and Exhaust

Gas Temperature

Accessory Drive Motor

V. COMPONENT DESCRIPTION (CONTINUED)

1. Turbine Impingement Starter

The engine is started by injecting high pressure air tangentially against the high pressure turbine rotor blades. The arrangement to perform this is illustrated in Figure 8.

The system conducts high pressure air from an external source through tubes in one strut of the fan exhaust duct. A manifold at the core engine distributes this air to four nozzles directed at the turbine blades. The nozzles are convergent-divergent to maximize the acceleration torque for a given air consumption.

2. External Oil System

The external oil system consists of a pressure pump supplying oil to the bearing jets, two scavenge pumps returning oil from the engine bearing cavities, an oil tank for oil storage and deaeration, a heat exchanger for oil cooling, and various items such as a filter, check valves, tubing, etc. This recirculating system was compared with an oil mist throw away system. Although the latter is potentially lighter and the quantity of oil discarded is small, it is unlikely that any preventable contamination of the atmosphere will be acceptable.

A comparison was also made between a lubrication system for each engine and a system where three engines share as many components as possible. Figures 14 and 15 are schematics of the two systems. There is little weight difference per engine between the two. If each engine has its own lubrication system, failure of a component can only affect one engine; i.e., aircraft reliability is enhanced. Also, the independent system enables engine placement in any pattern. In view of these advantages, each engine was given its own lubrication system.

The mechanical power to drive the oil pumps is shown as an electric motor. Alternatively, the pumps may be driven from the fuel pump motor to be discussed later. Since both oil pressure and fuel pressure are needed simultaneously, this arrangement was selected.

V. COMPONENT DESCRIPTION (CONTINUED)

3. Fuel and Control System

The engine is provided with a fuel control that regulates the fuel flow. It contains an electronic computation section that receives inputs from various sources. One input is received from a supervisory control that determines the necessary thrust level for the particular engine. Other inputs are produced by engine transducers for HP rotor speed, compressor discharge pressure, compressor inlet temperature, and exhaust gas temperature. Computation section output signals go to the fuel metering system, the ignition system and to the compressor stator actuation hydraulic control valve. See Figure 16.

A single ignition system is used to supply a group of four engines. See Figure 17.

The sensor for compressor speed is a variable reluctance pickup operating close to a toothed wheel. Conventional pressure and temperature transducers are used for measurement of the remaining engine variables.

The supervisory control, mentioned above, is responsive to aircraft performance and stability requirements. It may sense an uncommanded roll rate and signal for increased thrust on the appropriate engines. This supervisory control is not considered as part of the individual engine control system.

The drive motor for the fuel pump and lubrication pumps is an air turbine. It has been assumed that an appropriate source of air pressure is available on the aircraft for this purpose and also for supplying the impingement starter.

Similarly, a source of high pressure oil has been assumed to be available for actuating the hydraulic cylinders of the variable stator mechanism.

VI. DESIGN ANALYSIS AND DISCUSSION

The following section of the report documents analyses of critical components of the engine. In general, each analysis applies to the configuration shown in the component layouts, Figures 6-13. In some cases, the analysis showed a need for changes. These changes were incorporated in the assembly drawing, Figure 1, and in the engine weight estimate.

Unless otherwise specified, all calculated values are consistent with the 12,500 lb. thrust condition and section properties as defined in the engine specifications.

The various analyses indicate that the engine design solutions are feasible. There are some areas, however, where analysis alone is inadequate to insure the success of a design. The outstanding example in this engine is the use of composite blades. Intensive development experience is an absolute requirement to insure the success of such a design choice.

Each design solution has been reviewed with the appropriate specialist. In some instances approval was granted on the condition that experimental development would be permitted. An example is the hollow sheet metal blade for the LP turbine rotor. The sheet metal airfoil is to be electron beam welded to a forged butt. Problems of alignment and weld integrity can only be solved by process development. The problem is compounded by the choice of Rene 41 material which is difficult to weld.

A. Fan

This section contains a discussion of the analyses performed in the areas of Fan Rotor Blade Stresses, Overspeed Strength, Vibratory Strength, Attachment Strength, Natural Frequencies, Flutter Margin and Fan Rotor Disk Strength. The Fan Stator Vane design was considered mechanically conservative and was not analyzed in detail.

VI. DESIGN ANALYSIS AND DISCUSSION (CONTINUED)

1. Fan Rotor Blade Stresses

The fan rotor blade is loaded by centrifugal and gas forces. The centrifugal stresses are tabulated in Figure 18. At the root, the stress is 18,000 psi.

Gas bending moments at the root of the blade were estimated as:

3200 in. lbs. Tangential

3400 in. lbs. Axial

Blade flexibility reduces the gas bending stress since centrifugal forces produce a compensating moment.

2200 in. lbs. Tangential

2700 in. lbs. Axial

The consequent maximum bending stress is 57,000 psi.

Since this is a lift engine, it operates in a limited range of thrust, rotor speed and altitude. Consequently the blade can be leaned so that centrifugal moments cancel the gas bending moments, and the blade stress for steady state conditions approaches the centrifugal value of 18,000 psi. The blade lean shape for cancellation of gas bending moments is shown in Figure 19.

2. Fan Rotor Blade Overspeed Strength

For an overspeed condition of 15% above the top specified speed of 4100 RPM, the consequent root stress is 25,000 psi. The unidirectional strength of the composite is 130,000 psi. (NARMCO Modulite 5206). Consequently there is considerable margin of safety to allow for splitter weight, the effect of cross plies and the addition of leading edge protection.

VI. DESIGN ANALYSIS AND DISCUSSION (CONTINUED)

3. Fan Rotor Blade Vibratory Strength

Next consider the fatigue strength of the blade root.

Strength data from References 3 and 5 are plotted in Figure 20 and indicate an allowable vibratory stress for the graphite-epoxy composite of $\pm 60,000$ psi at a steady state stress of 18,000 psi.

It is a Curtiss-Wright design objective to permit a vibratory stress of two times the gas bending stress. This ratio is called the

$$\text{Vibratory Margin} = \frac{\text{Allowable Vibratory Stress}}{\text{Gas Bending Stress}}$$

Consider first the entire airfoil cantilevered from its attachment at the core root. Allowing for centrifugal support, the gas bending stress as stated earlier is 57,000 psi. The consequent vibratory margin is

$$VM = \frac{60,000}{57,000} = 1 \text{ approx.}$$

The blade has a specified thickness-to-chord ratio, t/c , of 8 percent. Increasing this to 12% will cut the bending stress in half and give a vibratory margin of two. See Figures 20 and 21.

It will be shown later that the concept of the entire airfoil vibrating as an unsupported cantilever is not consistent with attachment strength. The support of the splitter shroud is used and, consequently, the vibratory moment at the root of the fan blade is reduced. It will also be shown later that other considerations require the 12 percent thickness-to-chord ratio.

These factors result in a large vibratory margin for the airfoil at its core root.

VI. DESIGN ANALYSIS AND DISCUSSION (CONTINUED)

A similar analysis was made for the blade section at the root of the bypass annulus; i.e., just above the splitter shroud. Vibratory strength considerations are met with the specified 7 percent thickness-to-chord ratio. See Figure 21. Again, other factors will be shown to require a 12 percent thickness ratio.

4. Fan Rotor Blade Attachment Strength

The attachment consists of a dovetail on the composite blade and matching titanium tenons on the disk. Stresses were calculated for centrifugal and moment loads and account for stress concentrations and load proximity. The assumption was made that the analysis, developed for metal blade attachments, would be adequate for preliminary analysis.

The effect of the splitter shroud is especially important for the blade attachment. Significant blade vibration is characterized by phase differences in blade motion. As some blades swing to a tangentially leading position others swing to a trailing position. Consequently, a continuous shroud is acted on by opposing forces and does not participate in the vibratory motion.

Shrouds at the blade tip would be very effective in minimizing blade vibratory stresses. The splitter shroud is expected to be even more effective in reducing the vibratory moment felt by the blade attachment.

The analysis reported here assumed a shroud effectiveness as though it were located at the blade tip rather than at its true splitter location. As may be seen in Figure 21, the vibratory margins were satisfactory with the exception of the disk tenon. The increased effectiveness at the splitter location is expected to produce a satisfactory vibratory margin for the disk tenon. It will be necessary to interlock the splitter shrouds to make them an effectively continuous ring.

VI. DESIGN ANALYSIS AND DISCUSSION (CONTINUED)

5. Fan Rotor Blade Natural Frequencies

The natural frequencies of the bypass portion of the fan blade are presented in Figure 22. The blade as specified had a 7 percent thickness-to-chord ratio at its root and its bending frequency coincides with second order excitation near design speed. Because of inlet flow distortions in the aircraft installation it is good practice to have all blade frequencies above second engine order. Accordingly, the blade was tapered from the specified tip to 12 percent at the bypass root. The consequent frequencies also shown in Figure 22 were raised and avoid second engine order excitation.

Frequencies for the core portion of the fan blade are given in Figure 23. Values are very high. The number of stator blades behind the rotor is 19 and the specified 8% configuration avoids this excitation. However, to avoid an abrupt transition from the 12 percent bypass root, the core blade was made 12 percent also.

6. Fan Rotor Blade Flutter Margin

The fan blade has been checked for bending and torsional flutter by comparing the Reduced Frequency Parameter to limiting values.

$$\text{Reduced Frequency Parameter} = \frac{V}{bw}$$

V = relative flow velocity, feet per second

b = one half chord, feet

w = $2 \pi f$

f = natural frequency, hertz

Figures 24 and 25 give values of the parameter for both bending and torsional flutter. For stable operation the values should be less than:

6.6 for bending

2.0 for torsion

VI. DESIGN ANALYSIS AND DISCUSSION (CONTINUED)

The figures show that the blade is satisfactory in bending in either the 7 or 12 percent t/c configurations. In torsion, however, the 12 percent is necessary to avoid the flutter region.

The rotor blade root thickness-to-chord ratios to meet the combined requirements of vibratory strength, natural frequency and flutter are tabulated in Figure 26.

7. Fan Rotor Disk Strength

The fan rotor blades are supported on a titanium hoop. The total radial load of the blades, attachments and hoop is 400,000 lbs. The continuous cross-section area of the hoop is 1.10 square inches. The consequent hoop stress is:

$$\frac{400,000}{2 \pi \times 1.10} = 58,000 \text{ psi}$$

At an overspeed of 15% above the maximum operating speed, this stress becomes 80,000 psi. A strength criterion for overspeed is 90 percent of the disk material ultimate tensile strength.

Material, Titanium, 6Al - 4V

UTS = 150,000 psi

$$\frac{150,000 \times 90\%}{80,000} = 1.69$$

Consequently, the hoop meets the overspeed criterion with a large margin of safety. Increased thickness of the blades, as discussed earlier, can be accepted by this disk design.

B. Compressor

This section presents primarily the stress and vibrational results of analyses on the compressor rotor and stator blades.

VI. DESIGN ANALYSIS AND DISCUSSION (CONTINUED)

1. Compressor Rotor Blade Stresses

Stages 1, 5 and 9 were selected for analysis. Centrifugal and gas bending stresses at the blade root are tabulated in Figure 27.

All of the rotor blades are to be leaned to cancel gas bending stresses. Steady stresses are largely centrifugal and, even at the overspeed condition, the stresses are low.

2. Compressor Rotor Blade Vibratory Strength

The vibratory margin for the first stage airfoil is well in excess of the minimum design requirement of two. With the blade geometry as specified by NASA for aerodynamic considerations, the titanium stages did not have adequate airfoil vibratory margins. Changes in root thickness were required as follows:

	<u>Stage 5</u>	<u>Stage 9</u>
Present t/c	7%	7%
Required t/c	10%	12%

The consequent airfoil stresses and vibratory margins are presented in Figure 27. Blade attachment vibratory strengths are also listed in Figure 27 under Dovetail, Tenon and Drum. As shown in the figure, the stages have acceptable values.

3. Compressor Rotor Blade Natural Frequencies

The blade natural frequencies of compressor rotor stages 1, 5 and 9 were calculated. The frequencies and excitations for the first stage are presented in Figure 28. First bending and torsional frequencies are well above second order excitation. There are nineteen fan stators ahead of the first stage blade and 48 inlet guide vanes and first stage stators immediately adjacent to this blade. Resonances with these orders are confined to the low speed range.

A similar situation occurs for the 5th stage blade, see Figure 29. The 67th and 73rd order excitation represent the adjacent stator numbers. Frequencies have been shown for blades with a 7% and an 11%

VI. DESIGN ANALYSIS AND DISCUSSION (CONTINUED)

thickness to chord ratio. Flutter analysis reported later indicates that the 7% t/c ratio blade does not meet the limiting torsional flutter value. A change to 11% produces an acceptable flutter parameter value. From the standpoint of blade frequency, either blade avoids significant excitations and is acceptable.

The ninth stage blade frequencies are shown in Figure 30. For this stage, vibratory strength considerations require a 12% thickness-to-chord configuration. Adjacent stator numbers are very high and can excite the blade only at very low speeds. The excitation from the 12 struts in the exit diffuser is also shown. With the required 12% blade, bending resonance with the strut excitation is below 50% rotor speed, and torsional resonance is well above top speed. Thus the strength increase has resulted in a satisfactory frequency condition.

4. Compressor Rotor Blade Flutter Margin

The flutter parameters have been calculated for the compressor rotor blades of stages 1, 5 and 9, and the values are tabulated in Figures 24 and 25. For flutter considerations the 5th and 9th stages require an increase from the specified 7% thickness-to-chord ratio to an 11% ratio to lower the torsional flutter parameter by raising the torsional natural frequency.

As reported earlier, vibratory strength requires a thickness-to-chord ratio of 12 percent in the 9th stage rotor blade. Since this ratio exceeds the minimum required of 11%, the 12% blade is acceptable for both strength and flutter.

Refer to Figure 26 for a summary of the final thickness-to-chord ratios to satisfy vibratory strength, natural frequency and flutter requirements.

VI. DESIGN ANALYSIS AND DISCUSSION (CONTINUED)

5. Compressor Stator Vane Vibratory Strength

Again, stages 1, 5 and 9 were selected for analysis. The first stage vane with the specified geometry is adequate, but the vanes of stages 5 and 9 are considerably understrength. The following changes were required to obtain satisfactory vibratory margins.

Stage	1	5	9
Present t/c	7%	7%	7%
Required t/c	7%	12%	12%
Chord Increase	0	11%	15%

Stresses and vibratory margins are tabulated in Figure 31 for the revised vanes.

6. Compressor Stator Vane Natural Frequencies

Natural frequencies of the stator vanes for stages 1, 5 and 9 are given in Figures 32 and 33. First engine order excitation from rotor unbalance and higher order excitations from adjacent rotor blade numbers are shown. No major resonances are anticipated.

Thickness and chord changes required for vibratory strength will not alter this conclusion. See Figure 26.

C. COMBUSTOR

The mechanical design of the combustor was obtained by direct comparison with a combustor design from a Curtiss-Wright lift-cruise engine. Feasibility of the design concepts has been demonstrated by successful operation.

Thermal expansion loads have been largely eliminated by providing sliding joints between major components. The fuel manifold is isolated from casing radial growth by radial slots at the mounting bolts. Fuel nozzles and swirl cups are free to move relative to the burner head plate. The

VI. DESIGN ANALYSIS AND DISCUSSION (CONTINUED)

head plate mounting for the liners is, in turn, mounted on radial pins to the casing, again permitting relative radial growth. And finally, axial growth of the liners is accommodated with axially sliding seals at the HP stator vane shrouds.

Final design calculations of liner creep strength, outer liner buckling margin and minimum shell thicknesses are not expected to significantly alter the configuration.

The fact that the combustor is folded over the compressor has not created serious mechanical problems. Crowding of the variable stator mechanism and poor accessibility to the compressor are real but not critical problems. The short shafting that results from the folded flow path is beneficial from a critical speed standpoint. This, plus the lightweight composite components, contribute to high fan and compressor mode frequencies.

D. HIGH PRESSURE TURBINE

Stress and some vibrational analyses of the high pressure turbine rotor blade and disk and of the stator vane are discussed in this section.

1. H.P. Turbine Rotor Blade Stress Rupture Life

First consider the nominal condition of 10,000 lbs. thrust. Centrifugal stress and allowable stress are plotted in Figure 34. Since the stress is always far less than the allowable value for 2000 hours of life, this nominal condition can easily be tolerated.

The curve shows that the ratio of imposed stress to allowable stress reached a maximum at approximately one fourth of the blade span. This then represents the critical section for the assumed temperature distribution.

In the work that follows, it will be assumed, conservatively, that the peak temperature coincides with the stress at this critical section.

VI. DESIGN ANALYSIS AND DISCUSSION (CONTINUED)

Now consider the duty cycle shown in Figure 35. This is an interpretation of the cycle given in the Design Specification. In order to determine the blade life under duty cycle conditions, it is necessary to calculate the life for each operating condition. As an example, the life at the 12,500 lb. thrust condition is calculated below.

Rotor blade relative temperature = 1575°F

(Estimated before specification value of 1561°F was available.
Well within required accuracy.)

Temperature at critical section

$$(1575 + 460) 1.05 = 2140^{\circ}\text{R}$$

Stress at critical section

$$32,500 \times \left(\frac{14,700}{13,818}\right)^2 = 36,700 \text{ psi}$$

Larson-Miller Parameter = P

where

$$P = T (20 + \log t) \times 10^{-3}$$

$$T = \text{metal temperature, } ^{\circ}\text{R}$$

$$t = \text{time to rupture, hours}$$

From Figure 36, $P = 48.4$

Time to Rupture = 398 hours, based on average material properties.

Divide by two to account for minimum properties.

Rupture Life at 12,500 lbs. thrust = 200 hours

Similar calculations for the other conditions were made and combined using the assumption that the ratio

$$\frac{\text{Time at Condition } i}{\text{Life at Condition } i}$$

represents the fraction of life used up at Condition i.

VI. DESIGN ANALYSIS AND DISCUSSION (CONTINUED)

It follows then that:

$$\text{Life} = \frac{1}{\sum \frac{P_i}{L_i}}$$

Where P_i is the percentage of time at the Condition i and L_i is the life at Condition i .

This procedure results in a predicted Stress Rupture Life of 990 hours. Since an overhaul period for the engine is scheduled for 670 hours of lifting time, this blade life requires blade replacement at each overhaul. Thus the HP turbine rotor blade is only marginally acceptable. If final design cannot improve this condition by blade geometry changes or less conservative assumptions, then some form of blade cooling is indicated.

2. H.P. Turbine Rotor Blade Fatigue Strength

Gas bending moments on the blade root are:

78.5 in. lbs./blade axial
104.5 in. lbs./blade tangential

When these were resolved along the blades principal axes and combined with the airfoil section properties, the consequent blade bending stress was 12,600 psi at the leading edge, and the centrifugal stress was 46,000 psi.

Blade root temperature was estimated using total temperature relative to the blade and a factor of 0.95 to account for a radial temperature profile. The resulting temperature was 1440°F.

The blade material is Cast MAR-M-246 and has the following properties at this temperature:

Ultimate Tensile Strength 140,000 psi
Endurance Limit 35,000 psi

VI. DESIGN ANALYSIS AND DISCUSSION (CONTINUED)

The blade was leaned so that its steady stress is largely centrifugal. The consequent allowable vibratory stress is 23,000 psi.

The vibratory margin is

$$\frac{23,000}{12,600} = \underline{1.83}$$

In order to raise this to the design criterion of 2.0 the blade root region was increased in bending strength ten percent by lengthening the root chord ten percent without increasing blade thickness.

3. H.P. Turbine Rotor Blade Attachment Fatigue Strength

The computation of attachment stresses involves many factors. The method used at Curtiss-Wright considers:

- Tooth load distribution
- Stress concentrations
- Load proximity
- Non-axial slot effects

The configuration illustrated on the HP turbine layout, Figure 12, was calculated and the vibratory margin of the fir tree neck proved to be inadequate. Consequently a considerably strengthened three-tooth attachment was designed. See Figure 37. Its neck vibratory margin is satisfactory.

4. H.P. Turbine Rotor Blade Frequencies

Natural frequencies of the HP turbine rotor blade are presented in Figure 38. Radial lines representing excitation frequencies from 3 thick LP turbine stators, 38 HP stators, 55 LP stators, and 24 combustor nozzles are also shown.

The curves indicate a potential torsional resonance at design speed due to the 24 fuel nozzles in the combustor. Raising the blade

VI. DESIGN ANALYSIS AND DISCUSSION (CONTINUED)

frequency would result in serious resonance with the number of stators; therefore, it is recommended that the number of fuel nozzles be reduced to 20.

With 20 fuel nozzles, a bending resonance will occur at 9500 RPM (64% design speed). Since the turbine will only have to pass through this resonance, it is considered acceptable.

5. H.P. Turbine Stator Vane Stress Rupture Life

The HP turbine stator vane is mounted as a simply-supported beam. The bending moments are a maximum in the midspan and are calculated to be:

57.5 in. lbs. axial
42.5 in. lbs. tangential

The consequent stresses are:

Leading Edge	3000 psi	Compression
Back	2400 psi	Tension
Trailing Edge	1300 psi	Compression

The stator vane is cooled by a specified internal flow. The consequent metal temperatures have been calculated as:

1995°R Average
2100°R Leading Edge

Because of radial and circumferential distribution, the peak temperature will exceed these values. With an assumption of 1.15 stator temperature distribution factor, the peak leading edge temperature becomes:

$$2100 \times 1.15 = 2420^{\circ}\text{R}; 1960^{\circ}\text{F}$$

VI. DESIGN ANALYSIS AND DISCUSSION (CONTINUED)

Although the leading edge stress is compression, it was conservatively used for the stress rupture criterion.

Vane Stress	3000 psi
Vane Material	MAR-M-246
Larson-Miller Parameter	58
Stress Rupture Life at 12,500 lbs. thrust	5000 hours

This life represents 5000 hours of continuous operation at the maximum normal thrust. Since the duty cycle requires considerably less than this, the design is more than adequate. During final design, other materials and weight reduction can be considered.

6. H.P. Turbine Rotor Disk Stress

The HP turbine disk was analyzed for centrifugal stresses. Two configurations were investigated. The first is consistent with the blade geometry as pictured on the layout. Figure 12. The final configuration is consistent with the increased strength blade and attachment as discussed previously.

The radial and tangential stresses for the final configuration are presented in Figure 39. For this preliminary analysis, only centrifugal stresses were considered.

The disk material selected is Udimet 700. Temperatures of the disk are low enough that yield strength governs. This preliminary design was sized so that maximum stresses approximate yield values.

VI. DESIGN ANALYSIS AND DISCUSSION (CONTINUED)

E. LOW PRESSURE TURBINE

Analyses of the L.P. Turbine rotor blade and disk strengths and vibrational frequencies as well as the L.P. Turbine first stage stator vane strength are presented in this section. The areas of the L.P. Turbine that were not analyzed and therefore not discussed were considered either conservative from a mechanical design standpoint or covered by analyses of neighboring components.

1. L.P. Turbine Blade Strength

The third stage rotor blade was selected for analysis. This stage has the longest span and greatest tip speed.

Centrifugal stress is 14,000 psi at 4000 RPM. The blades were leaned so as to minimize the effects of the gas loading.

This turbine incorporates tip shrouds that are interlocked and pre-loaded in torsion to form a continuous rim. As a consequence, relative tangential tip motion of the blades is prevented and the blades are effectively tip supported tangentially for vibratory conditions. The tip supported gas bending stress is 9100 psi and is the value used to compute the vibratory margin.

With a relative blade temperature of 1574°R and a profile factor of 0.95, the blade root temperature is 1040°F. The Rene 41 material has an endurance limit of 50,000 psi and an ultimate tensile strength of 125,000 psi at this temperature. At a steady stress of 14,000 psi the allowable vibratory stress is 44,000 psi and the vibratory margin

is $\frac{44,000}{9,100} = 4.8$.

Although this margin seems high, this Rene 41 blade is envisioned as a hollow sheet metal blade butt welded to a forged shroud and butt. Consequently there will be a weld near the root section, and some

VI. DESIGN ANALYSIS AND DISCUSSION (CONTINUED)

mismatch is probable. There is adequate allowance in the vibratory margin for a stress concentration factor of two.

2. L.P. Turbine Blade Attachment Fatigue Strength

The attachment of the LP turbine rotor blades was checked in the same way as discussed for the HP rotor blade. The third stage blade was selected since it has the smallest attachment radius and, consequently, the least space for its fir tree

Early calculations indicated that the attachment was too crowded for satisfactory vibratory strength. The basic assembly drawing was changed to incorporate increased chord blades in the second and third stages. This change is consistent with reduced numbers of blades in these stages and, consequently, room for stronger attachments.

A recent calculation, however, shows that a satisfactory vibratory strength can be achieved by axially widening the attachments significantly, without reducing the number of blades. It was necessary to widen the third stage attachment to full projected chord length in order to get a satisfactory vibratory margin. See Figure 40.

The basic assembly drawing was not changed back to the original blades. It still shows the increased chords. Engine weight is based on the latest configuration with the specified blade numbers.

The space for attachment is quite limited in this third stage. Conservatively, it is recommended that a smaller number of blades be considered for this stage and the preceding one. This change would be necessary if an all-cast blade is considered since its fatigue strength would be lower.

3. L.P. Turbine Blade Natural Frequencies

The natural frequencies for fundamental bending and torsion have been calculated for the first and third stages. The first stage frequencies

VI. DESIGN ANALYSIS AND DISCUSSION (CONTINUED)

for fundamental bending and torsion have been calculated for the first and third stages. The first stage frequencies are shown in Figure 41. The torsional frequency of the original layout configuration is excited in the high speed range by the 55 first stator vanes of the LP turbine just upstream of this rotor.

As a fix for this problem it is proposed that a shank be introduced under the blade shelf to lower the blade frequencies. Figure 41 shows the effect of such a shank on the blade frequencies. The resonance with 55 engine order has been lowered to a satisfactory speed.

The situation for the third stage blade is given in Figure 42. Adjacent stator orders are shown and present no resonance problems in the high speed range.

Third engine order is shown for both blades since this order was introduced or emphasized by the use of three thick stator vanes in the LP first stage of the turbine. Blade frequencies are much higher than this excitation. This is also true for the first harmonic of this excitation, i.e., 6 E.O. Consequently the three thick stator vanes are acceptable from a vibration standpoint.

4. L.P. Turbine First Stator Vane Strength

The first stator vanes are used structurally in the turbine bearing support. The following loads have been considered.

Gas loads on the vanes.

Inner shroud and bearing support cone axial pressure load.

Radial bearing loads from rotor unbalance, gyroscopic effect and high pressure turbine blade loss.

VI. DESIGN ANALYSIS AND DISCUSSION (CONTINUED)

The consequent bending moments in the vane are tabulated below:

<u>Load</u>	<u>Vane Tip Bending Moments</u>	
	<u>Axial</u>	<u>Tangential</u>
<u>Steady State</u>		
Gas on Vane	49.6	129 <u>in. lbs.</u> blade
Shroud & Cone Pressure	159	0
Turbine Unbalance (200 lbs.)	15.3	39.2
<u>Gyro Loading*</u>	87	319
<u>Total Steady State</u>	224	168 <u>in. lbs.</u> blade
<u>Gyro plus Steady State</u>	311	487

The consequent stresses in the leading edge of the stator vane tip are:

Steady State	13,000 psi
Gyro plus Steady State	31,000 psi

Blade temperature is 1350°F. At this temperature MARM 246 cast vanes or Rene 41 sheet metal vanes have adequate strength. Final design calculations may allow use of a lower strength material.

Now consider the loss of a high pressure turbine rotor blade. As discussed later under Critical Speeds, this engine operates above the critical speed of its turbine suspension. Consequently, the loss of a blade results in a small shift of the center of rotation of the turbine rotors and the consequent bearing load is determined by the spring rate of the turbine suspension.

(*) Based on rotor inertias of 75.4 lb.in.sec² (LP) and 14.5 lb.in.sec² (HP) at 1 rad/sec rpm.

VI. DESIGN ANALYSIS AND DISCUSSION (CONTINUED)

For an airfoil weight of 0.20 lbs. and a combined turbine weight of 180 lbs. (LP and HP), the shift of the center of rotation is 0.012 inches. For a turbine support spring rate of 27,000 lbs./in. the load on the vane assembly is only 320 pounds. This value will magnify as the engine decelerates through its turbine critical speed but even a factor of ten only results in a blade stress close to the gyro value.

5. L.P. Turbine Rotor Disk Strength

The hoop type of rotor disk used for each low pressure turbine stage is loaded by centrifugal forces of the blades, their attachments and the continuous hoop itself.

For the third stage, the tangentially continuous hoop is 1.2 inches wide as required for attachment fatigue strength and effectively one half inch in radial dimension.

At 4000 RPM the loads are:

97 Blades	149,000 lbs.
Attachments	24,000 lbs.
Hoop	<u>22,000 lbs.</u>
	195,000 lbs.

and the consequent hoop stress is:

$$\begin{aligned}\sigma_t &= \frac{195,000}{2\pi} \times \frac{1}{1.2 \times .5} \\ &= \underline{52,000 \text{ psi}}\end{aligned}$$

Rene 41 at the full total temperature of this stage has a 0.2% creep strength of 96,000 psi for 100 hours. This stage then has ample hoop section.

The earlier stages are somewhat hotter but have shorter blades so that similar hoop area is required.

VI. DESIGN ANALYSIS AND DISCUSSION (CONTINUED)

F. BEARINGS AND LUBRICATION

The following analyses are reported here:

Bearing Thrust Loads

Bearing Selection and Lubrication

1. Bearing Thrust Loads

Rotor thrust loads have been calculated for the engine. The results are tabulated in Figure 43. Compressor spool thrust is a function of the radius of the compressor rotor exit seal. The tabulated values are consistent with a seal located at the inner diameter of the compressor exit annulus.

For the 12,500 lb. thrust condition, the loads are:

Fan Spool	3695 lbs.
Compressor Spool	2745 lbs.

The thrust load on the compressor spool can be reduced by moving the compressor rotor exit seal to a larger radius. Because the compressor exit diffuser curves outward this change is readily accomplished and has been incorporated. See Figures 1 and 12. The radius chosen lowers the calculated thrust on the compressor bearing to 600 pounds.

The thrust loads for the condition of 12,500 pounds of engine thrust were estimated using compressor and turbine interstage conditions provided by NASA. Because of insufficient interstage flow conditions, the thrust loads for the case of 10,000 lbs. of thrust were scaled from those for the case of 12,500 lbs. thrust. It was assumed that the pressure force on each component of the engine is proportional to the overall static pressure rise through that component at each operating condition and that the force due to axial momentum change is proportional to weight flow.

VI. DESIGN ANALYSIS AND DISCUSSION (CONTINUED)

2. Bearing Selection and Lubrication

Bearing capacity, life and lubrication requirements are summarized in Figure 44. They are based on early estimates of bearing loads and sizes, yet agree well with the configuration finally selected. As pointed out in the previous section, compressor spool thrust loads are readily adjustable to the load range of 1000 pounds assumed here. Bearing sizes were altered to suit improved arrangements, but the data are still a good approximation and the design is clearly feasible.

Later studies indicated that a larger oil flow may be needed for the bearings. Resolution of this question has been left for final design.

An analysis was made of the oil tubes in the LP turbine first stage stator. Figure 45 shows the installation configuration. An important consideration is that the oil tube walls remain below the temperatures that will degrade the oil. The calculation results are given in Figure 46. The oil tube temperature of 410°F is acceptable.

The calculation was based on the 12,500 lb. thrust condition and considered only the oil return or scavenge tube. The fact that a similar quantity of cooler oil will be flowing in the double tube has been ignored. However, the calculation was based on an increased oil flow to the rear bearings. If this larger flow is found to be unnecessary for the bearings, then the tube cooling requirement will need further attention.

There is considerable design freedom in this area. Compressor exit air is readily available at the LP turbine stator vanes and can be used for cooling these three vanes. However, the present analysis indicates that this is not needed.

VI. DESIGN ANALYSIS AND DISCUSSION (CONTINUED)

G. CRITICAL SPEEDS

The critical speeds of this engine were investigated by studying the behavior of the following three subsystems:

The combined mass of the LP and HP turbine rotors on a single flexible support.

The complete LP shaft with fan and LP turbine, on two flexible supports.

The complete HP shaft with compressor and HP turbine, on two flexible supports.

It was a design objective to flexibly suspend the heavy turbine rotors and to operate above the turbine mode critical speed. This approach avoids the need for a rigid and consequently heavy rear bearing support. In addition, the flexible suspension isolates the turbine structure from turbine unbalance forces. It is especially important in this design since it reduces the vibratory loading of the LP turbine first stators being used as bearing supports.

The first subsystem approximates this turbine mode. The frequency of the mode is given as a function of rear bearing support spring rate in Figure 47. For a spring rate of 27×10^3 lbs/inch the frequency is 1800 cpm. This is excited by LP turbine unbalance at 1800 RPM which is above idle speed and below operating speed.

The second subsystem, the fan spool on two supports, was used to determine the natural frequency of the fan rotor suspension. Figure 48 illustrates the effect of varying the front support spring rate. For a spring rate of 300×10^3 lbs/in. the natural frequency is 8600 cpm. This is above the maximum fan speed so that fan spool unbalance cannot excite this fan mode. This mode corresponds to the second mode of the fan shaft system. The third mode involves the mass of the fan shaft between bearings and is

VI. DESIGN ANALYSIS AND DISCUSSION (CONTINUED)

similar to the "bent shaft" critical speed. For the selected spring rates, this frequency is 12,000 cpm which is above excitation by fan shaft unbalance.

The third subsystem, the compressor spool on two supports, was used to determine the natural frequency of the compressor rotor suspension. See Figure 49. For a front spring rate of 900×10^3 lbs/inch, the natural frequency is 20,200 cpm. This is above the maximum compressor speed so that compressor spool unbalance cannot excite this compressor mode.

The relationship of the various mode frequencies and their excitations are given in Figure 50. The significant critical speeds avoid operating speeds.

The requirement for a softer front support spring rate for the fan than for the compressor is resolved by selection of bearing spring rates. The assumed spring rates appear to be reasonable and attainable in the final design.

H. IMPINGEMENT STARTER

A parametric study of the impingement starter system is summarized below. An engine resistance torque curve, Figure 51, was obtained by scaling from the resistance characteristics of an existing engine. Compressor spool polar inertia is 14.5 lb.in.sec^2 .

In Figure 52, the light-off time is plotted versus light-off speed for convergent-divergent nozzles with the required airflow as a parameter. Convergent-divergent starter nozzles were chosen to maximize acceleration torque for a given air flow. The required total nozzle area, both at the throat and at the exit, is shown for each flow. See Figure 53. The number of nozzles can be determined for any nozzle size selected.

To minimize pressure loss in the flow passage upstream of the nozzles, supply pipes of four times the throat area are recommended. A converging

VI. DESIGN ANALYSIS AND DISCUSSION (CONTINUED)

angle of 60 degrees and a diverging angle of between 24 and 36 degrees are considered adequate to achieve proper contraction and expansion. The nozzles were designed for a jet Mach number of 1.9.

The specific design selection obtained from the parametric curves is:

Source Pressure	100 psia
Source Temperature	950°R
System Flow	1.0 lb/sec
Nozzle	
Throat Area	0.58 in ²
Exit Area	0.90 in ²
Number of Nozzles	4
Supply Tube Area	2.3 in ² min.
Time to 10% Speed	2.2 secs

I. ENGINE WEIGHT

Engine weights are summarized in Figure 54. Two configurations are shown. Configuration 1 is the engine as described by the individual layouts of Figures 6 through 13. All blading in Configuration 1 conforms to the geometry as originally specified.

Configuration 2 incorporates blading strength increases to attain acceptable vibratory margins. In some cases the consequent weight increases provide for heavier attachments and disks to support the heavier blades.

These changes were included in the engine basic assembly drawing, Figure 1. There is, however, one exception to this. The assembly drawing shows the fan turbine rotor with increased chord blades in the second and third stages. This change had been introduced to reduce the number of blades and give room for a stronger attachment. A recent calculation indicated that the desired vibratory strength in the attachment can be attained with the original numbers of blades by increasing attachment width. Although

VI. DESIGN ANALYSIS AND DISCUSSION (CONTINUED)

The assembly drawing was not changed back, the weights are consistent with the original blade chords, blade numbers, and wider disks.

The accessory weight of 65.6 pounds includes the following items:

- Fuel Control
- Fuel Manifold and Nozzles
- Fuel Pump
- Ignition System
- Oil Pressure and Scavenge Pumps
- Oil Tank
- Heat Exchanger
- Filter, Check Valves, Tubing
- Air Turbine Drive Motor

Configuration 2 represents the completed engine design. The estimated engine weight for this configuration is 1011.7 pounds.

VII. CONCLUSIONS

1. On the basis of this preliminary design, the Integral Lift Engine is considered mechanically feasible and suitable for final design.
2. The use of composite material in the fan and compressor rotor blades appears to be feasible and will result in weight savings and favorable blade vibratory characteristics, but extensive experimental development will be required to assure success.
3. To avoid vibratory excitation and to achieve adequate vibratory strength, some of the blade geometry supplied by NASA will require modification.
4. To reduce vibratory loads on the fan blade attachment and to increase the fan blade vibratory frequencies, the splitter shroud on the fan rotor blade must provide blade support under operating conditions.
5. This preliminary design indicates that the required lifting time life of 2000 hours and overhaul life of 670 hours can be achieved for the engine.
6. Although the high pressure turbine rotor blades have a relatively short predicted life, they will exceed the required overhaul life.
7. The low pressure turbine rotor blades of welded Rene 41 sheet metal construction will require process development to produce high strength welds.
8. Use of the low pressure turbine first stage vanes for turbine bearing support is feasible from a standpoint of strength and lubrication requirements.
9. The first stage rotor blades of the low pressure turbine will require detuning to avoid torsional resonance from the upstream stator vanes, and this detuning can be accomplished by providing torsional flexibility in the blade attachment.

VII. CONCLUSIONS (CONTINUED)

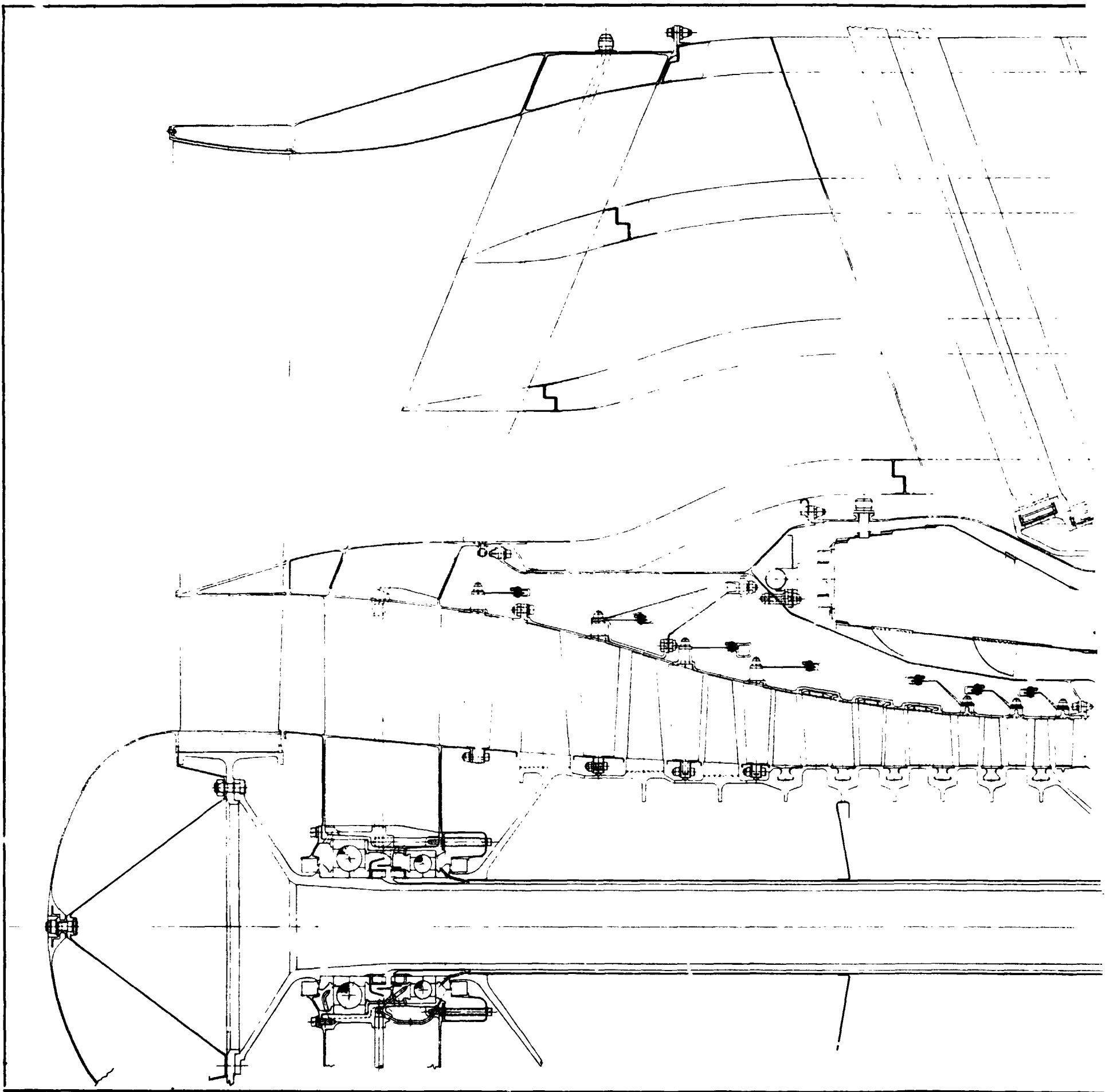
10. Although locating the combustor outboard of the compressor results in accessibility problems, there are beneficial effects on rotor critical speed as a result of the shortened rotor shaft.
11. This engine design satisfies the requirement of noise reduction by means of proper spacing between the fan rotor and stator blades and by the installation of acoustical material in the fan duct, but there is some accompanying penalty in overall engine weight.

VIII. REFERENCES

1. Jaklitsch, R.; Leto, A.; Pratt, W. and Schaefer, R.: Tip-Turbine Lift Package Design. NASA CR 72974, July 1971, Prepared by the Curtiss-Wright Corp. for the NASA Lewis Research Center.
2. Jaklitsch, R.; Leto, A.; Schaefer, R.: Tip-Turbine STOL Fan Package Preliminary Design, Sept. 30, 1971. A Final Report Prepared by Curtiss-Wright Corp. for the NASA Lewis Research Center, Report No. CW-WR-71-083.
3. Brandmaier, H.; Katz, H.; McInnis, W.: Molding Compressor Blades From Preimpregnated Composite Materials, SAMPE Quarterly VI. No. 3, April 1970.
4. Watson, H.; Thompson, J.; Rucker, C.: Structural and Environmental Studies of Acoustical Duct-Lining Materials, NASA SP-189 Report, Oct. 1968.
5. Owen, M.; Morris, S.: An Assessment of the Potential of Carbon Fibre Reinforced Plastics as Fatigue Resistant Materials. 25th Annual Technical Conference, 1970, Reinforced Plastics/Composites Div. The Society of the Plastics Industry, Inc.

FOLDOUT FRAME |

ENGINE ASSEMBLY DRAWING



THE ASSEMBLY DRAWING

EOLDOUT FRAME 2

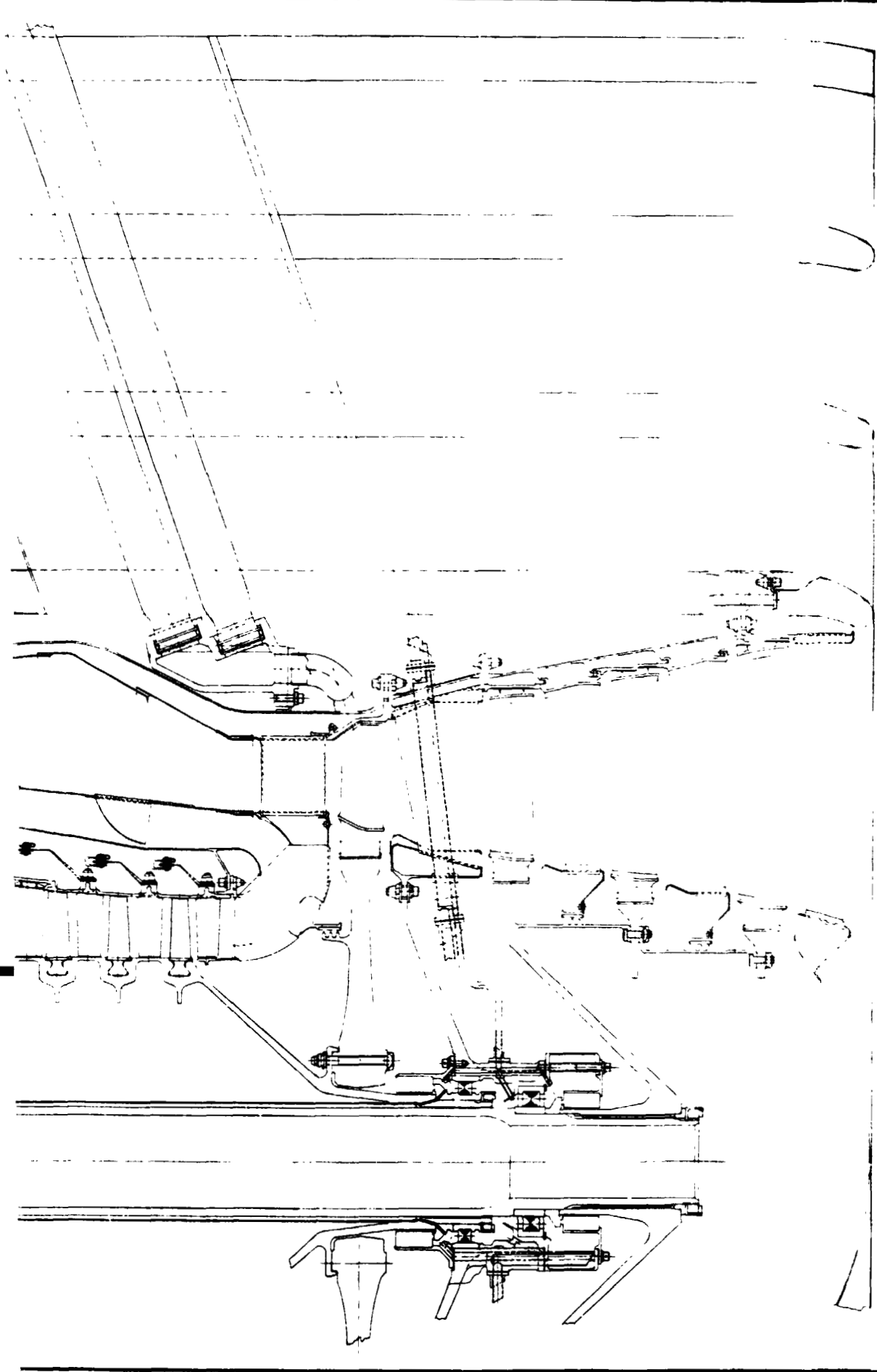


FIG. 12	REVISION	DATE	BY	APPROVED BY	REVISION	DATE
1						
2						
3						
4						
5						
6						
7						
8						
9						
10						
11						
12						
13						
14						
15						
16						
17						
18						
19						
20						
21						
22						
23						
24						
25						
26						
27						
28						
29						
30						
31						
32						
33						
34						
35						
36						
37						
38						
39						
40						
41						
42						
43						
44						
45						
46						
47						
48						
49						
50						
51						
52						
53						
54						
55						
56						
57						
58						
59						
60						
61						
62						
63						
64						
65						
66						
67						
68						
69						
70						
71						
72						
73						
74						
75						
76						
77						
78						
79						
80						
81						
82						
83						
84						
85						
86						
87						
88						
89						
90						
91						
92						
93						
94						
95						
96						
97						
98						
99						
100						

Figure 1

COMPONENT PERFORMANCE

Condition	<u>All Engines Operating</u>		<u>Engine Out Operation</u>	
	Nominal	Maximum Control	Nominal	Maximum Control
Thrust, Lbs	10,000	12,500*	11,450	12,880
<u>FAN</u>				
Inlet Temp., °R	549	549	549	549
Inlet Total Press., Atm	1.00	1.00	1.00	1.00
Outlet Temp., °R	582	591	587	592
Outlet Total Press., Atm	1.20	1.25	1.23	1.25
Pressure Ratio	1.20	1.25	1.23	1.25
Air Flow, Lb/Sec	487	540	517	547
Bleed Flow, Lb/Sec	0	0	0	0
Efficiency	.839	.878	.886	.866
Speed, RPM	3,556	4,000	3,800	4,100
Percent Design Speed	88.9	100	95.0	102.5
<u>CORE FAN</u>				
Inlet Temp., °R	549	549	549	549
Inlet Total Press., Atm	1.00	1.00	1.00	1.00
Outlet Temp., °R	564	568	566	569
Outlet Total Press., Atm	1.09	1.11	1.10	1.11
Pressure Ratio	1.09	1.11	1.10	1.11
Air Flow, Lb/Sec	63.7	71.0	68.0	71.8
Bleed Flow, Lb/Sec	0	0	0	0
Efficiency	.897	.886	.892	.879
<u>COMPRESSOR</u>				
Inlet Temp., °R	564	68	566	569
Inlet Total Press., Atm	1.09	1.11	1.10	1.11
Outlet Temp., °R	1050	1103	1080	1170
Outlet Total Press.	7.27	8.5	7.92	8.68
Pressure Ratio	6.67	7.65	7.20	7.82
Air Flow, Lb/Sec	63.7	71.0	68.0	71.8
Bleed Flow, Lb/Sec	0	0	0	0
Efficiency	.822	.820	.839	.814
Speed, RPM	13,818	14,700	14,259	14,994
Percent Design Speed	94.0	100	97.0	102.0

*Aerodynamic Design Point

COMPONENT PERFORMANCE - Continued

Condition	All Engines Operating		Engine Out Operation	
	Nominal	Maximum Control	Nominal	Maximum Control
Thrust, Lbs	10,000	12,500*	11,450	12,880
<u>COMBUSTOR</u>				
Inlet Temp., °R	1,050	1,103	1,080	1,120
Inlet Total Press., Atm	7.27	8.5	7.92	8.68
Outlet Temp., °R	2,070	2,260	2,175	2,312
Outlet Total Press., Atm	6.72	7.86	7.35	8.08
Air Flow, Lb/Sec	63.7	71.0	68.0	71.8
Fuel Flow, Lb/Sec	1.0	1.30	1.15	1.36
Total Flow, Lb/Sec	64.7	72.3	69.1	73.1
Efficiency	.98	.98	.98	.98
SFC	.3606	.3735	.3662	.3780
<u>HIGH PRESSURE TURBINE</u>				
Inlet Temp., °R	2,070	2,260	2,175	2,312
Inlet Total Press., Atm	6.72	7.86	7.35	8.08
Outlet Temp., °R	1,650	1,811	1,740	1,860
Outlet Total Press., Atm	2.46	2.86	2.69	2.96
Pressure Ratio	2.73	2.74	2.73	2.73
Flow, Lb/Sec	64.7	72.3	69.1	73.1
Bleed Flow, Lb/Sec	0	0	0	0
Efficiency	.920	.924	.920	.926
<u>LOW PRESSURE TURBINE</u>				
Inlet Temp., °R	1,650	1,811	1,740	1,860
Inlet Total Press., Atm	2.46	2.86	2.69	2.96
Outlet Temp., °R	1,420	1,528	1,470	1,560
Outlet Total Press., Atm	1.16	1.23	1.20	1.24
Pressure Ratio	2.12	2.32	2.24	2.39
Flow, Lb/Sec	64.7	72.3	69.1	73.1
Efficiency	.826	.829	.828	.829
<u>EXHAUST NOZZLES</u>				
Fan Exhaust Flow, Lb/Sec	487	547	517	547
Fan Exhaust Velocity, Ft/Sec	582	647	625	657
Core Exhaust Flow, Lb/Sec	64.7	72.3	69.1	73.1
Core Exhaust Velocity, Ft/Sec	833	990	916	1020

*Aerodynamic Design Point

ENGINE SPECIFICATIONS PROVIDED BY NASA

Fan

Computer Print Outs	YON1313	Crouse
	013	1-27-71
	172	1-27-71
	018	4-28-71

Compressor

Computer Print Outs	YON1313	Crouse
	396	2-27-71
	157	3-9-71
	011	3-10-71
	043	4-15-71
	018	4-28-71

Combustor

Table of Conditions - 12-21-70
Flow Path Chart and Accompanying Table - 12-21-71

Turbine

High Pressure Turbine Aerodynamics - 3-9-71
Layout Drawings of Blade Sections and Flow Path
Low Pressure Turbine Computer Print Outs YON2200 Erickson

	084	3-24-71
	088	3-24-71

Figure 3

ENGINE SERVICE TIME REQUIREMENTS

Total Engine Life 30,000 Cycles

Engine Operation Per Cycle:

Idle	2 Minutes
Takeoff	1 Minute at 10,000 Pounds Nominal Thrust
Landing	3 Minutes at 9,000 Pounds Nominal Thrust
Idle	1 Minute

Idle Time 1500 Hours

Lifting Time 2000 Hours

TBO 10,000 Cycles

ENGINE THRUST VARIATION CHARACTERISTICS

	Nominal	Emergency
Rated Lift	$L_{NR} = 10,000 \text{ Lbs}$	$L_{ER} = 11,450 \text{ Lbs}$
Max. Control Lift	$L_{NM} = 12,500 \text{ Lbs}$	$L_{EM} = 12,880 \text{ Lbs}$

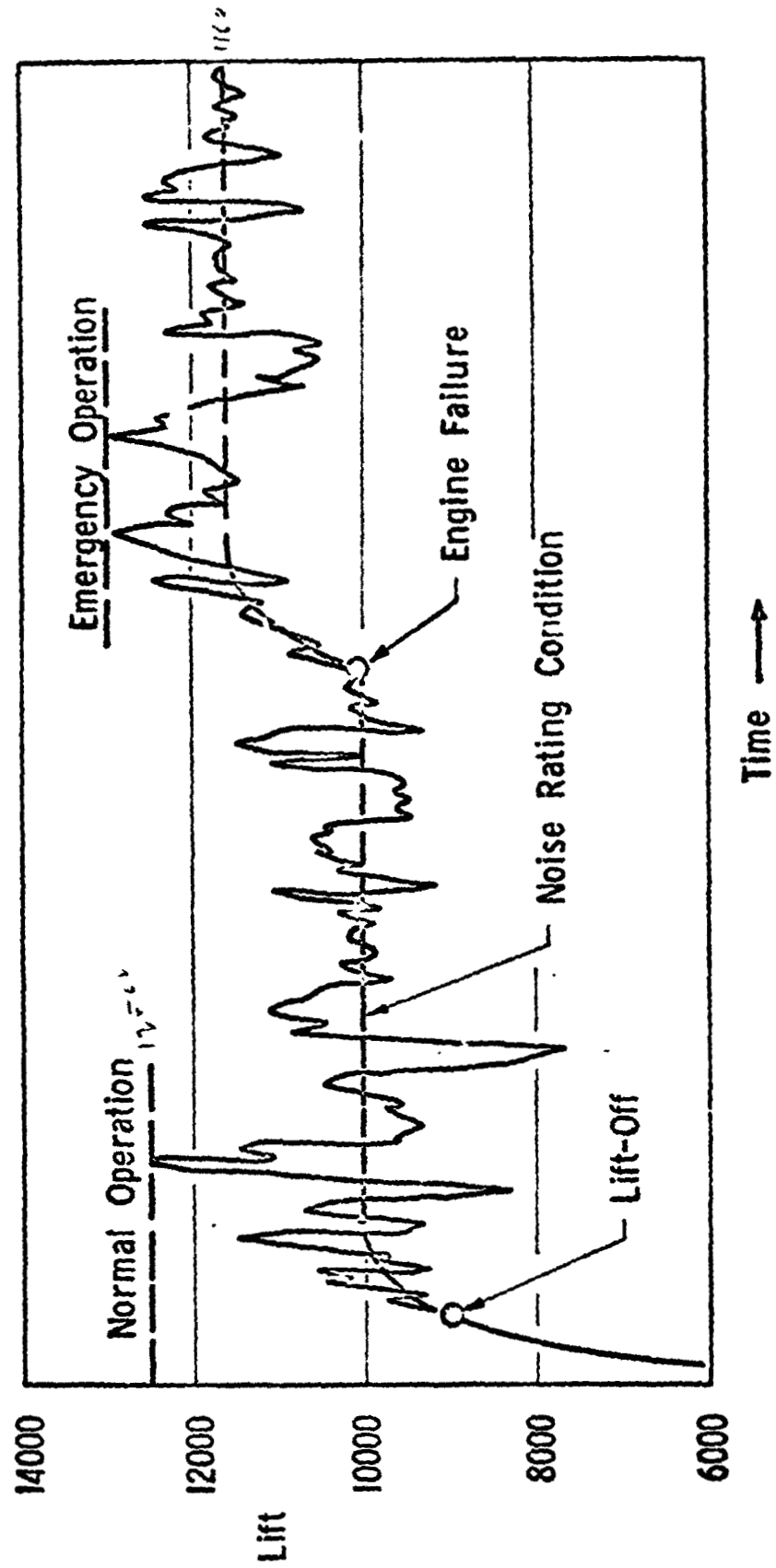


Figure 5

FAN ROTOR

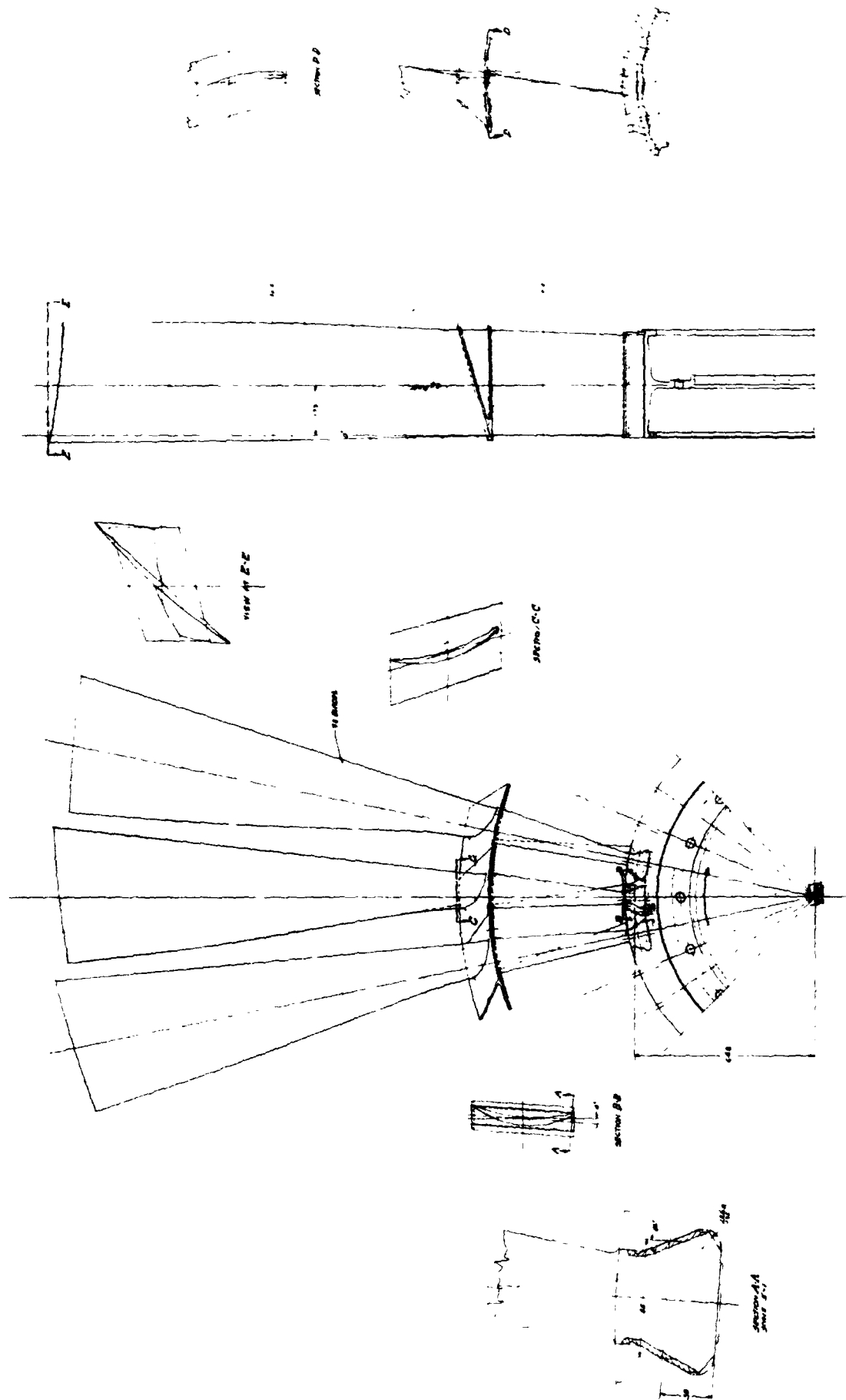
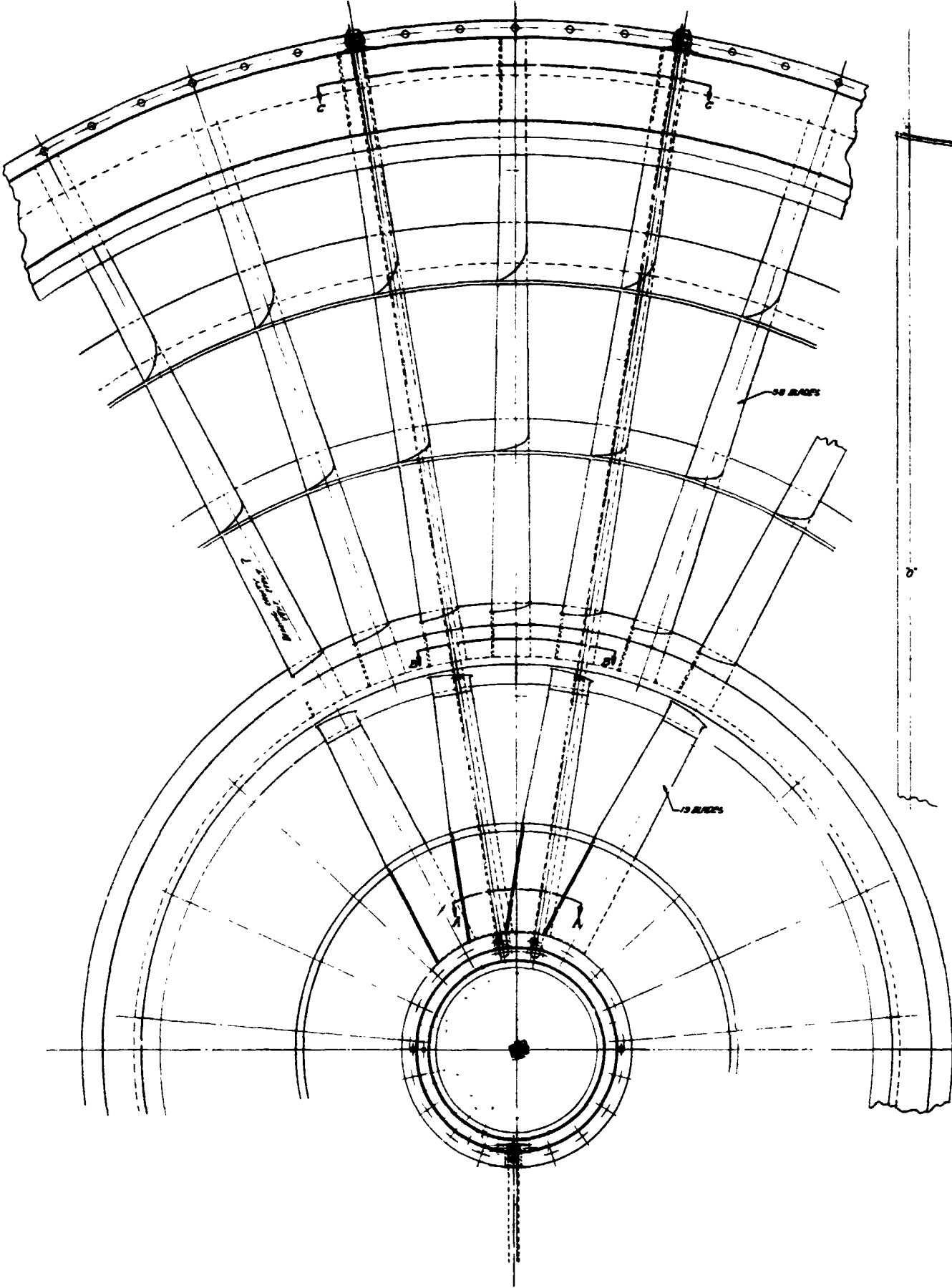
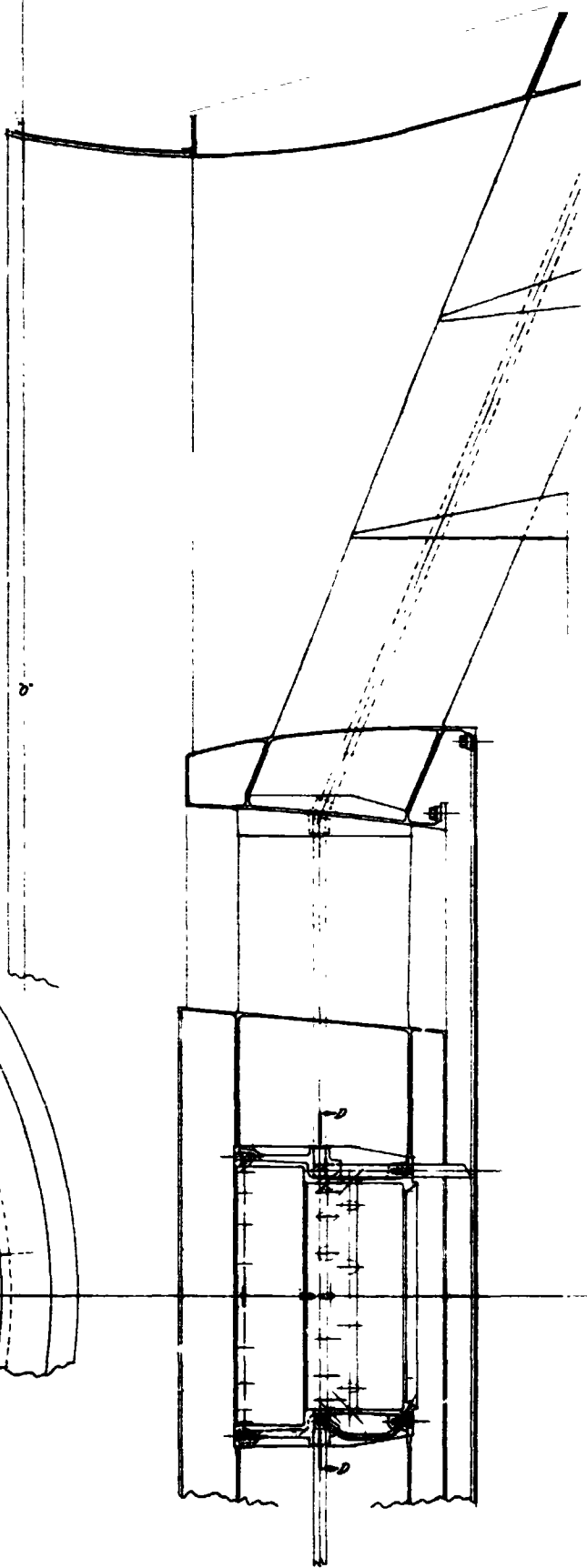


Figure 6

FOLDOUT FRAME

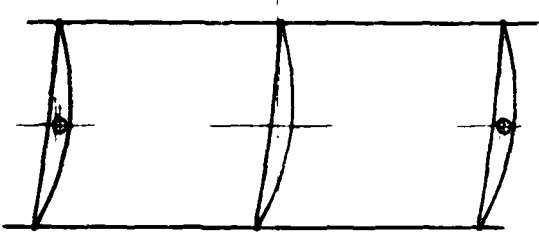
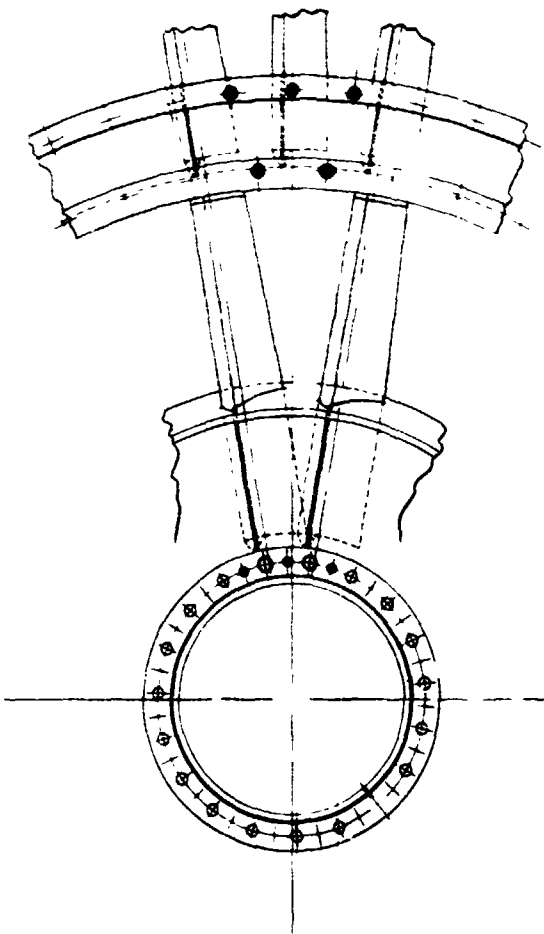
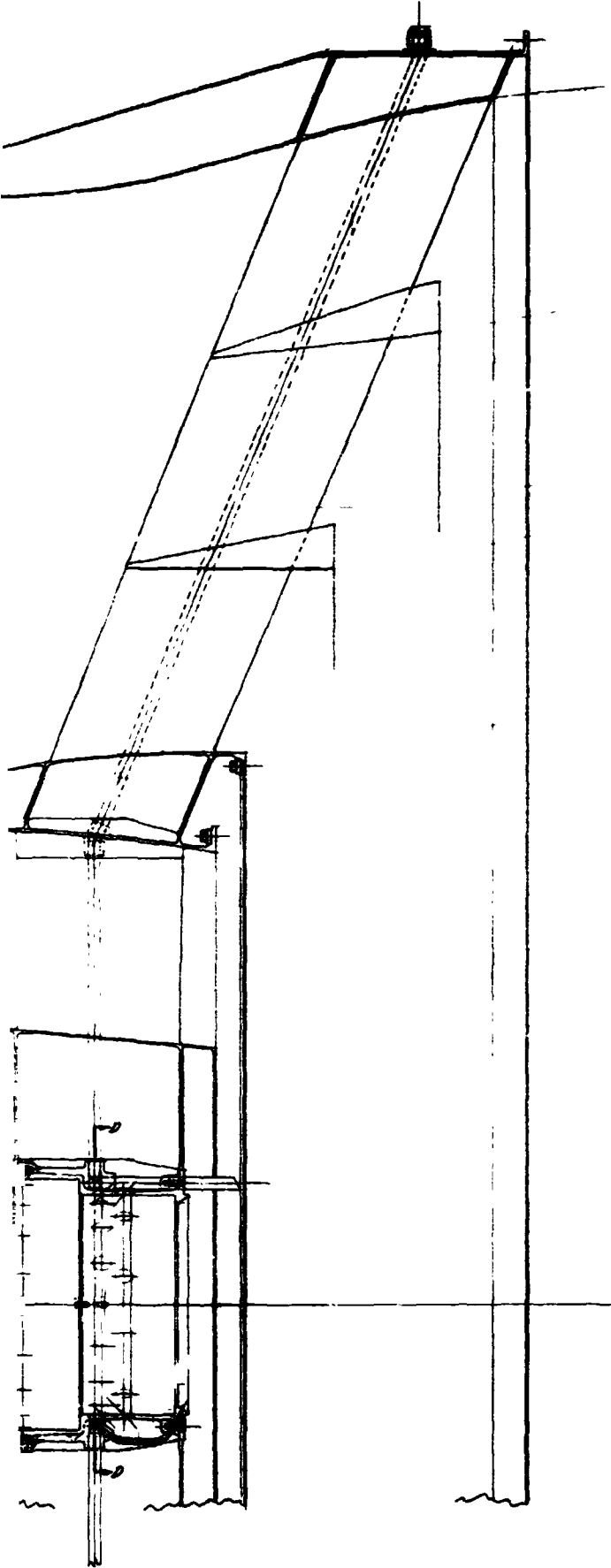


FAN STATOR HOUSING

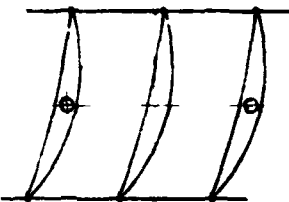


FAN STATOR HOUSING

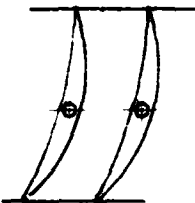
FOLDOUT FRAME 2



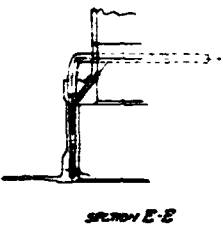
SECTION C-C



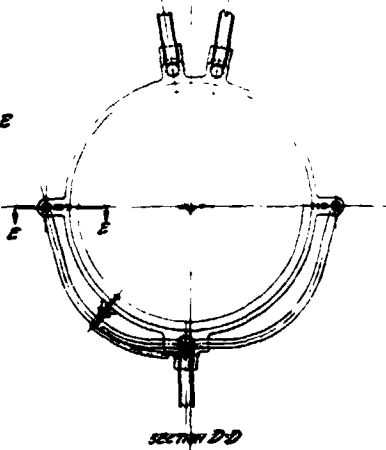
SECTION B-B



SECTION A-A



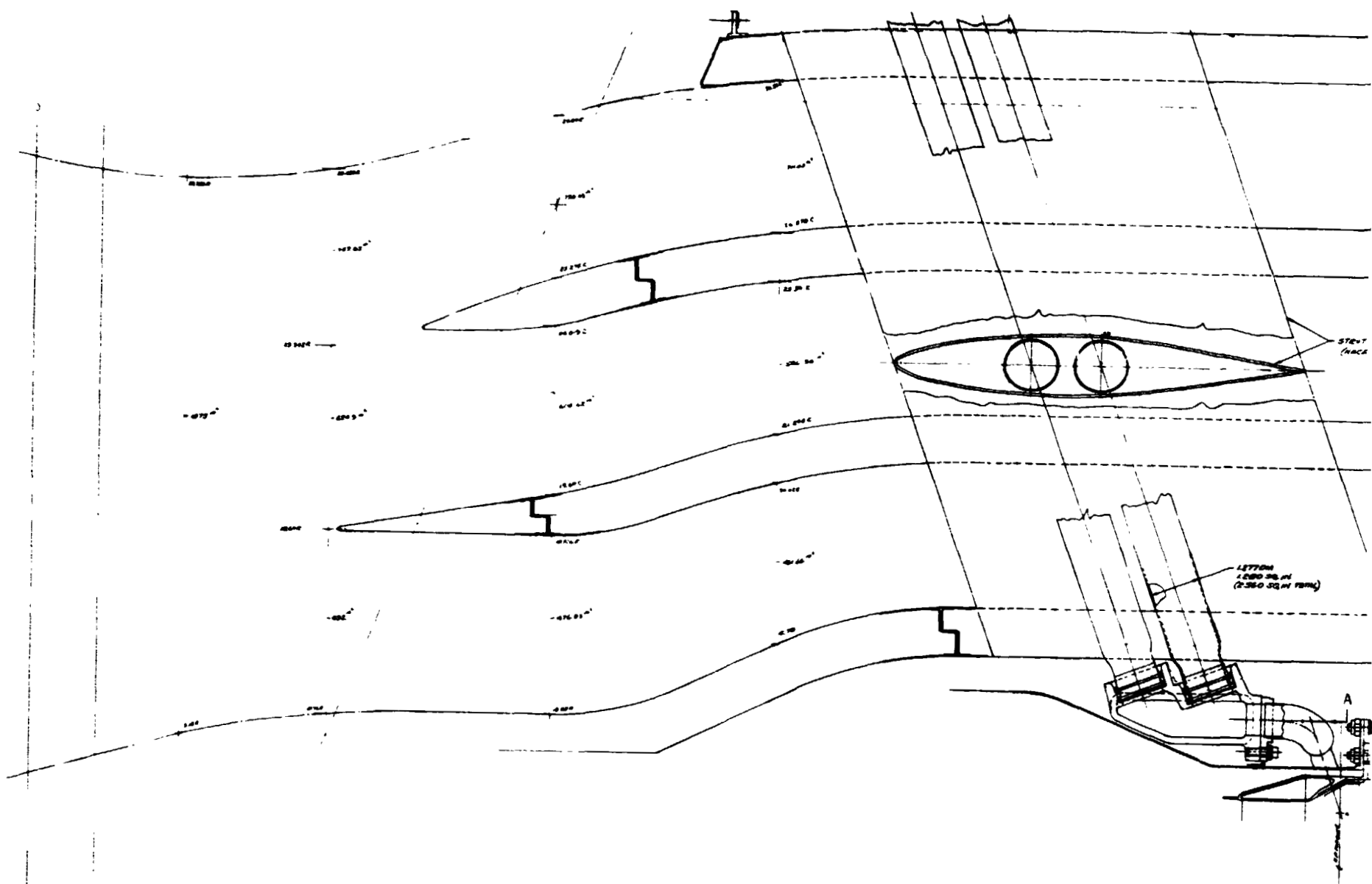
SECTION E-E



SECTION D-D

Figure 7

FOLDOUT FRAME



4 & 8 O'CLOCK STRUTS
MCA 684008

FOLDOUT FRAME 2

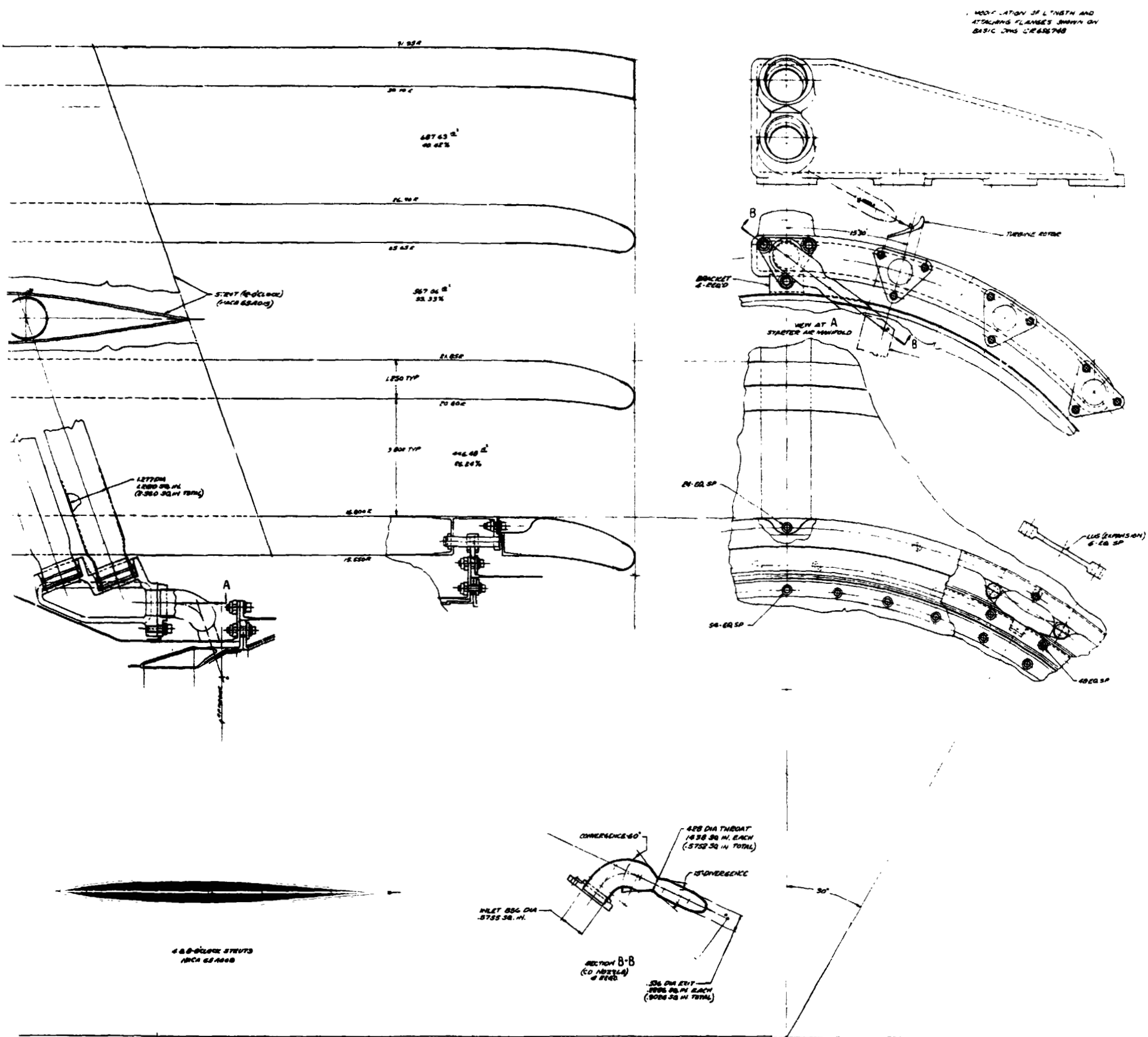
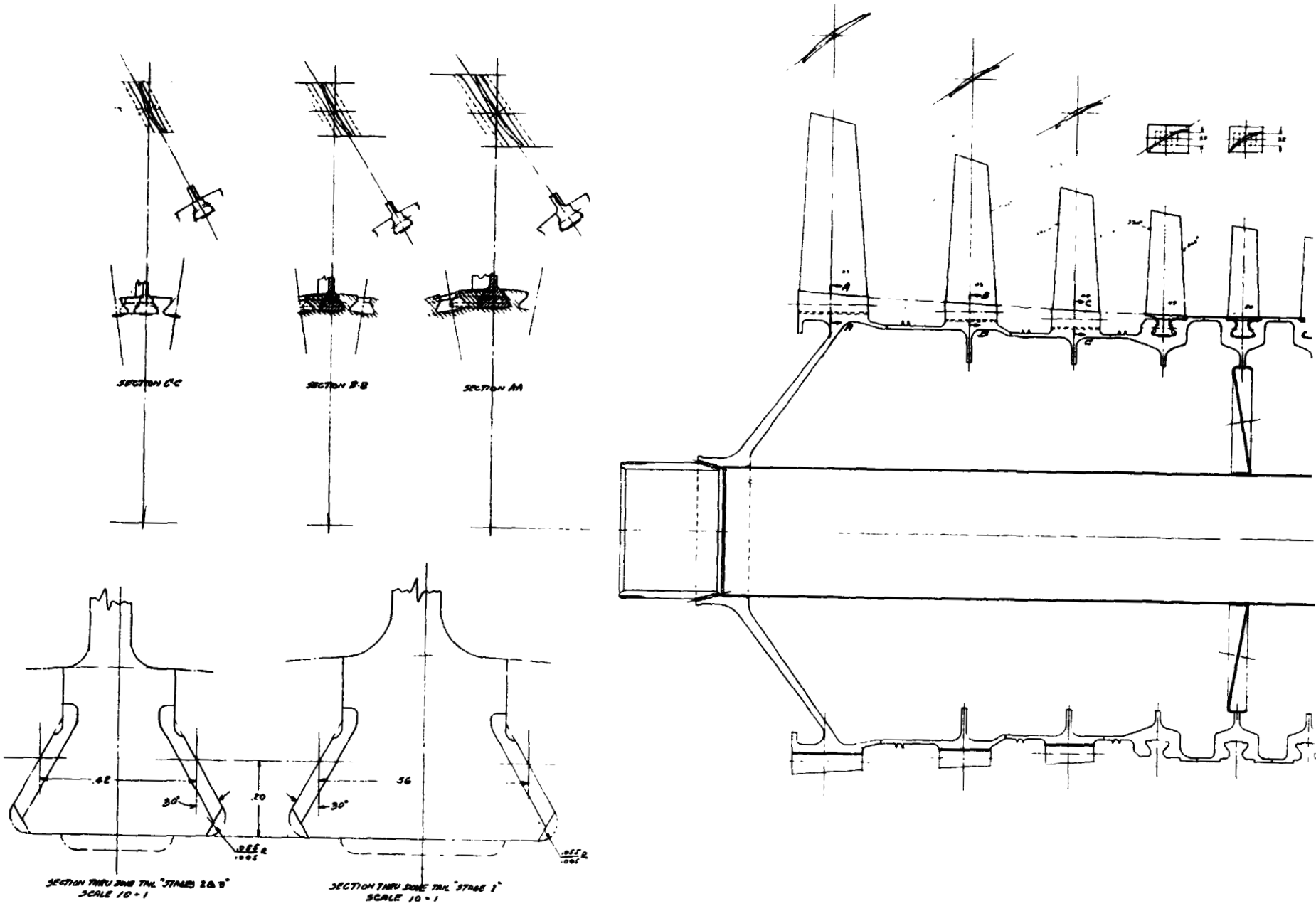


Figure 8

FOLDOUT FRAME

COMPRESSOR ROTOR



FOLDOUT FRAME 2

COMPRESSOR ROTOR

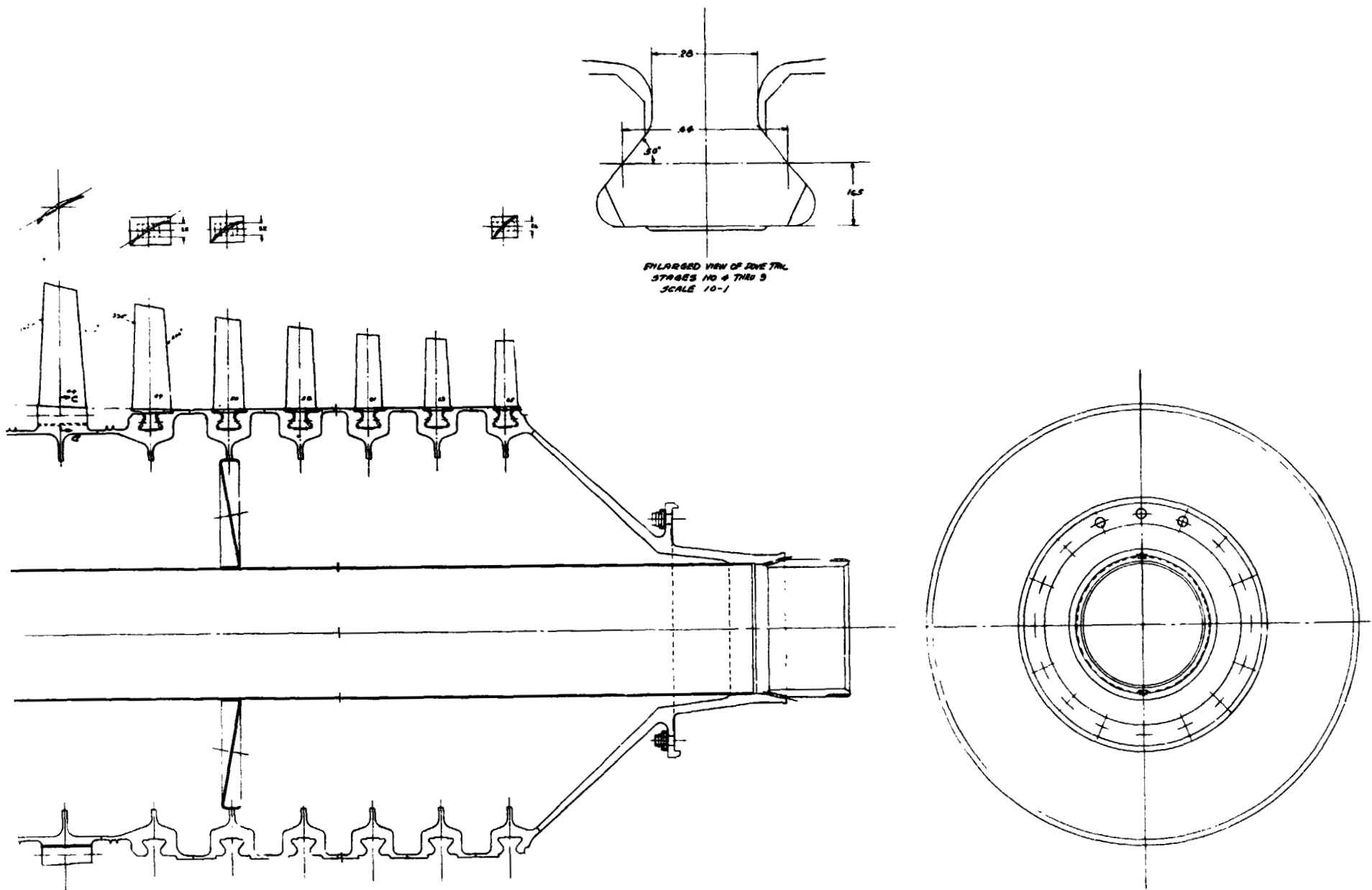
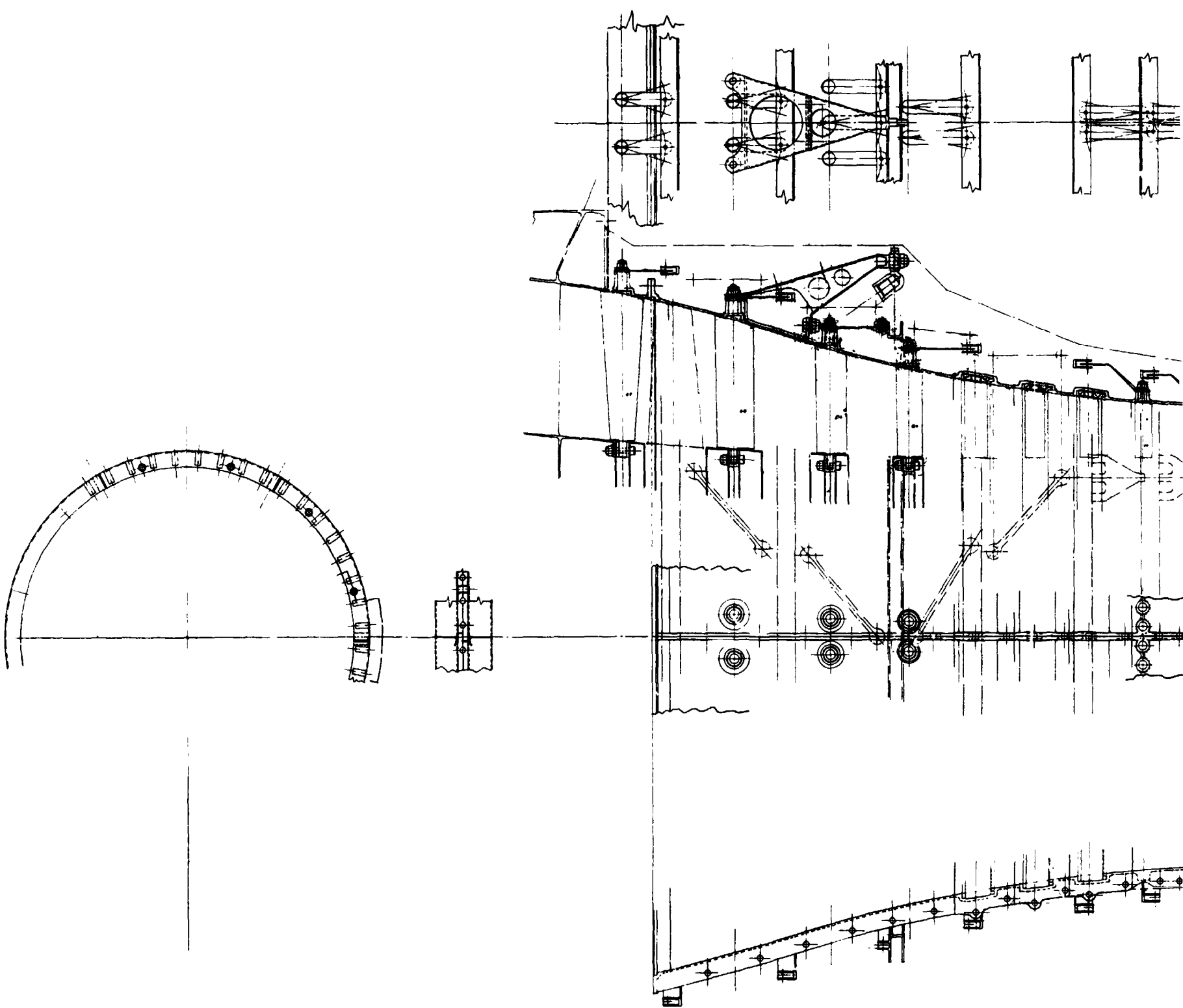


Figure 9

FOLDOUT FRAME

COMPRESSOR STATOR HOUSING



FOLDOUT FRAME 2

OMPRESSOR STATOR HOUSING

1. TO OBTAIN SATISFACTORY RESULTS
STRENGTHENING RINGS HAVE BEEN
ADOPTED AS SHOWN ON BASIC
DWS CR.56749

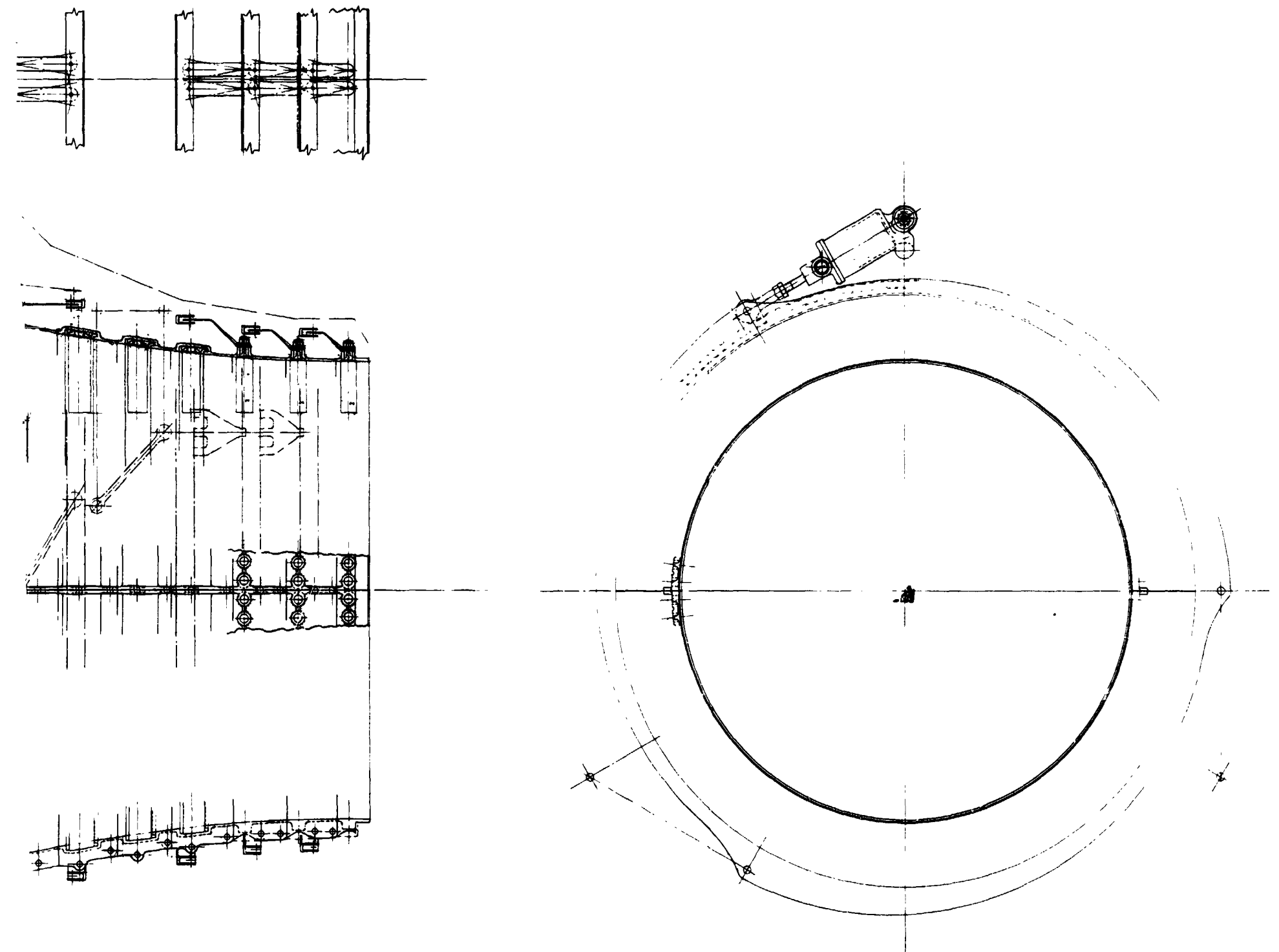
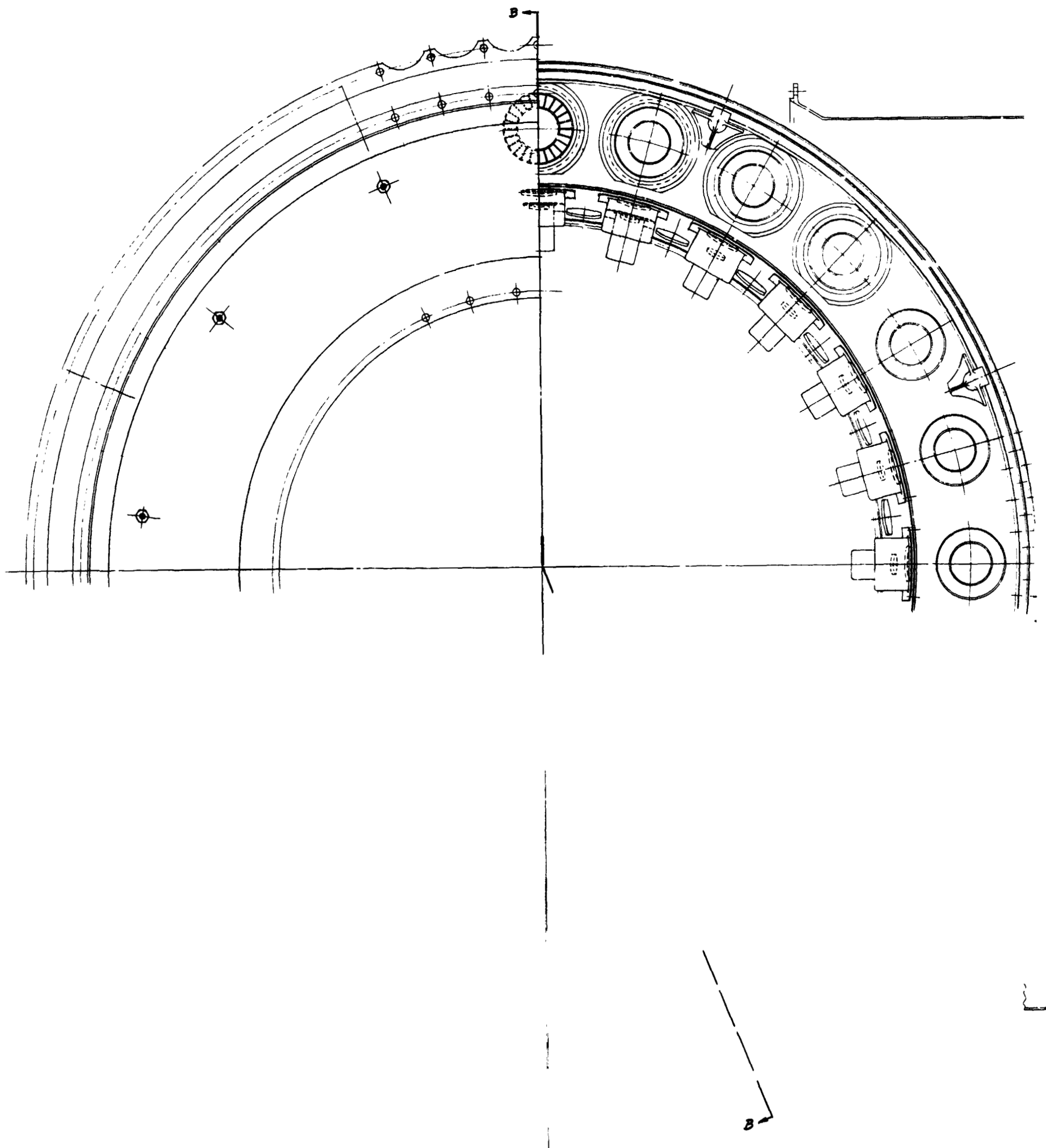


Figure 10

FOLDOUT FRAME I

COMBUSTOR



COMBUSTOR

FOLDOUT FRAME 2

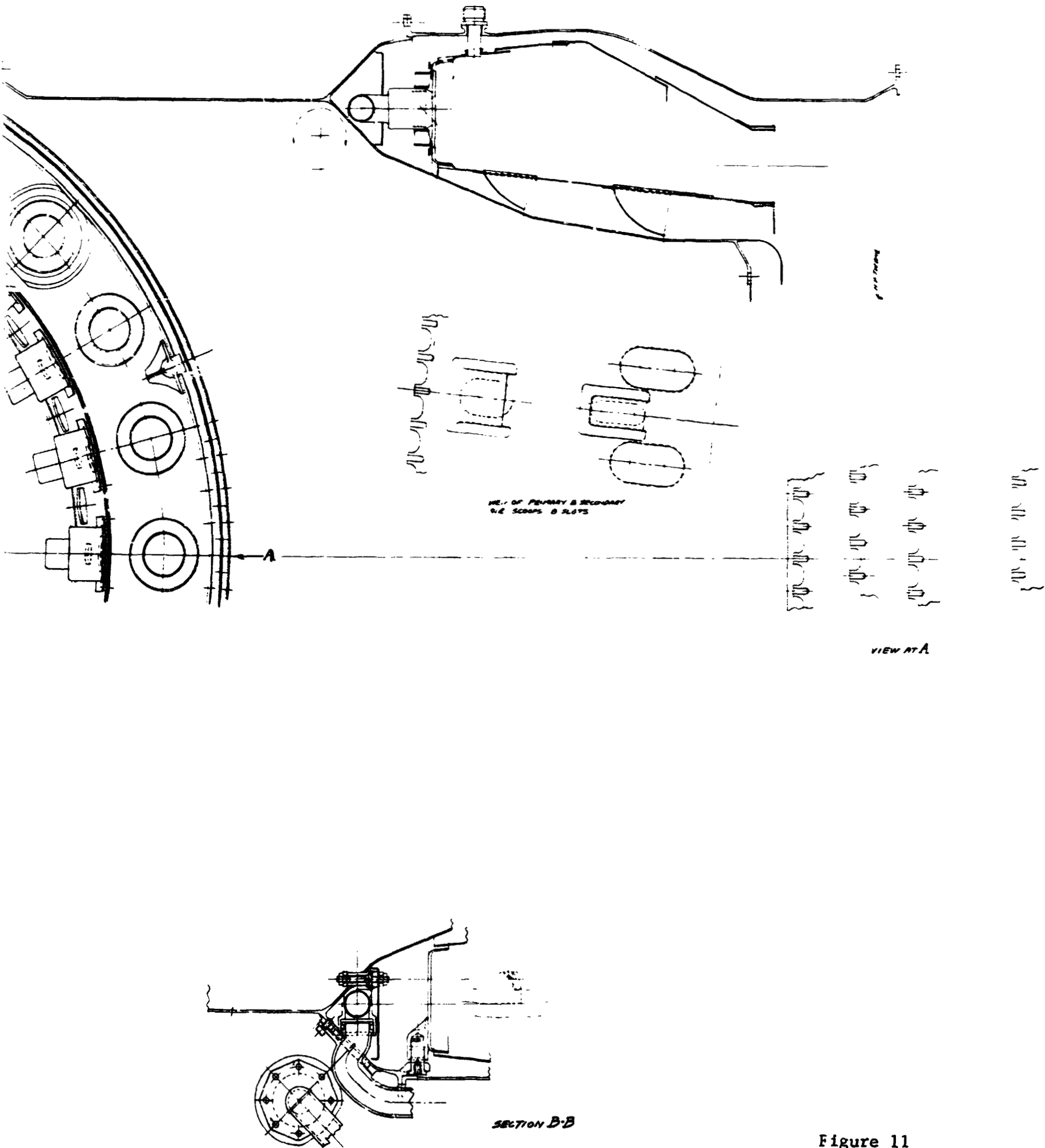
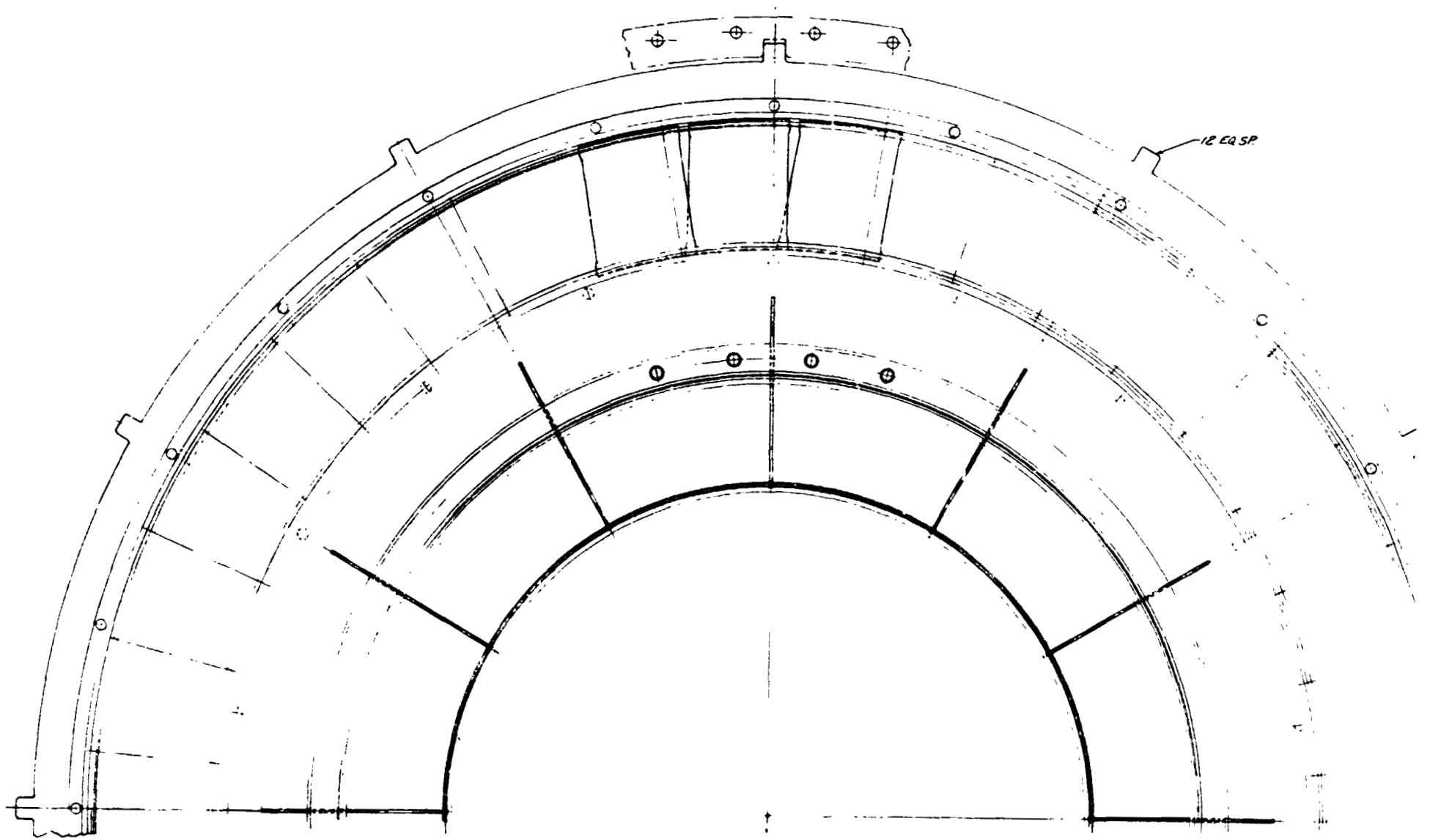


Figure 11

FOLDOUT FRAME 1

HIGH PRESSURE TURBINE



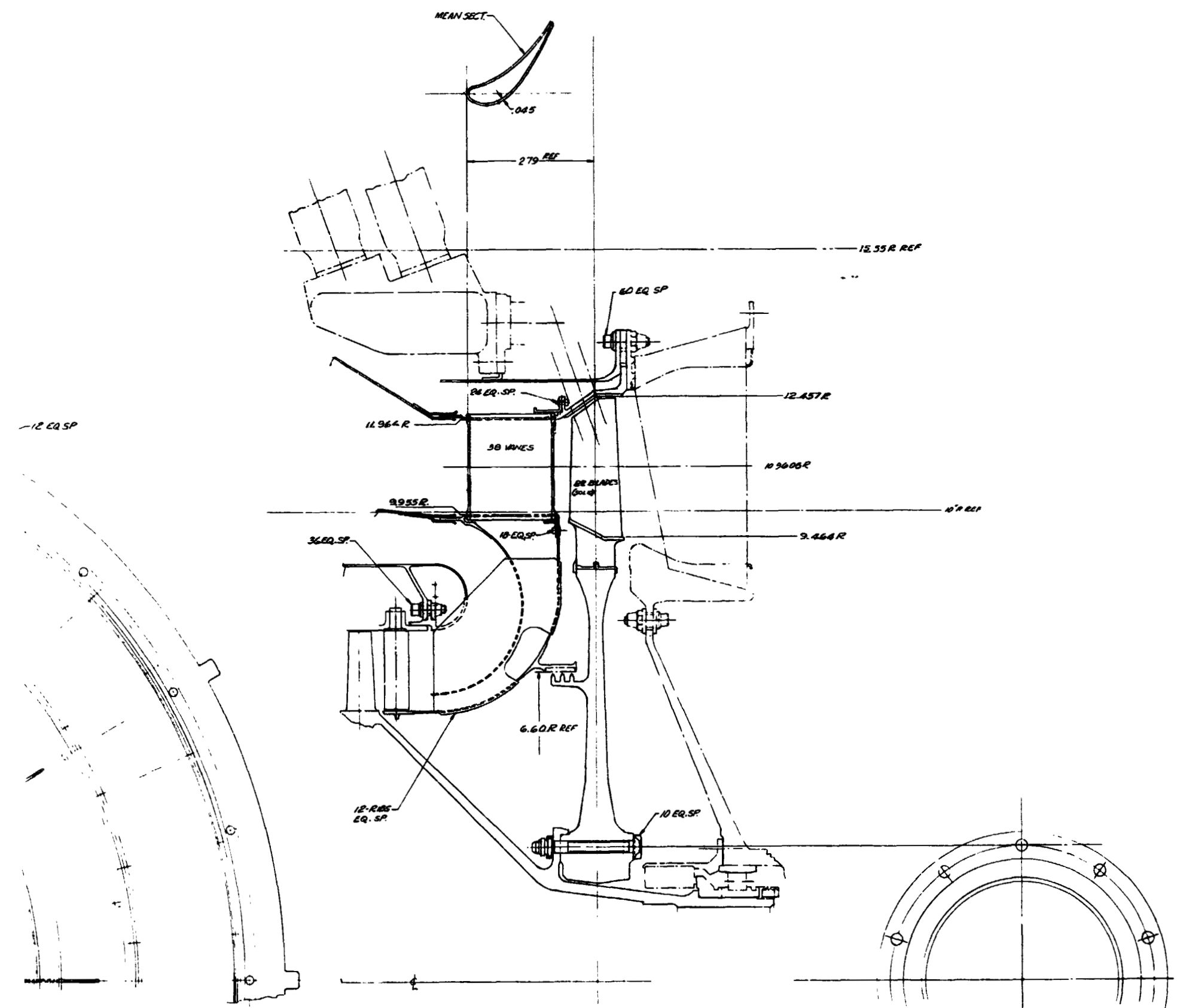


Figure 12

TO OBTAIN SATISFACTORY INFORMATION
STANDING TIME, AND THE BLACKS & AFFILIATIONS
WHICH WERE ASSIGNED AS SHOWN ON
BASIC DATA CAP 656 708



Figure 13

SINGLE ENGINE LUBKICATION SCHEMATIC

BILL OF MATERIAL		
ITEM QUANT	DESCRIPTION	
1 1	T-2, ALUM. VENT - 2" x 0.95 x 3'	
2 1	TUBE, AL. V. PRESS. - 1/2" x 0.28 x 2'	
3 3	TEE, ALUM. - AN824-3D	
4 1	TUBE, ALUM. PRESS. - 1/2" x 0.28 x 1'	
5 1	FILTER - PALL #ACQ-2466-62 PBP	
6 1	TUBE, ALUM. PRESS. - 1/2" x 0.28 x 1'	
7 1	HEAT EXCHANGER	
8 1	VALVE, PRESS. RELIEF - CIRCLE SEAL - 1/2" x 0.28 x 1'	
9 1	THERMOSTAT	
10 1	VENTED FILLER - TEDECO #F-973	
11 1	TANK, LUBE - 3 QT.	
12 1	SCREEN - PALL #AC 4022E-67A	
13 1	MOTOR, ELECT.	
14 1	PUMP, LUBE - 3 ELEMENT	
15 2	TUBE, ALUM. RETURN - 1/2" x 0.35 x 3'	

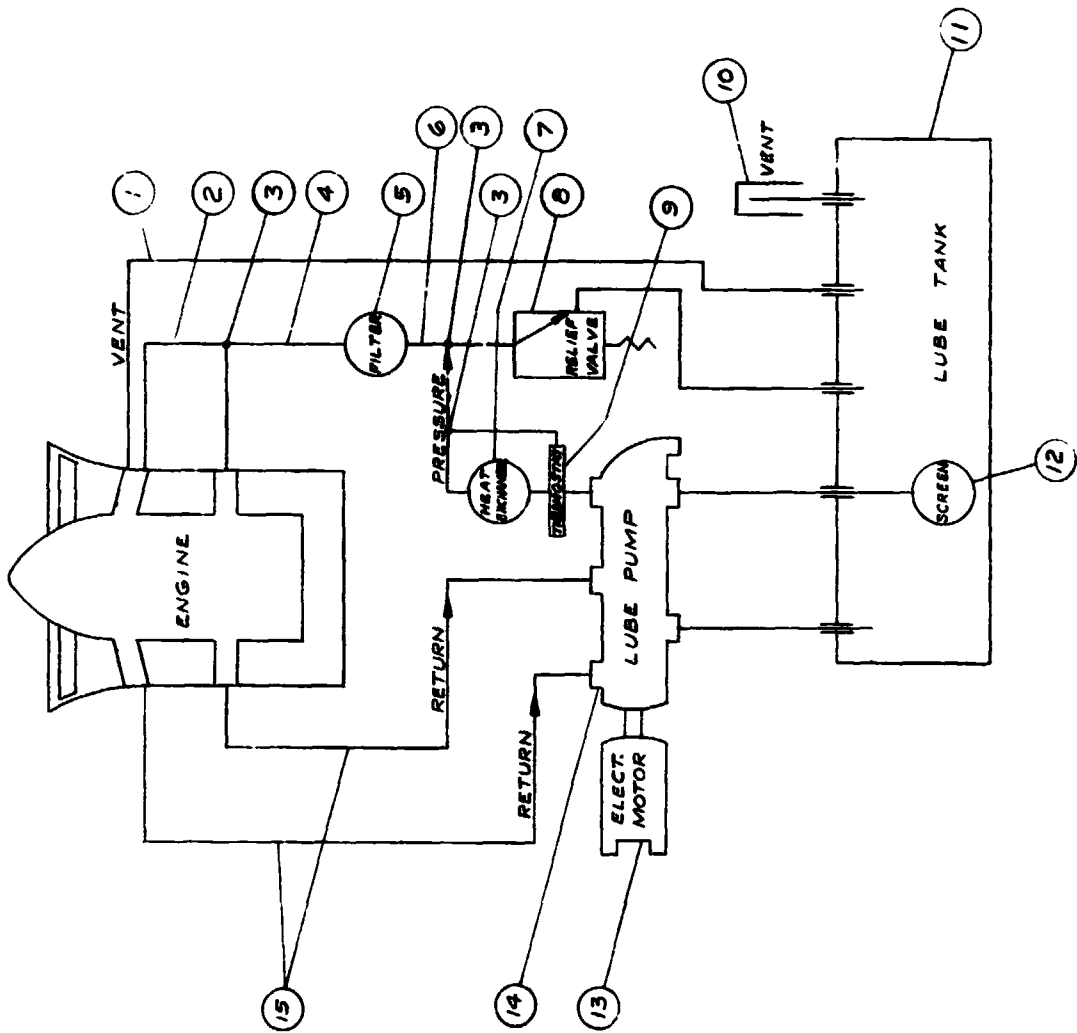
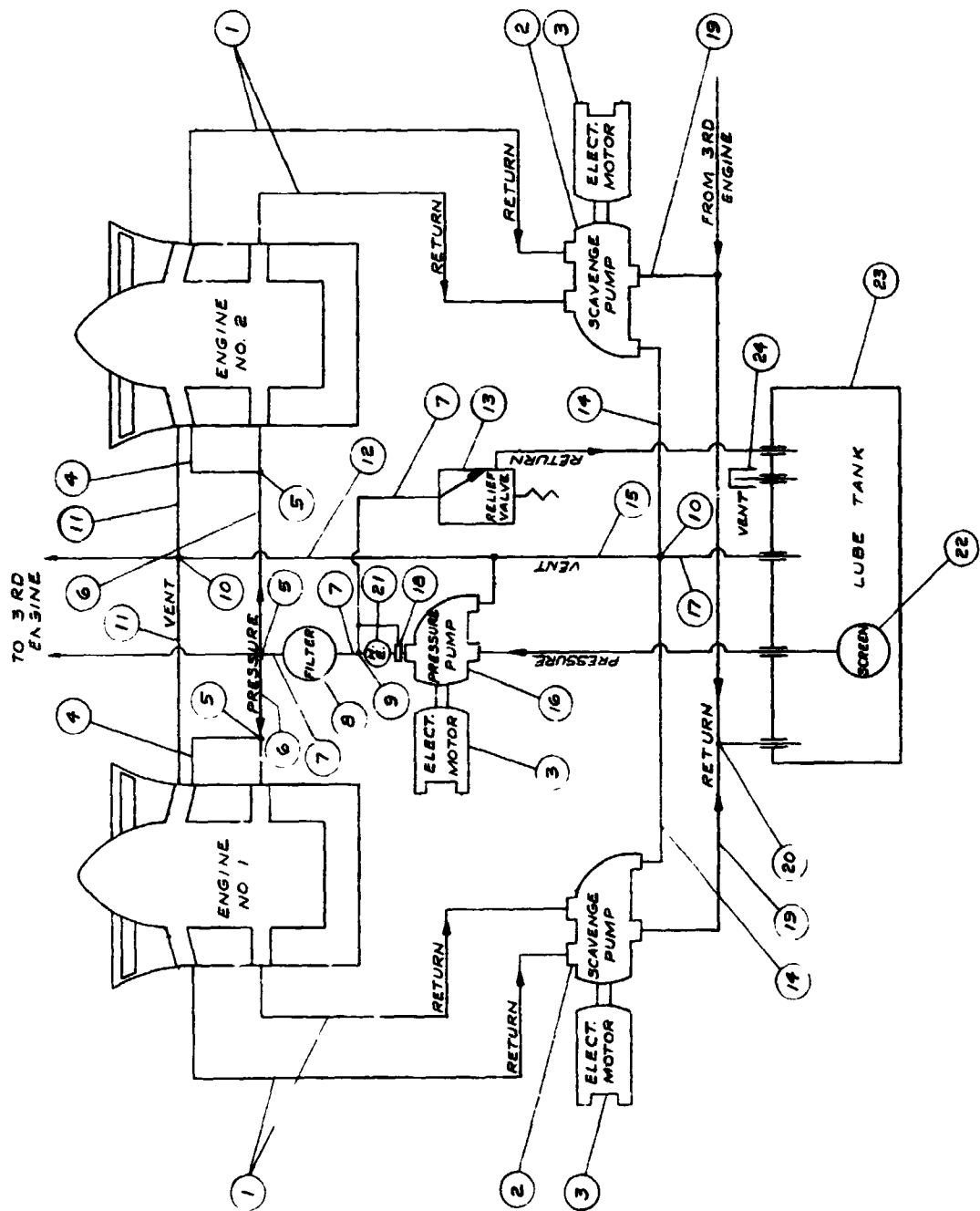


Figure 14

THREE ENGINE LUBRICATION SCHEMATIC



BILL OF MATERIAL	
ITEM NO.	DESCRIPTION
1	6 TUBE, ALUM. RETURN - $\frac{1}{8}$ x .035 x 3'
2	3 SCAVENGE PUMP - 2 ELEMENT
3	4 ELECT. MOTOR
4	3 TUBE, ALUM. PRESS - $\frac{1}{8}$ x .028 x 2'
5	6 TEE, ALUM. - ANB24-3D
6	3 TUBE, ALUM. - $\frac{1}{8}$ x .028 x 1'
7	3 TUBE, ALUM. - $\frac{1}{8}$ x .028 x 1'
8	1 FILTER - PALL PACQ-2466-62 PBP
9	1 TEE, ALUM. - ANB24-6D
10	6 TEE, ALUM. - ANB24-12D
11	3 TUBE, ALUM. - $\frac{1}{8}$ x .035 x 1'
12	1 VALVE, PRESS. RELIEF - CIRCLE SEAL 1/2" NPT
13	3 TUBE, ALUM. - $\frac{1}{8}$ x .028 x 2'
14	1 PUMP, PRESS. - 1 ELEMENT
15	1 TUBE, ALUM. - $\frac{1}{8}$ x .035 x 1'
16	1 TUBE, ALUM. - $\frac{1}{8}$ x .035 x 5'
17	1 THERMOSTAT
18	3 TEE, ALUM. - ANB24-16D
19	1 HEAT EXCHANGER
20	1 SCREEN - PALL #AC-2466E-74
21	1 TANK, LUBE - 10 QT
22	1 VENTED FILLER - TEDCO #F-910
23	
24	

Figure 15

FUEL CONTROL BLOCK DIAGRAM

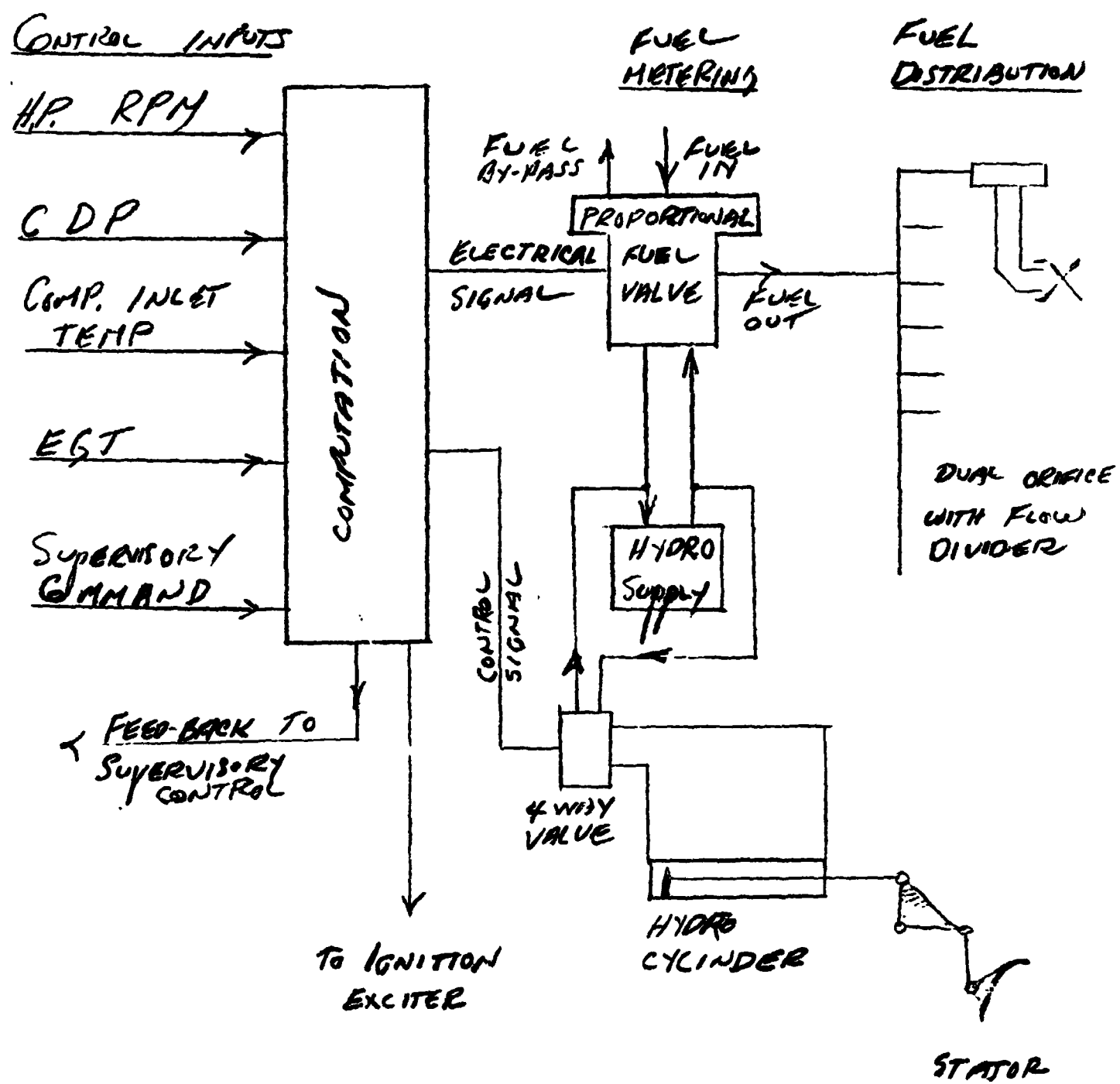
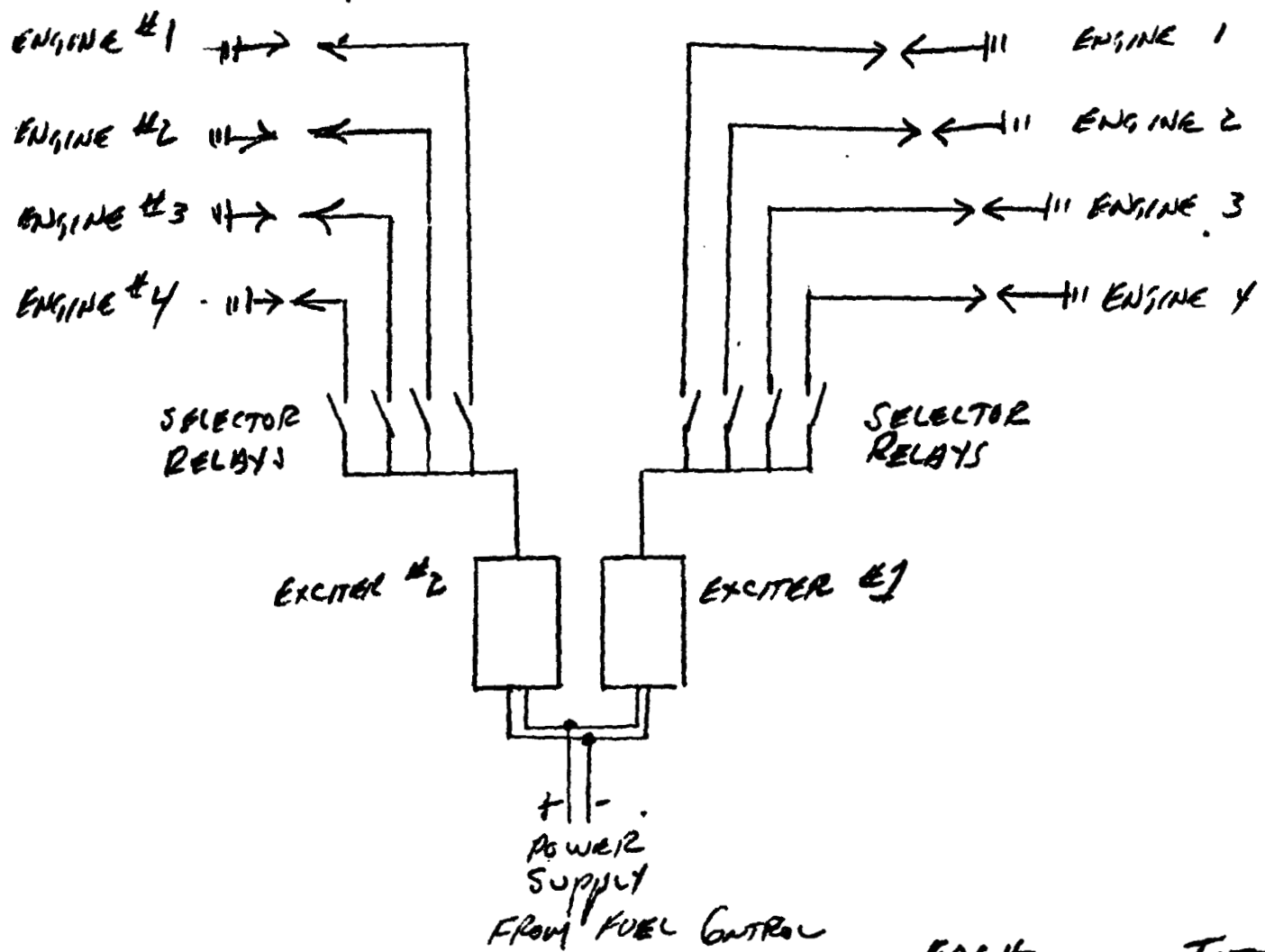


Figure 16

IGNITION SYSTEM DIAGRAM



	<u>EACH</u>	<u>TOTAL</u>
EXCITER WEIGHT - EACH UNIT INCLUDES SELECTOR RELAYS.	2 LBS	4
IGNITOR WT. (2 PER ENGINE)	.25 LBS	.5
LEAD WT. (2 PER ENGINE)	1.2 LBS	2.4
∴ FOR A FOUR ENGINE POD - IGNITION WT. PER ENGINE IS	<u>3.9 LBS</u>	

Figure 17

FAN ROTOR BLADE CENTRIFUGAL STRESSES

<u>Radius In.</u>	<u>Area In²</u>	<u>Centrifugal Force Lbs.</u>	<u>Centrifugal Stress Lbs./Sq. In.</u>
27.9	1.24	0	0
26.8	1.2112	1010.66	834.43
25.3	1.1689	2285.25	1955.05
23.8	1.1293	3445.12	3050.67
22.3	1.0901	4496.78	4125.11
20.8	1.0597	5449.16	5142.18
19.3	1.011	6302.66	6234.08
17.8	.9682	7057.41	7289.2
16.3	.9246	7720.84	8350.46
14.8	.8779	8297.04	9451.01
13.3	.8206	8787.62	10708.8
12.42	.79	9037.42	11439.8
12	.772	9147.2	11848.7
11.25	.7408	9327.96	12591.7
10.4	.7032	9510.05	13524.
9.55	.6713	9669.77	14404.5
8.7	.6313	9808.24	15536.6
7.85	.591	9926.06	16795.4
7.2	.55	10002.5	18186.5

Total Static Weight	1.17358 Lbs.
Radial C.G.	20.5342 In.
Axial C.G.	0 In.
Tangential C.G.	0 In.
RPM	4000
Material Density	.0603

Figure 18

FAN ROTOR BLADE LEAN TO CANCEL GAS BENDING MOMENTS

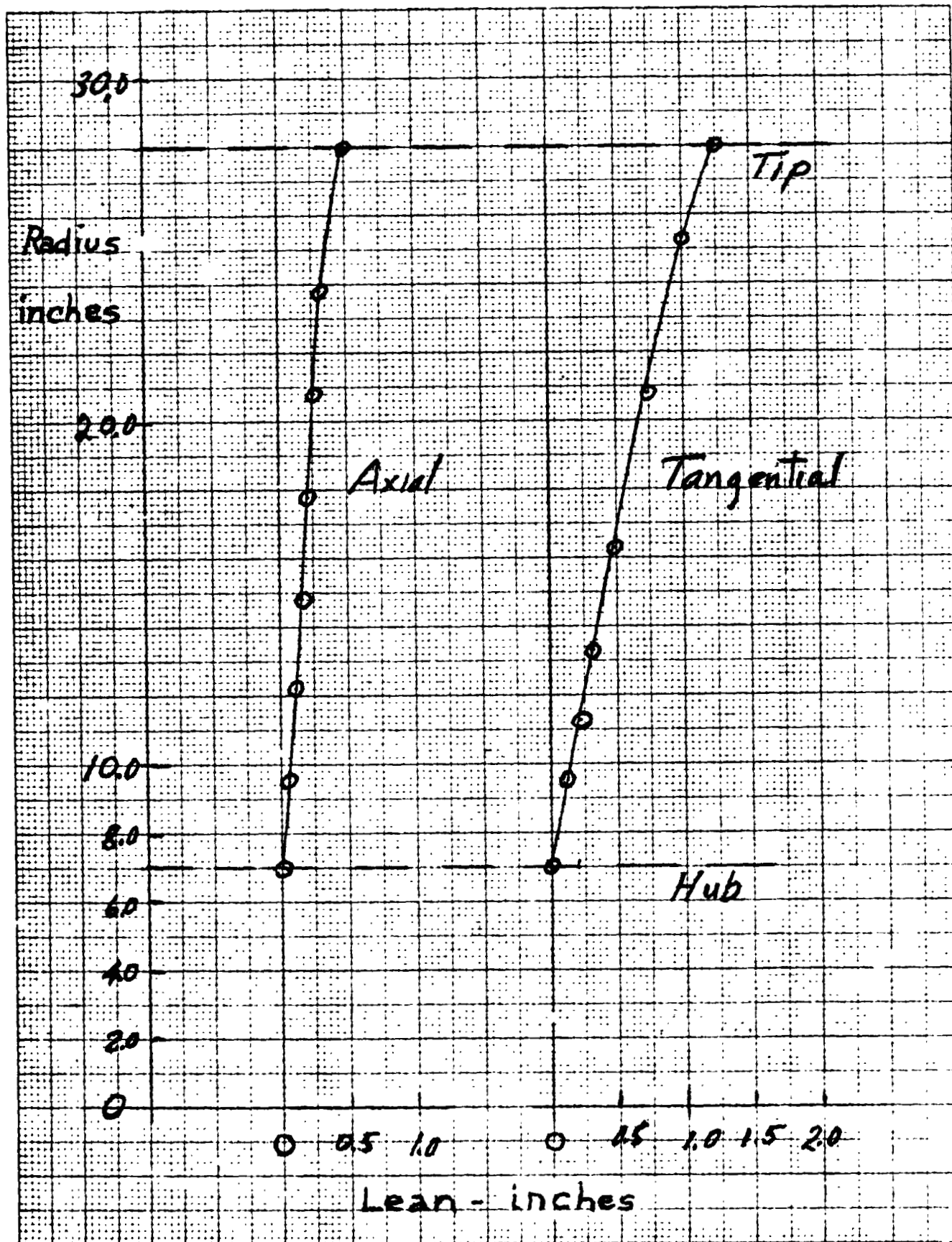


Figure 19

FAN ROTOR BLADE FATIGUE STRENGTH

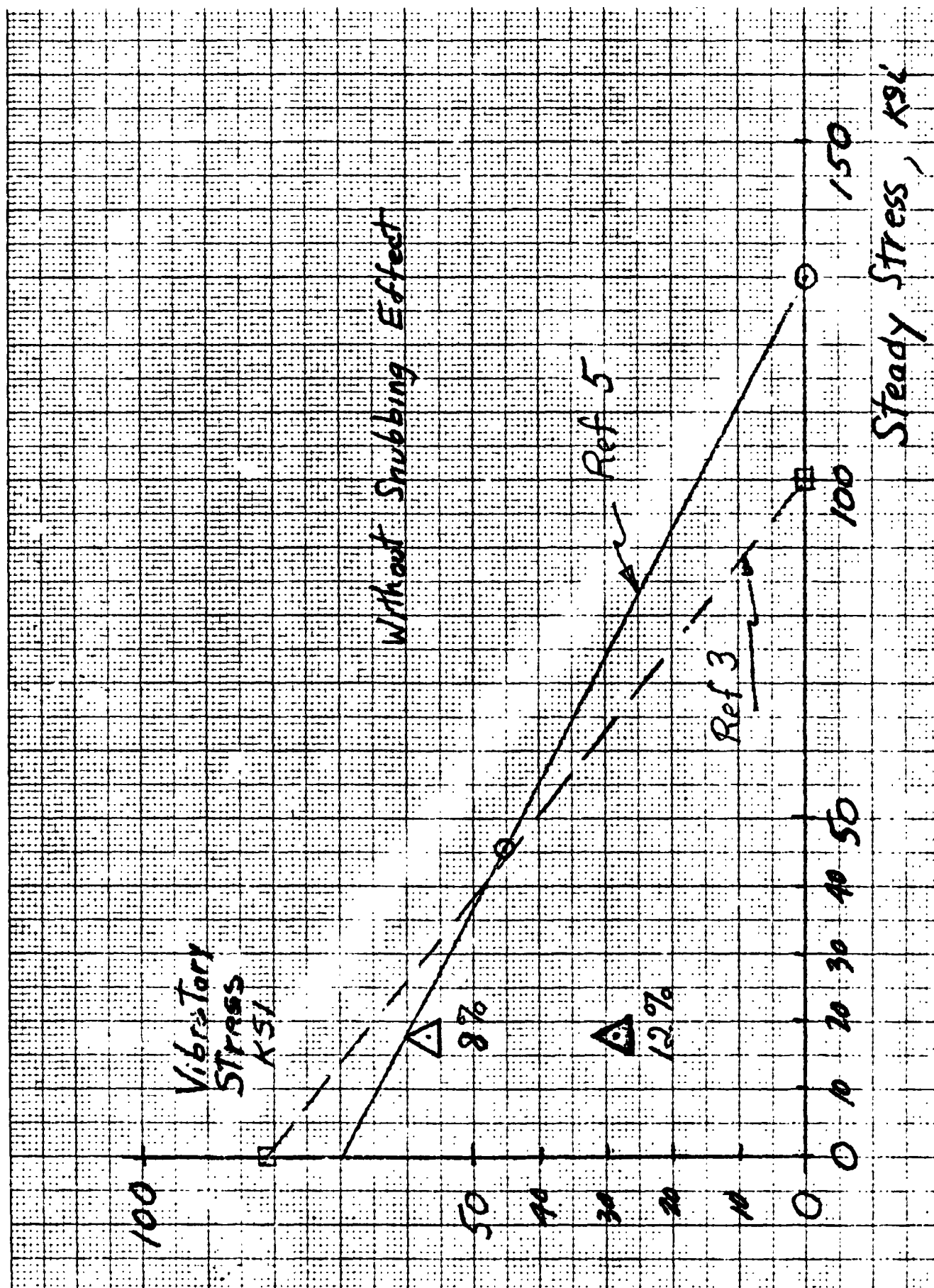


Figure 20

FAN ROTOR BLADE VIBRATORY STRENGTH

[illegible]

Figure 21

FAN ROTOR BLADE INTERFERENCE DIAGRAM - BY-PASS PORTION

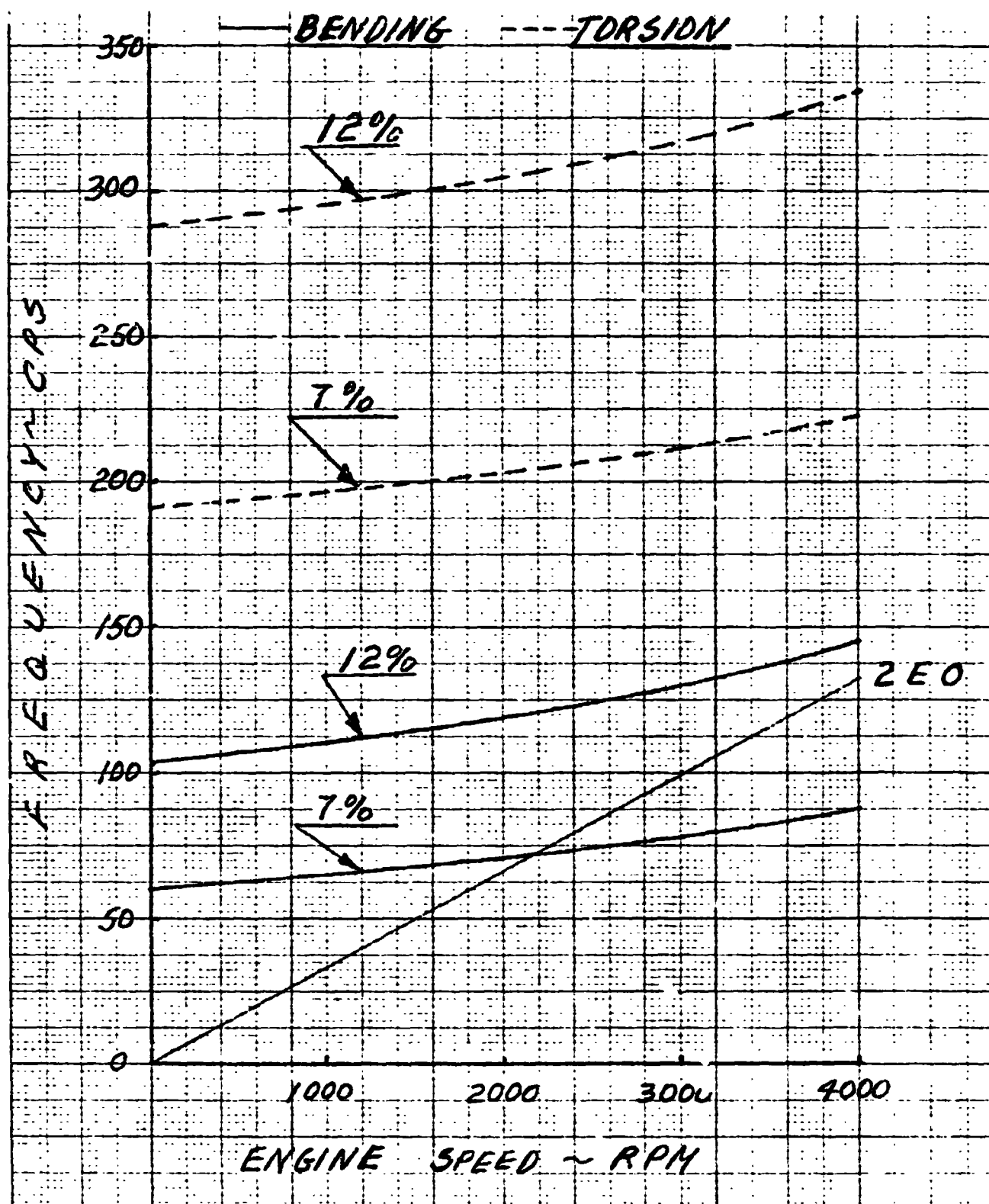


Figure 22

FAN ROTOR BLADE INTERFERENCE DIAGRAM - CORE PORTION

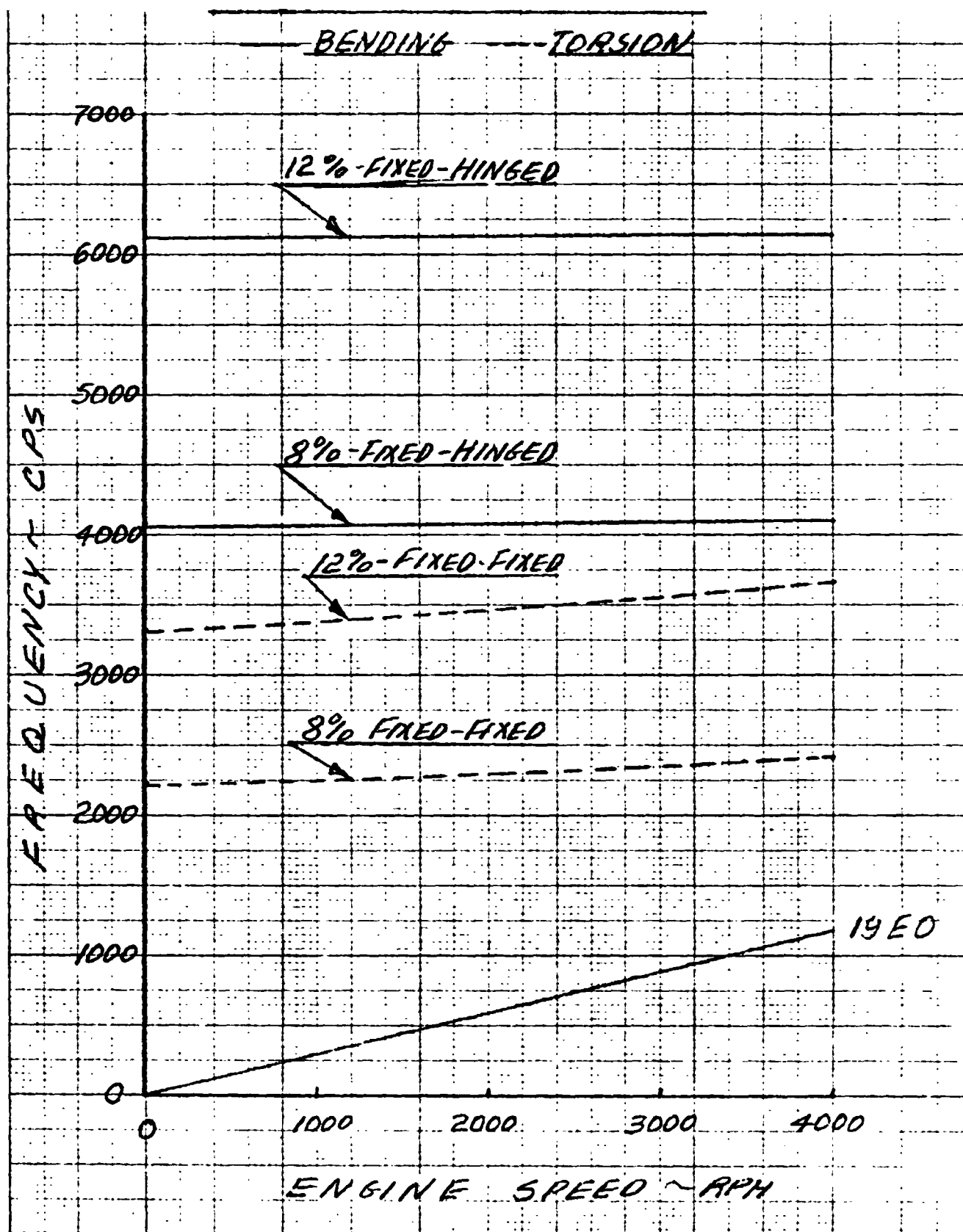


Figure 23

FAN AND COMPRESSOR ROTOR BLADE BENDING FLUTTER PARAMETER

STAGE	Z t/c	RELATIVE VELOCITY = V ft/sec	CHORD/2 = b ft.	NATURAL FREQUENCY CPS	$\frac{V}{bw}$
Fan Core	8	653*	.160	4100	.160
Fan Core	12	653	.160	6150	.100
Fan Bypass	7	1060*	.249	87	8.26
Fan Bypass	12	1060	.249	145	5.00
1st Rotor	7	1382 ⁺	.100	585	3.76
5th Rotor	7	1186 ⁺	.042	765	5.87
5th Rotor	11	1186	.042	1200	3.74
9th Rotor	7	1057 ⁺	.033	900	5.66
9th Rotor	11	1057	.033	1260	4.04

* Based on 4000 RPM

+ Based on 14,700 RPM

Figure 24

FAN AND COMPRESSOR ROTOR BLADE TORSIONAL FLUTTER PARAMETER

STAGE	% t/c	RELATIVE VELOCITY = V ft/sec	$\frac{\text{CHORD} = b}{2}$ ft.	NATURAL FREQUENCY CPS	$\frac{V}{bw}$
Fan Core	8	653*	.160	2400	0.270
Fan Core	12	653	.160	3650	0.18
Fan Bypass	8	1060*	.249	220	3.12
Fan Bypass	12	1060	.249	335	2.00
1st Rotor	7	1382 ⁺	.100	1105	1.99
5th Rotor	7	1186 ⁺	.042	1400	3.20
5th Rotor	11	1186	.042	2220	1.99
9th Rotor	7	1057 ⁺	.033	2040	2.49
9th Rotor	11	1057	.033	3200	1.59

* Based on 4000 RPM

+ Based on 14,700 RPM

Figure 25

• ROTOR BLADE ROOT THICKNESS-TO-CHORD REQUIREMENTS

	Fan	Fan	Comp.	Comp.	Comp.	Comp.	Comp.	Comp.
	Rotor	Rotor	Rotor	Rotor	Rotor	Stator	Stator	Stator
STAGE		1	1	5	9	1	5	9
	Bypass	Core						
<u>SPECIFIED</u>	7	8	7	7	7	7	7	7
<u>REQUIRED</u>								
Vib. Str.	7	8	7	10	12	7	12	12
							11*	15*
Frequency	12	8	7	7	7	7	7	7
Flutter	12	8	7	11	11	—	—	—
Combined	12	12	7	11	12	7	12	12
							11*	15*
	All Ratios expressed as per cent							
	of chord length							
	* Chord Increase Ratio							

Figure 26

COMPRESSOR ROTOR BLADE VIBRATORY STRENGTH

	Thick/ Chord		Steady Stress	Gas Bend Stress	End. Limit	Ult. Tens. Strength	Allow. Stress	Vib. Margin
First Stage								
Airfoil	7%		11,300	18000	70,000	130,000	64000	3.6
Dovetail			12600	5900	70,000	130,000	63000	10.7
Tenon			30,400	17800	61,000	150,000	48,500	2.7
Second Stage								
Airfoil	10%		13000	22000	53000	126000	46000	2.1
Dovetail			24800	19500	53000	126000	42000	2.2
Drum			7800	22100	53000	126000	41000	2.2
Ninth Stage								
Airfoil	12%		10000	20400	48000	117000	44000	2.2
Dovetail			14700	16500	48000	117000	42000	2.5
Drum			6800	17800	48000	117000	45000	2.5

Figure 27

• FIRST STAGE COMPRESSOR ROTOR BLADE INTERFERENCE DIAGRAM

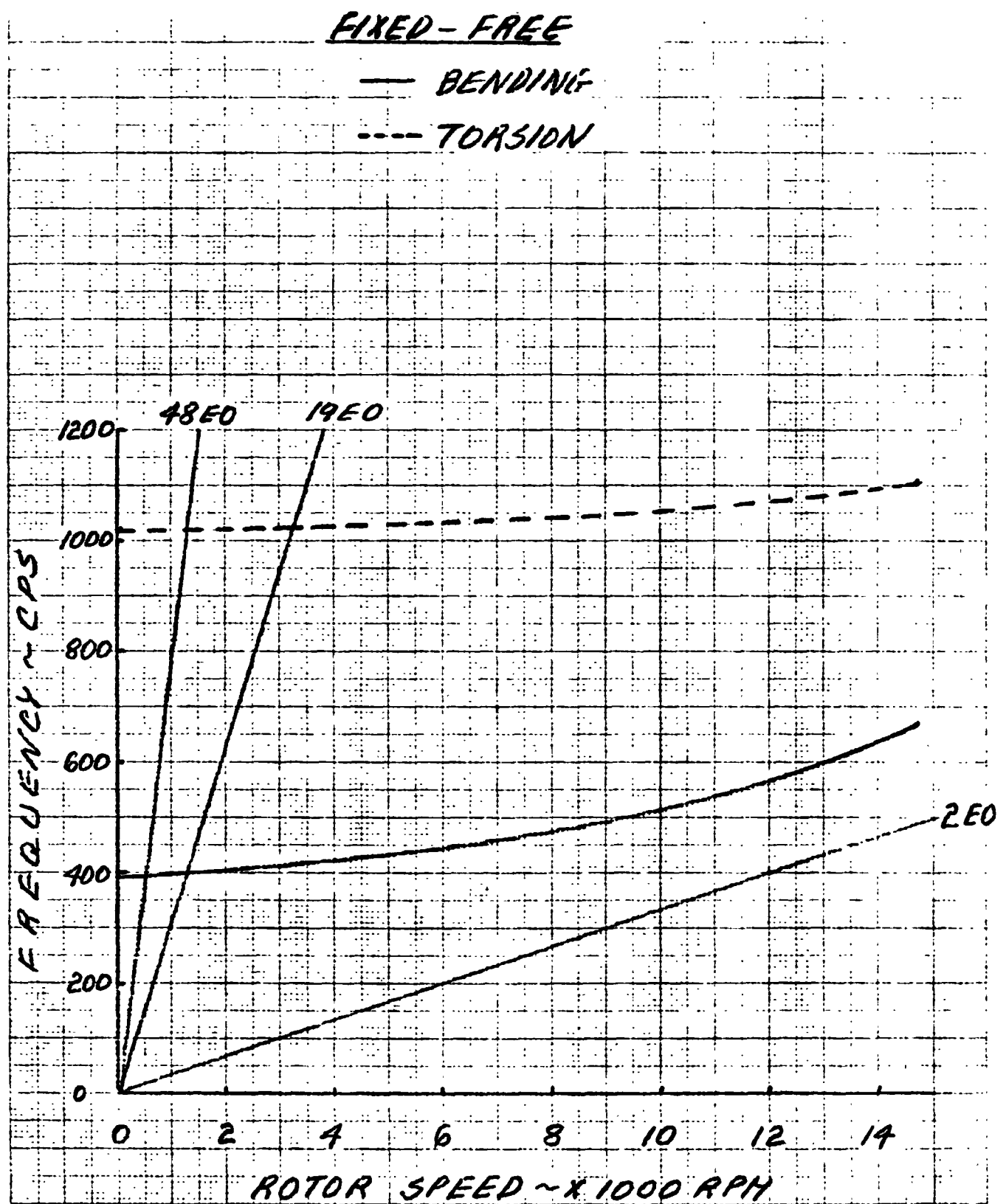


Figure 28

FIFTH STAGE COMPRESSOR ROTOR BLADE INTERFERENCE DIAGRAM

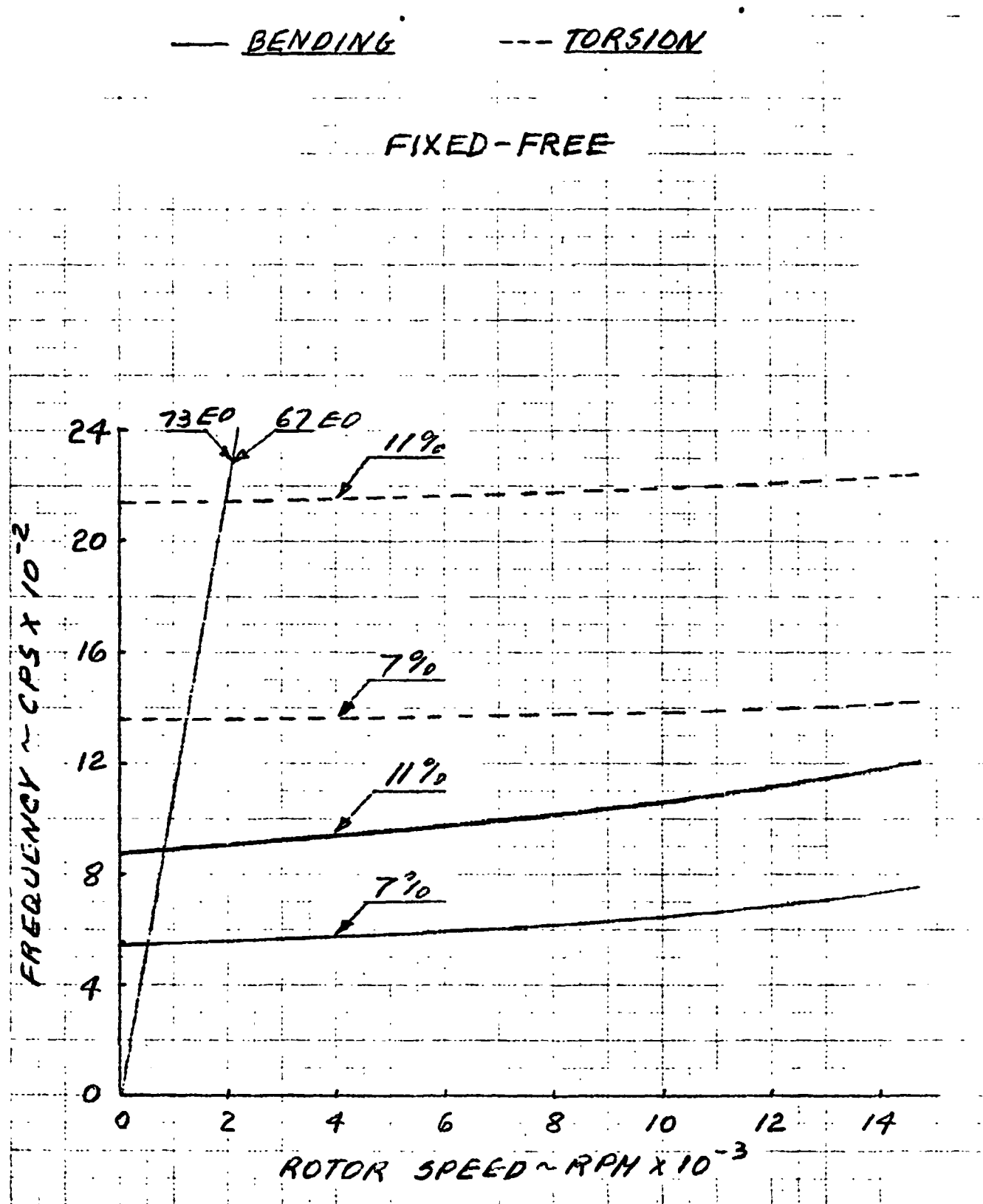


Figure 29

NINTH STAGE COMPRESSOR ROTOR BLADE INTERFERENCE DIAGRAM

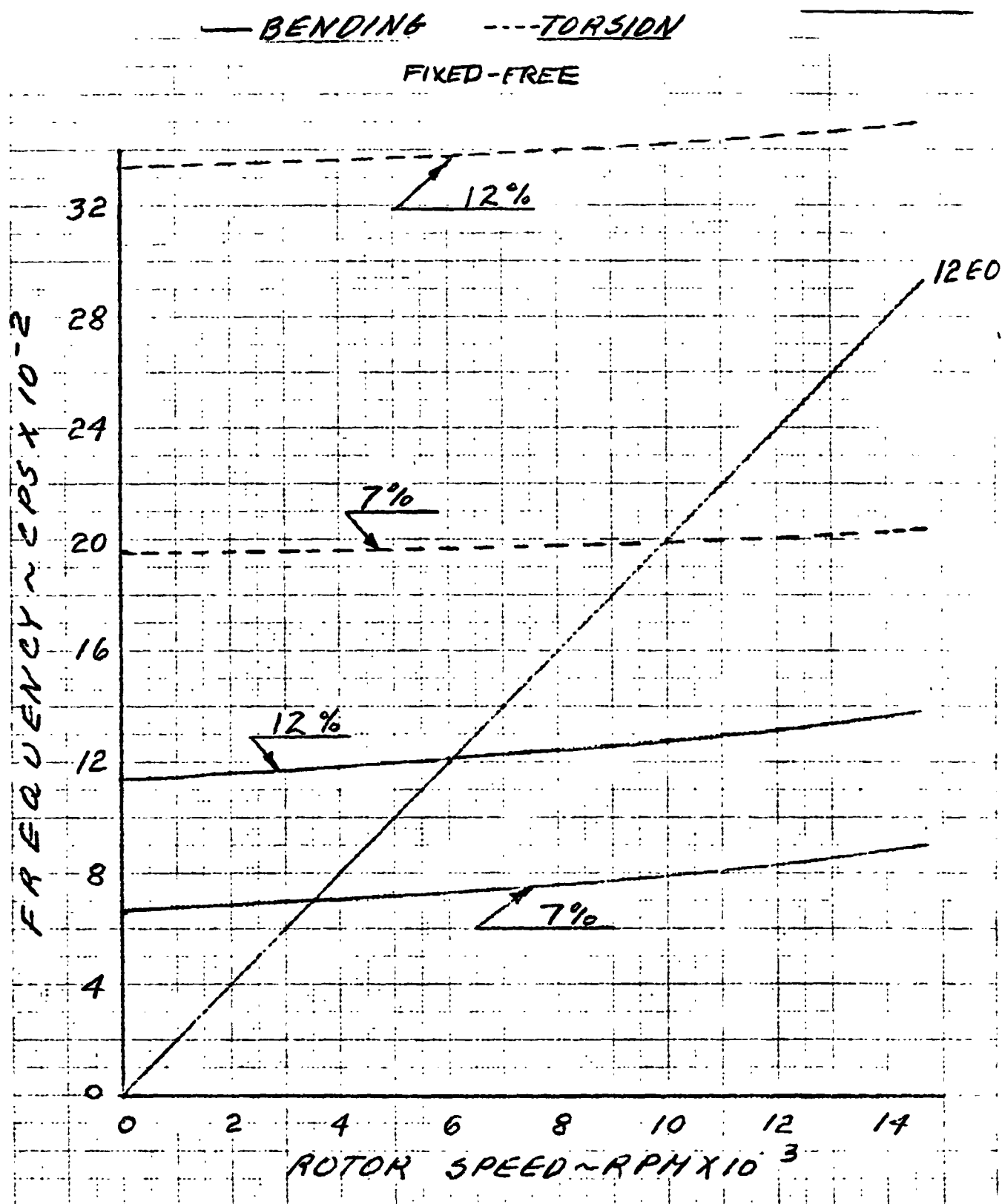


Figure 30

COMPRESSOR STATOR VANE VIBRATORY STRENGTH

	Thick Chord	New Chord	Steady Stress	Gas. Bend Stress	End. Limit	Ult. Tens. Strength	Allow. Stress	Vib. Margin
<u>First Stage</u>								
Airfoil	7%	1.00	30,000	9,100	52000	160000	41000	4.5
Button			43,100	12,600	52000	160000	37000	2.9
Shank			9,700	4,500	52000	160000	48000	10.7
<u>Fifth Stage</u>								
Airfoil	12%	1.11	21,000	21,000	52000	126000	43000	2.0
<u>Ninth Stage</u>								
Airfoil	12%	1.15	19500	19,500	48000	116000	40000	2.1
Button			19500	19,500	48000	116000	40000	2.1
Shank			6200	6200	48000	116000	46000	7.4

Figure 31

COMPRESSOR STATOR VANE BENDING INTERFERENCE DIAGRAM

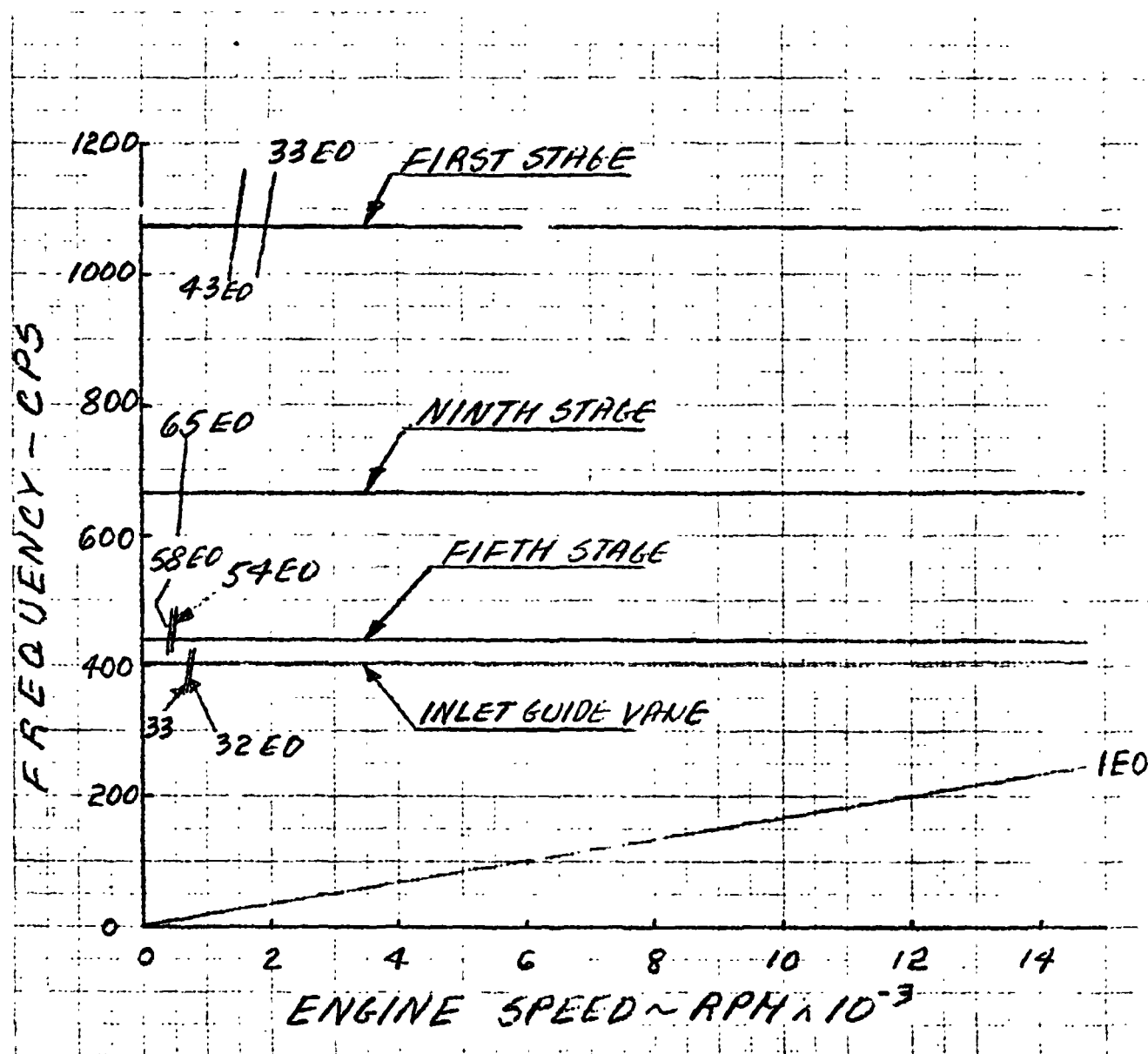


Figure 32

COMPRESSOR STATOR VANE TORSIONAL INTERFERENCE DIAGRAM

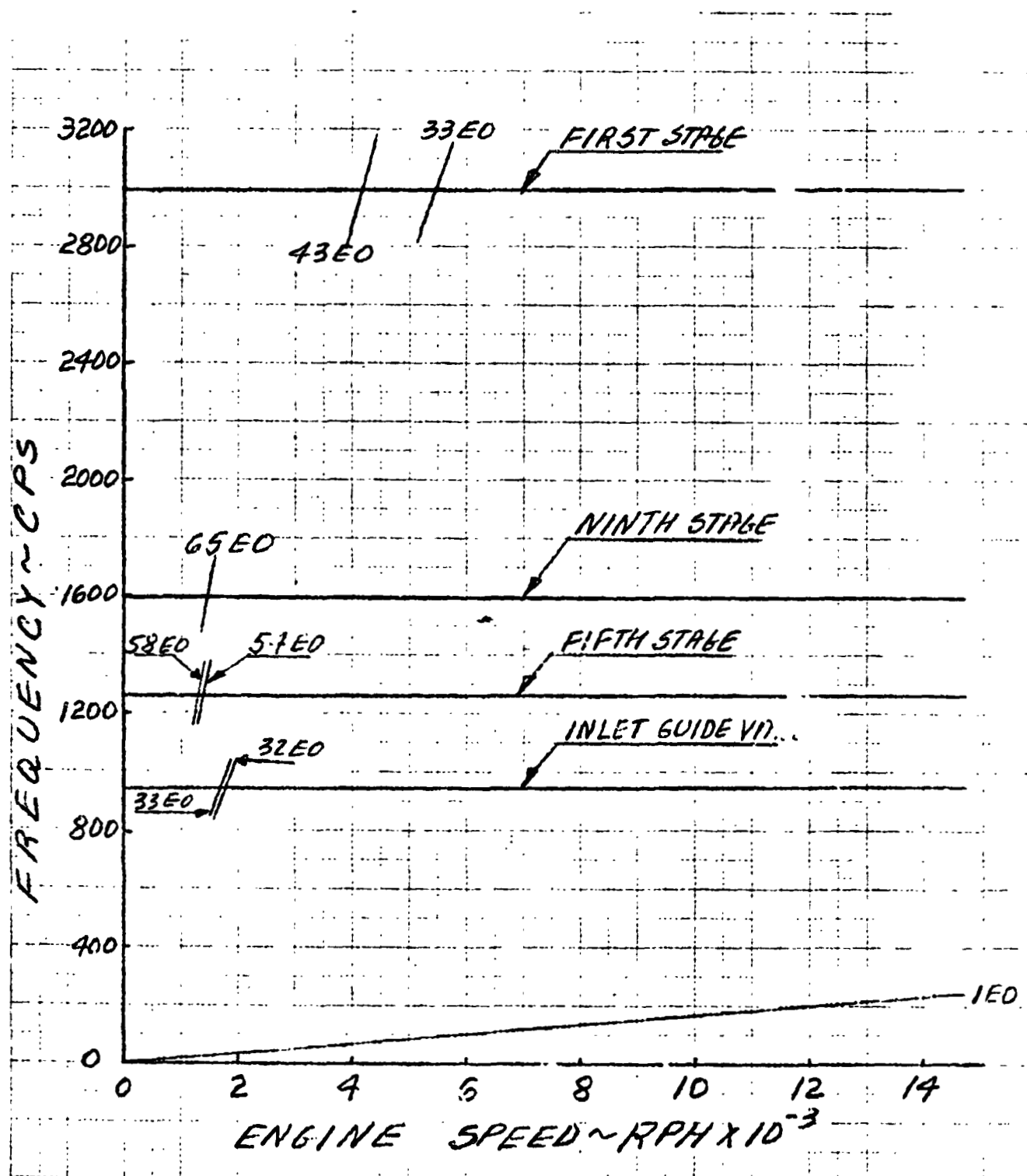


Figure 33

HIGH PRESSURE TURBINE ROTOR BLADE STRESSES

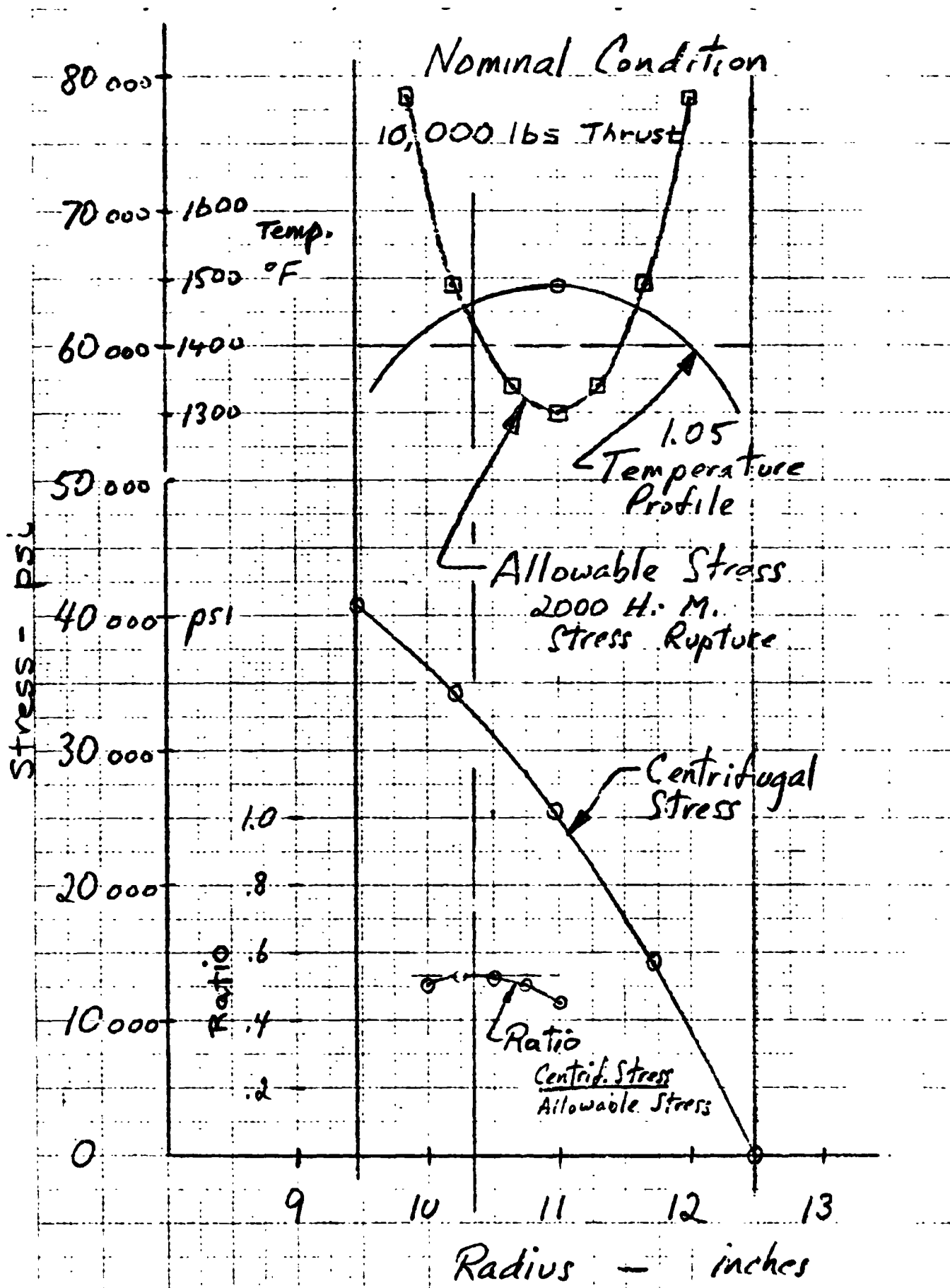
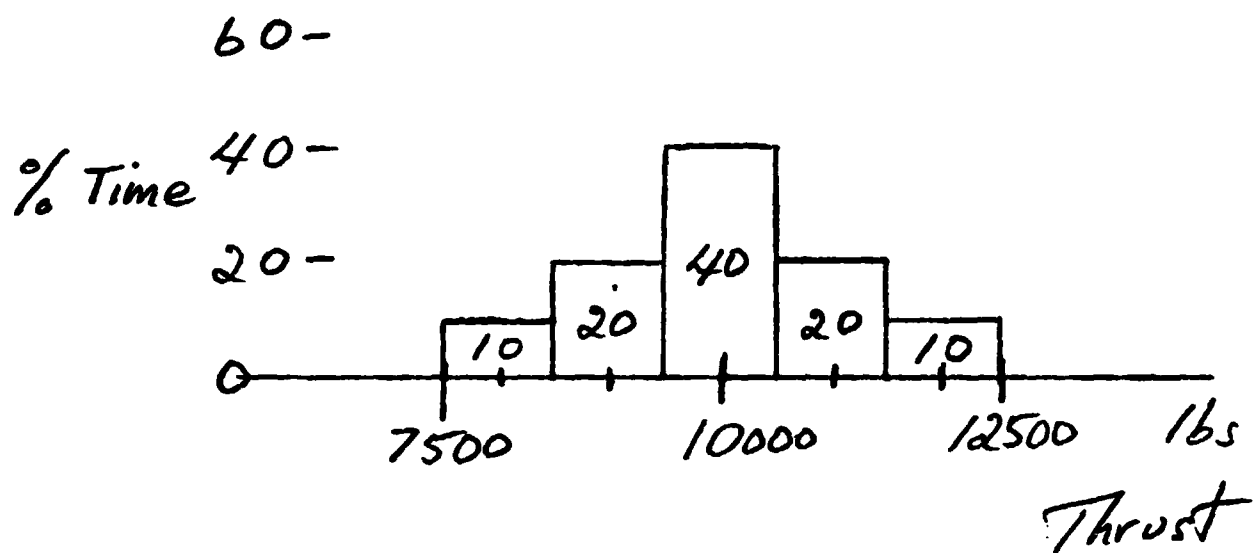


Figure 34

ENGINE DUTY CYCLE

Duty Cycle

Normal Operation (90% of time)



Emergency (10% of time)

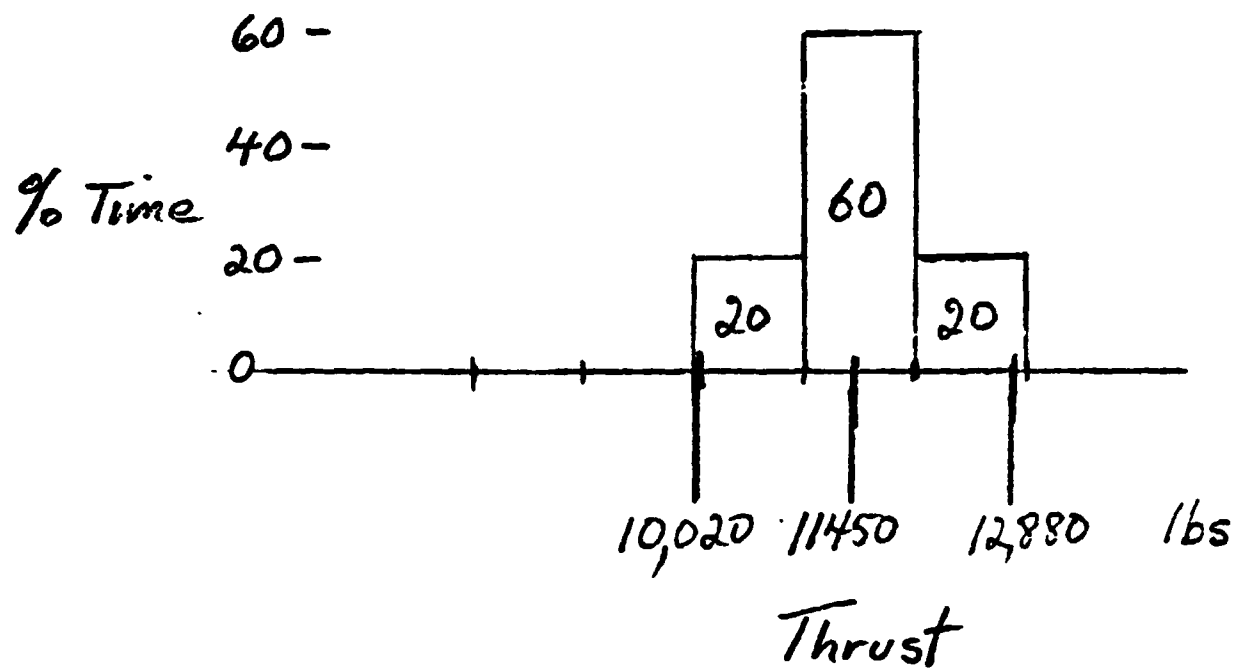


Figure 35

HIGH PRESSURE TURBINE ROTOR BLADE MATERIAL STRESS RUPTURE PROPERTIES

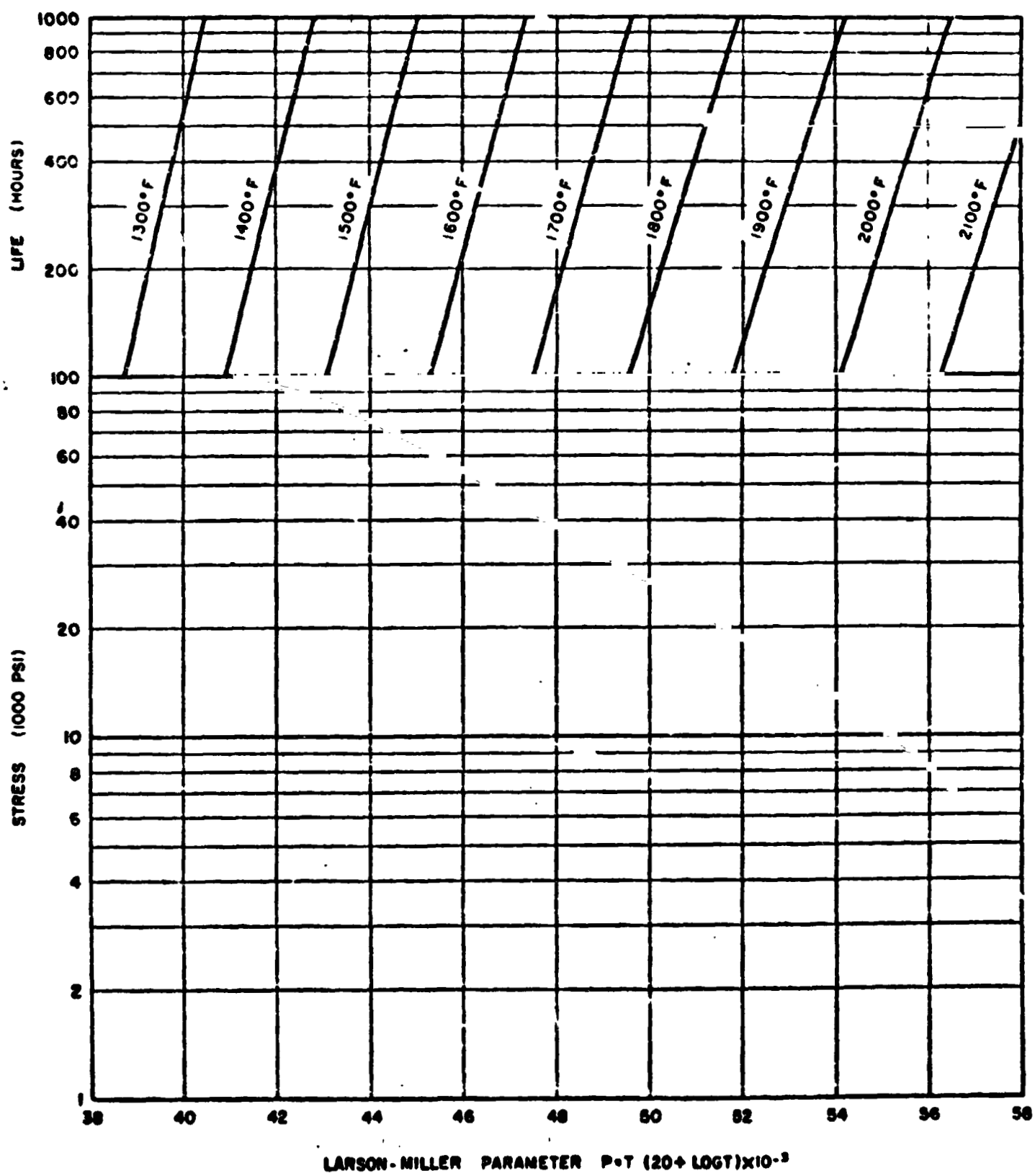


Figure 36

HIGH PRESSURE TURBINE ROTOR

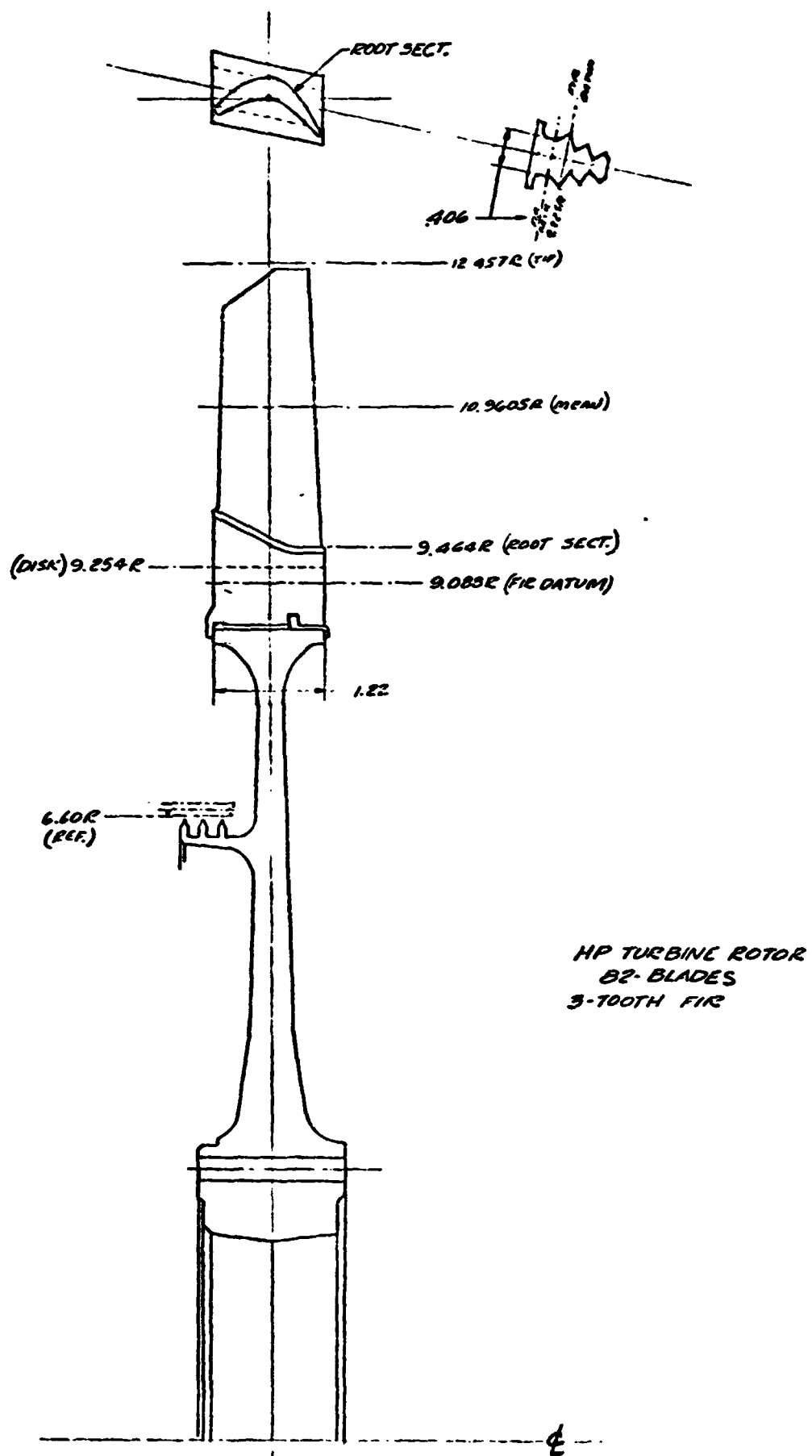


Figure 37

HIGH PRESSURE TURBINE ROTOR BLADE INTERFERENCE DIAGRAMS

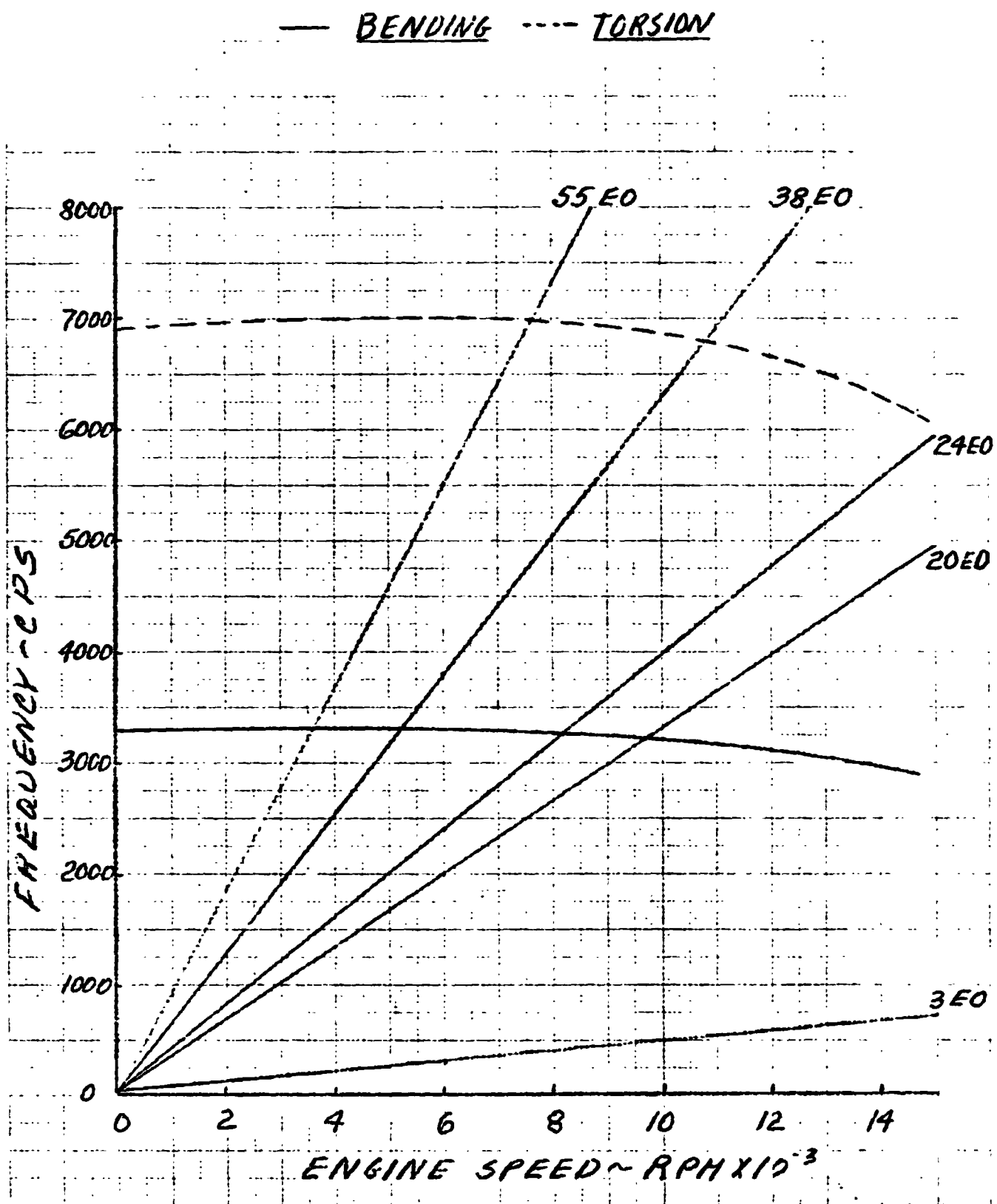


Figure 38

HIGH PRESSURE TURBINE ROTOR DISK STRESSES

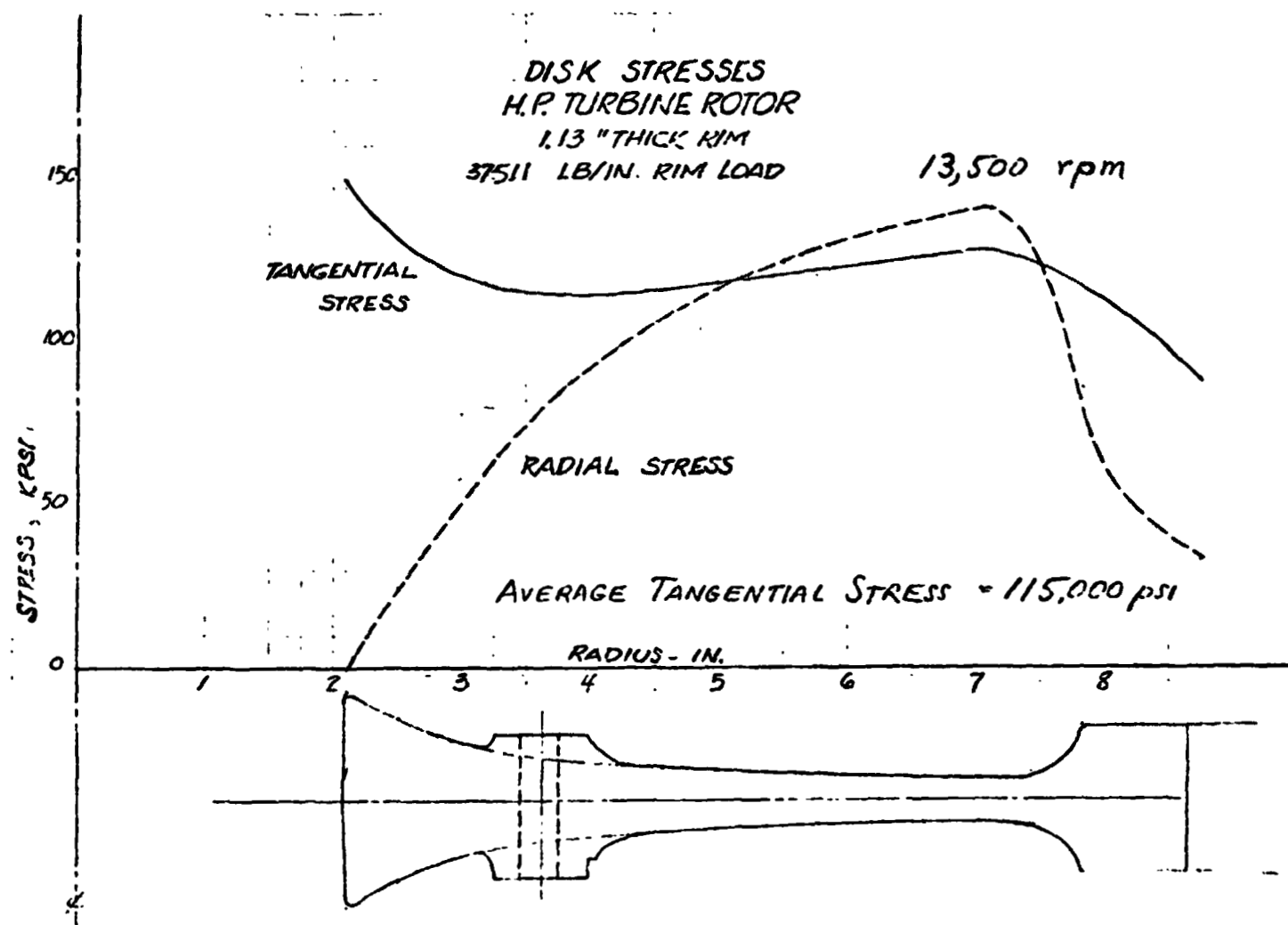
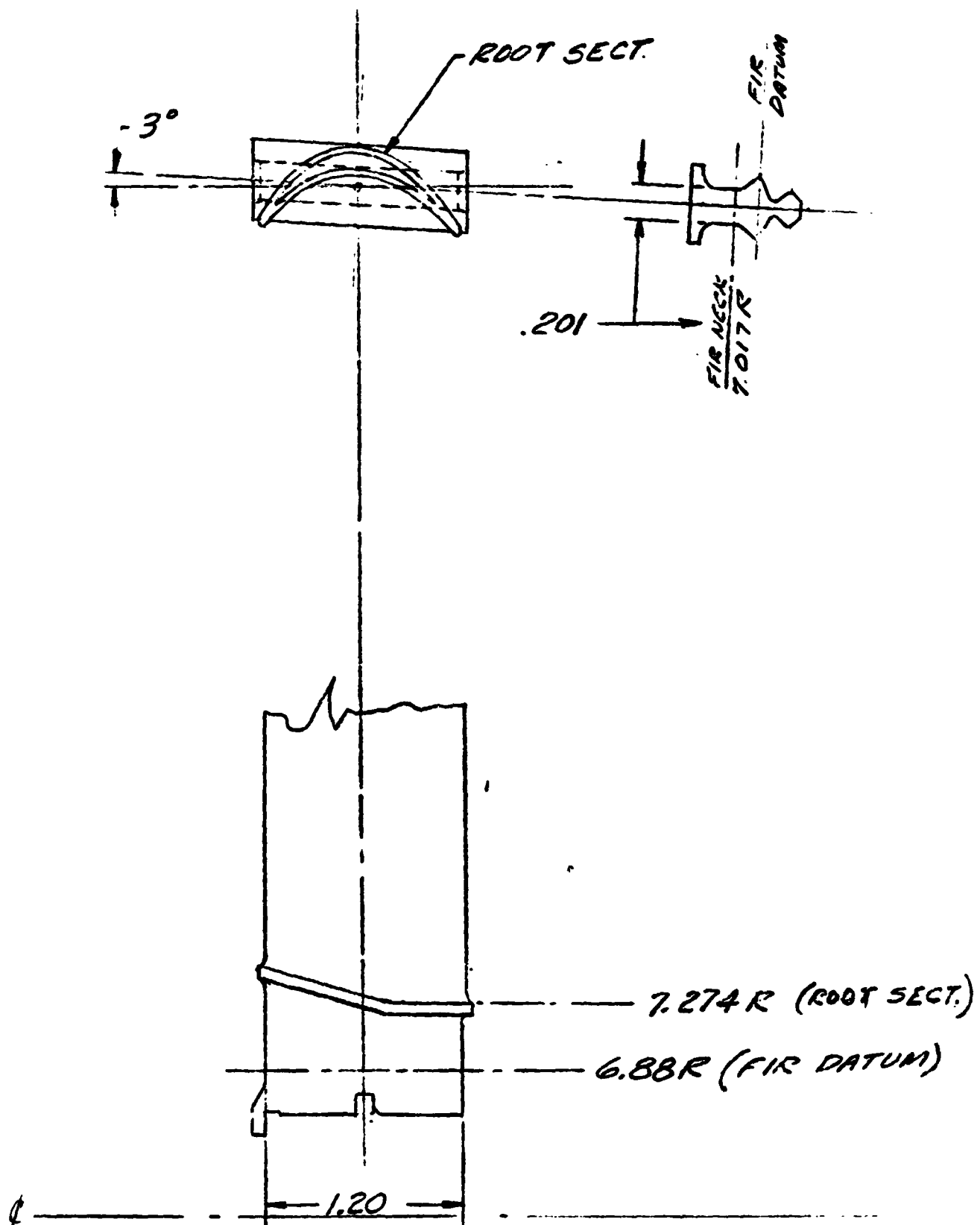


Figure 39

LOW PRESSURE TURBINE THIRD STAGE ROTOR BLADE



3RD L.P. TURBINE ROTOR
97 BLADES
2- TOOTH FIR

Figure 40

LOW PRESSURE TURBINE FIRST STAGE ROTOR BLADE INTERFERENCE DIAGRAM

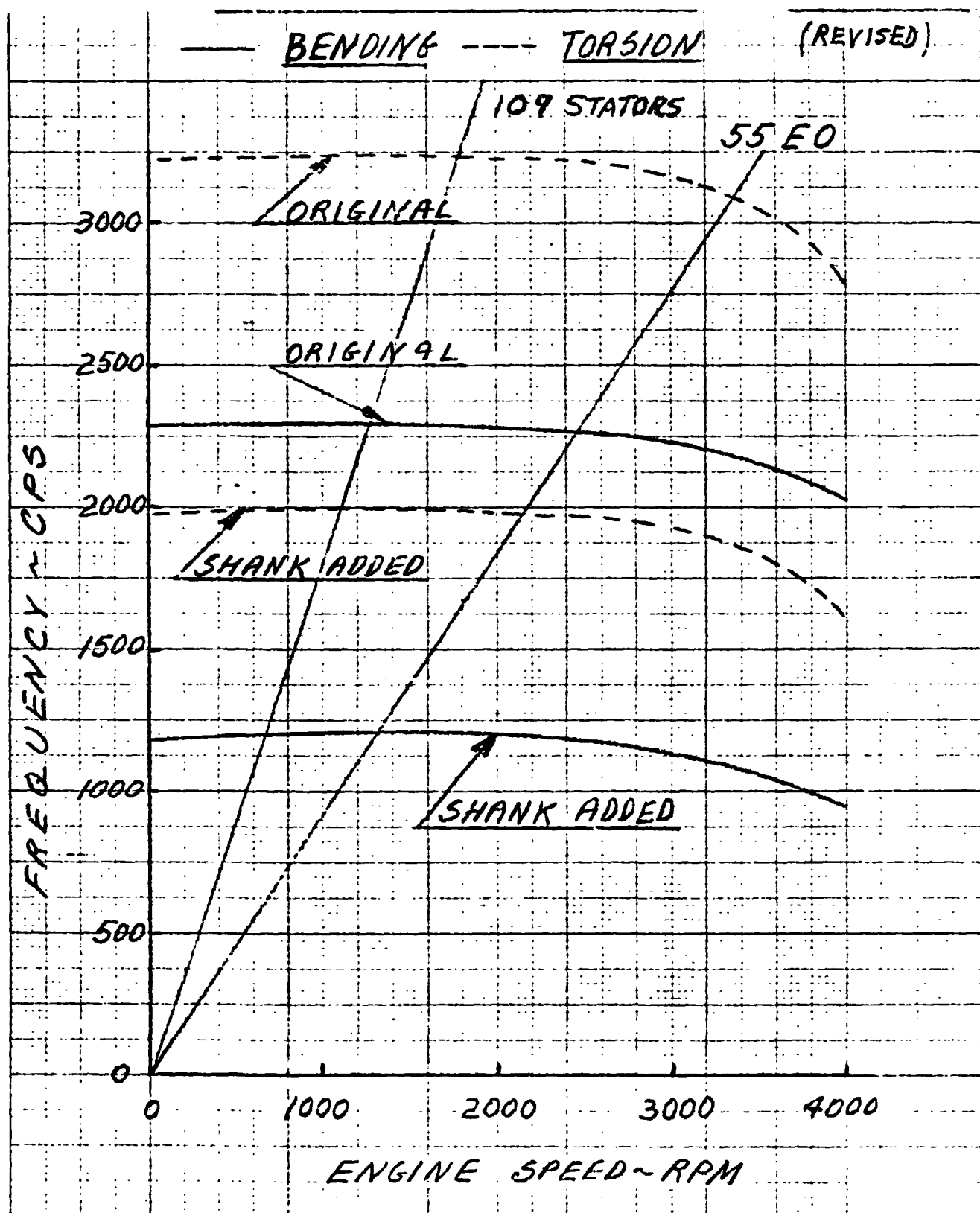


Figure 41

LOW PRESSURE TURBINE THIRD STAGE ROTOR BLADE INTERFERENCE DIAGRAM

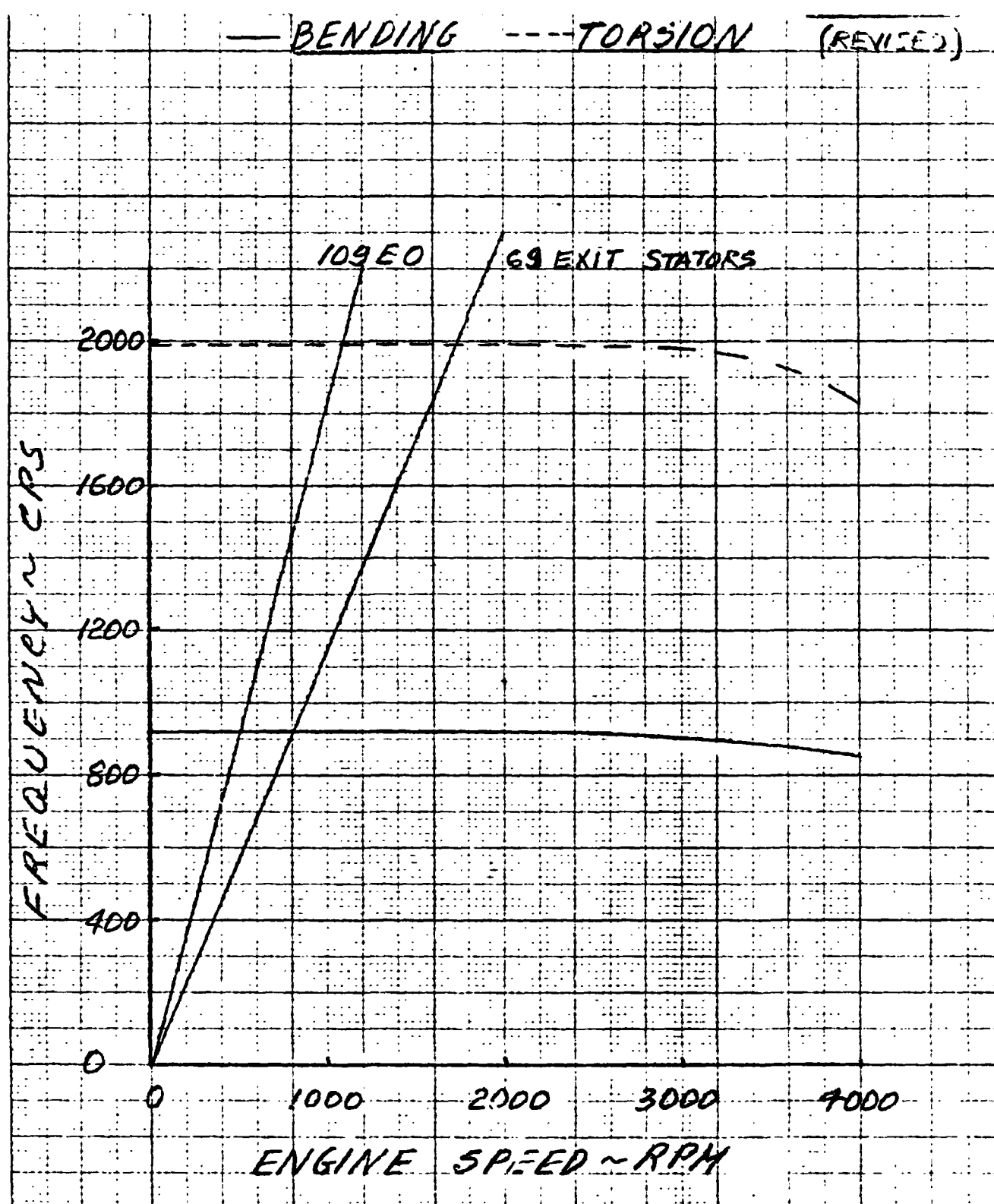


Figure 42

ROTOR THRUST LOADS

OPERATING THRUST LOADS (LBS)		10,000# ENGINE THRUST	12,500# ENGINE THRUST
LP SPOOL	FAN	4350 FORWARD	5505 FORWARD
	TURBINE	7175 AFT	9200 AFT
	NET THRUST LOAD	2825 AFT	3695 AFT
	COMPRESSOR	6240 FORWARD	7568 FORWARD
HP SPOOL	TURBINE	3830 AFT	4823 AFT
	NET THRUST LOAD	2410 FORWARD	2745 FORWARD

Figure 43

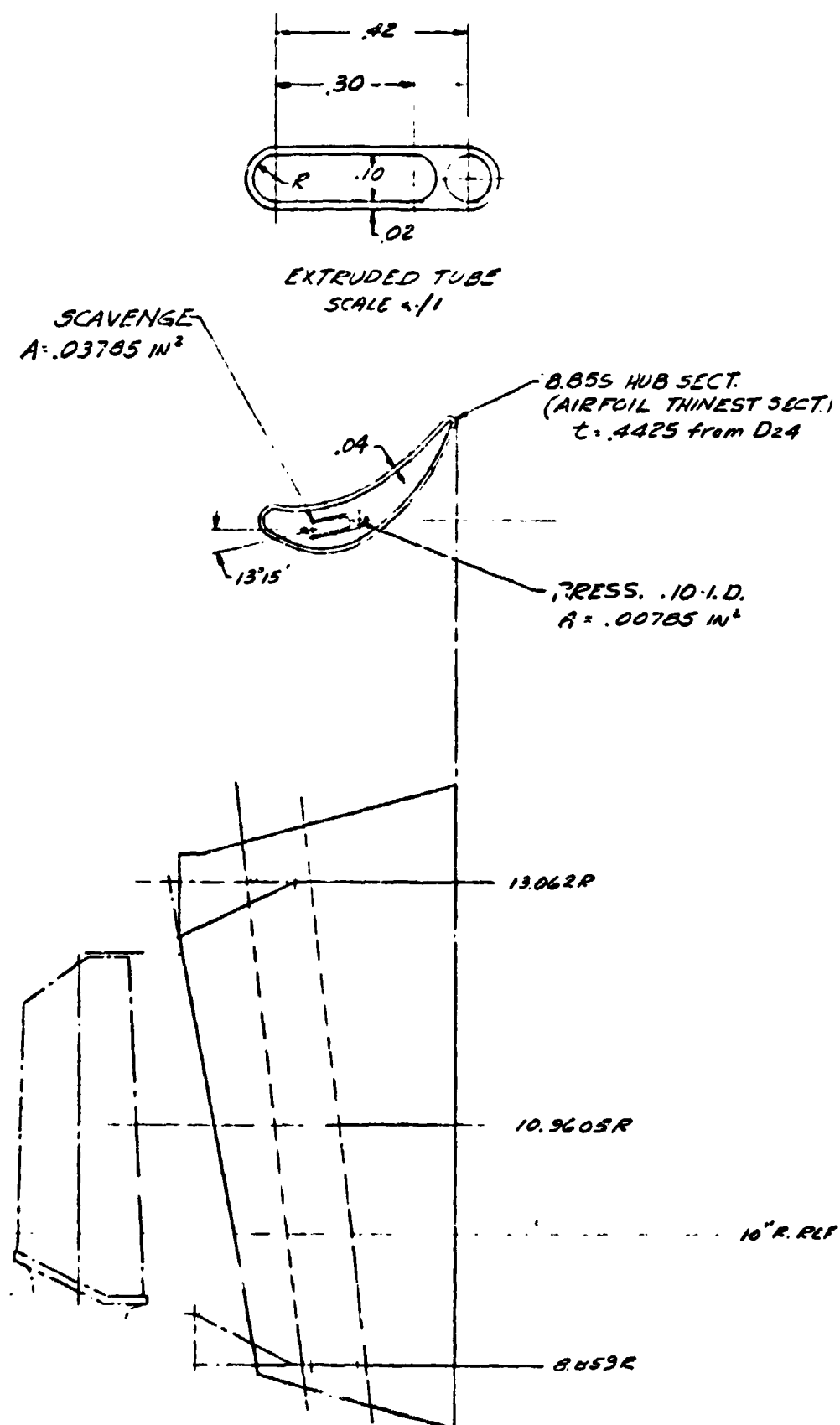
ROTOR SHAFT BEARING CHARACTERISTICS

BEARING TYPE	THRUST BEARING		ROLLER BEARING	
LOCATION	LP	HP	HP	LP
NUMBER	218	1018	1918	1918
CAPACITY - LB.	21240	13310	15500	15500
LOAD - LB.	3860	1000	1500	1000
EQUIV. RADIAL LOAD - LB.	2930	870	1500	1000
SPEED - RPM	4000	14860	14860	4000
DN - $\times 10^6$.36	1.34	1.34	.36
C/P	7.25	15.3	10.3	15.5
L-10-HR	4750*	$> 10^4$ *	8000	9250
LOSS - BTU/MIN.	17	25	28	4
LUBE FLOW - LB/MIN.	1.52	1.52	1.52	.76
TEMP. RISE - °F	22	33	37	10.5
JET SIZE - IN.	2 @ .031	2 @ .031	2 @ .031	1 @ .031
LUBE PRESS. - PSIG	20	20	20	20

* A life factor of 3 is used.

Figure 44

CIL TUBE IN LOW PRESSURE TURBINE STATOR



1ST LP STATOR
(THICK VANE FOR OIL TUBING)

Figure 45

...AR BEARING OIL TUBE CALCULATED TEMPERATURES

(12,500 LB ENGINE THRUST)

TOTAL OIL FLOW	7.3 — 8.3 LB/MIN
NUMBER OF TUBES	3
TOTAL HEAT GENERATION IN BEARING CAVITY	163 BTU/MIN
INITIAL OIL TEMPERATURE	180°F
OIL TEMPERATURE RISE IN INLET TUBE	28°F
OIL TEMPERATURE RISE IN BEARING CAVITY	44°F
OIL TEMPERATURE RISE IN SCAVENGE TUBE	22°F
FINAL OIL TEMPERATURE	274°F
OIL TUBE WALL TEMPERATURE	410°F

CRITICAL SPEEDS - TURBINE MODE FREQUENCY

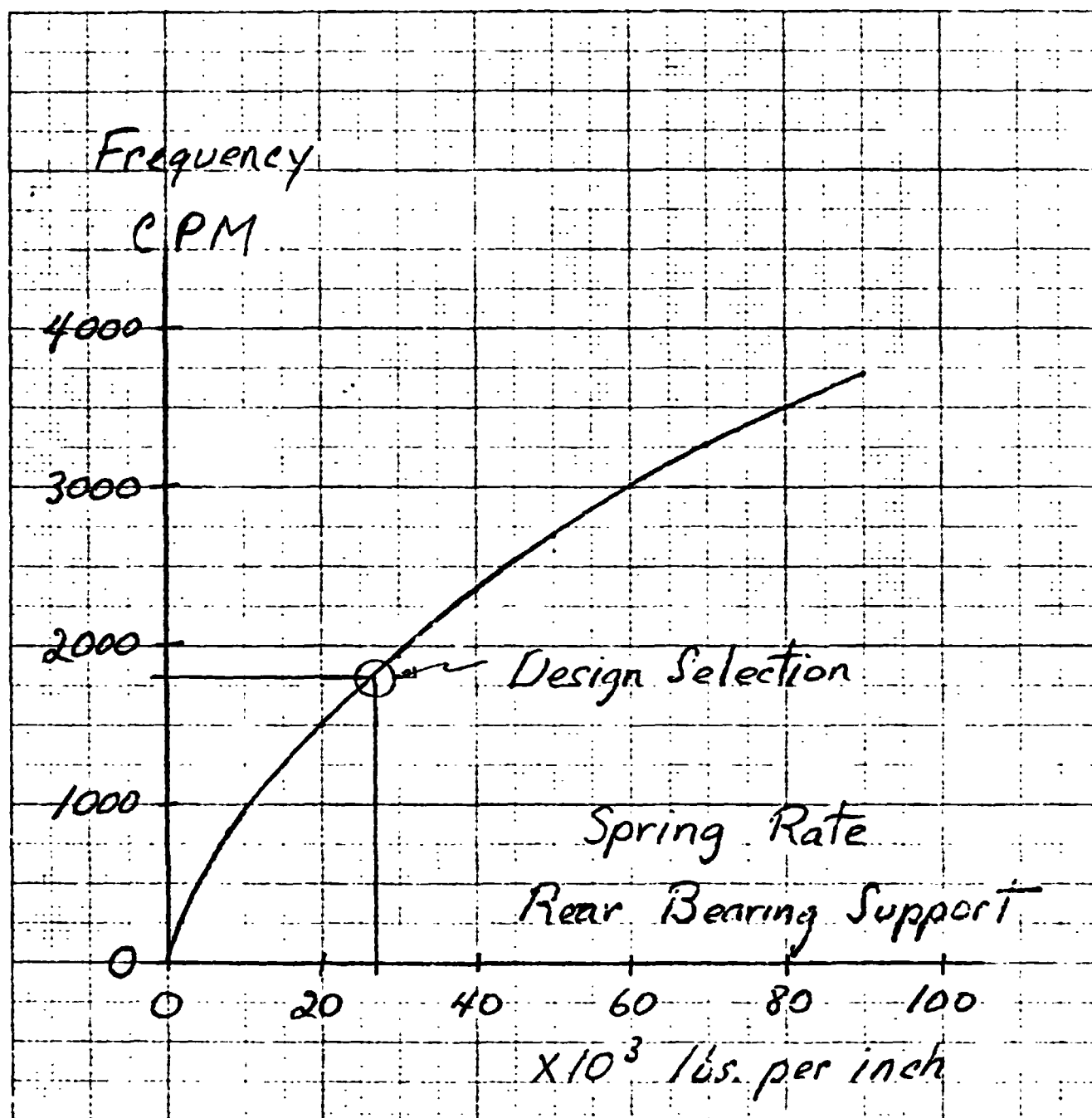


Figure 47

CRITICAL SPEEDS - FAN MODE FREQUENCY

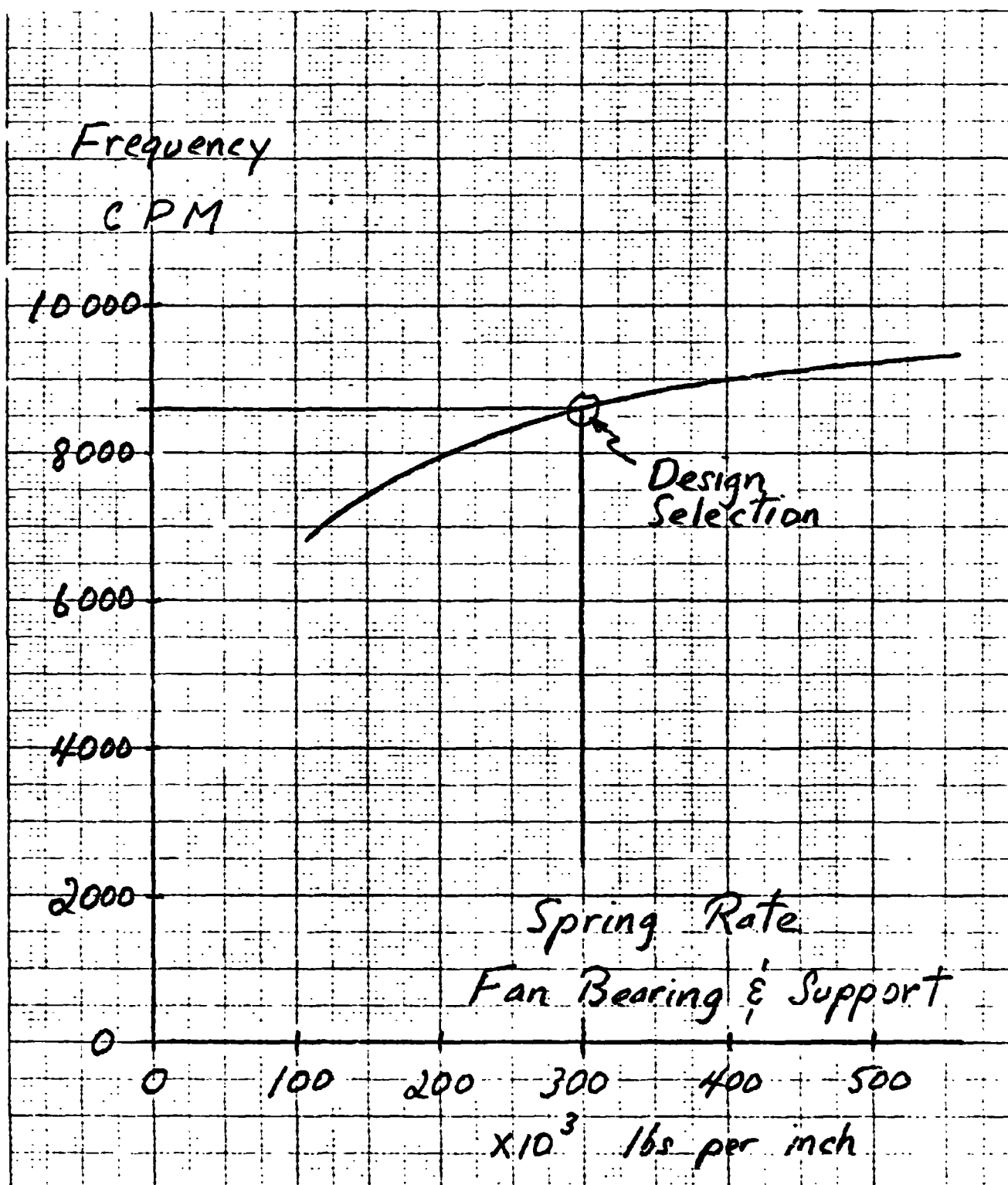


Figure 48

CRITICAL SPEEDS - COMPRESSOR MODE FREQUENCY

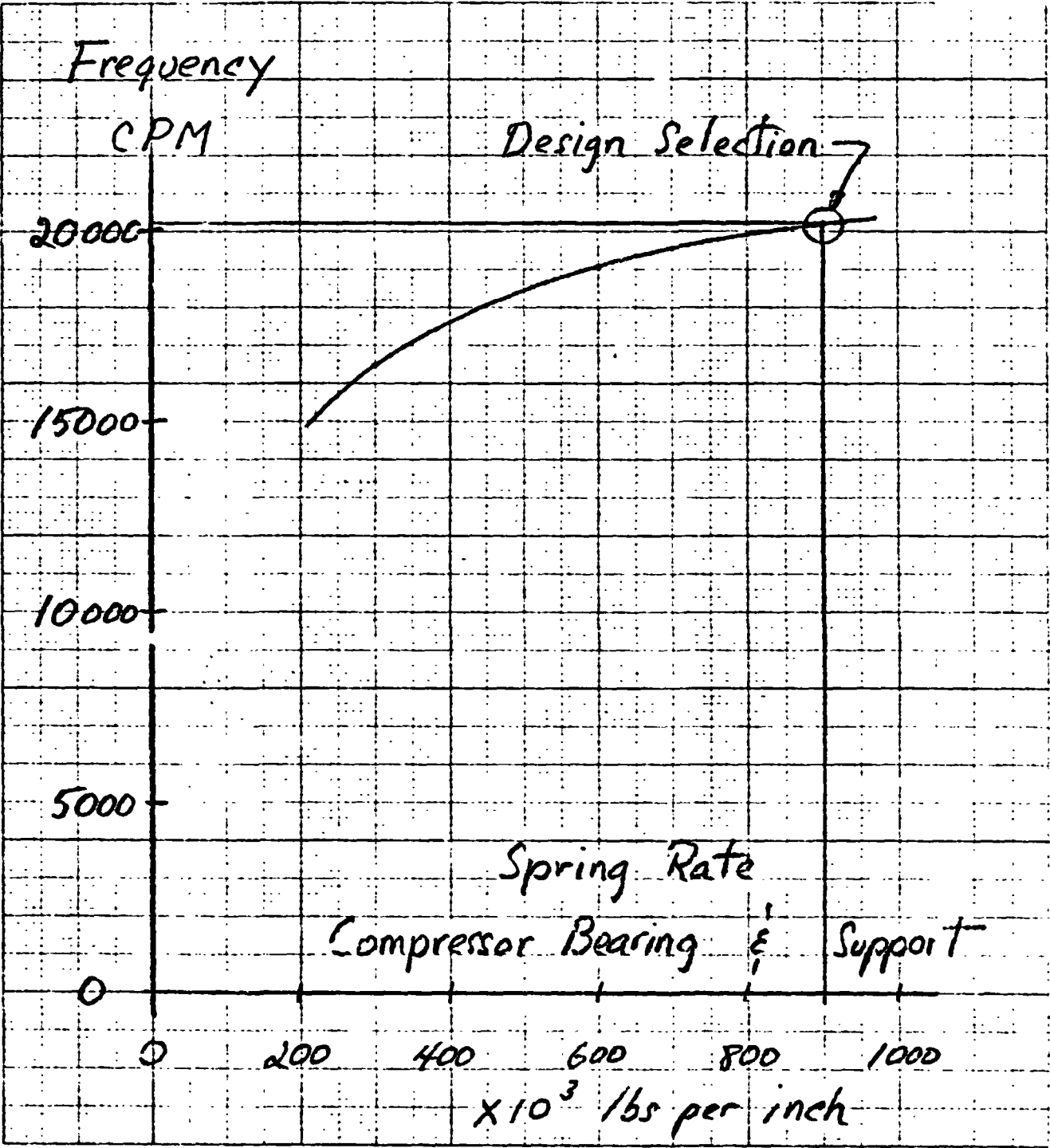


Figure 49

CRITICAL SPEED MAP

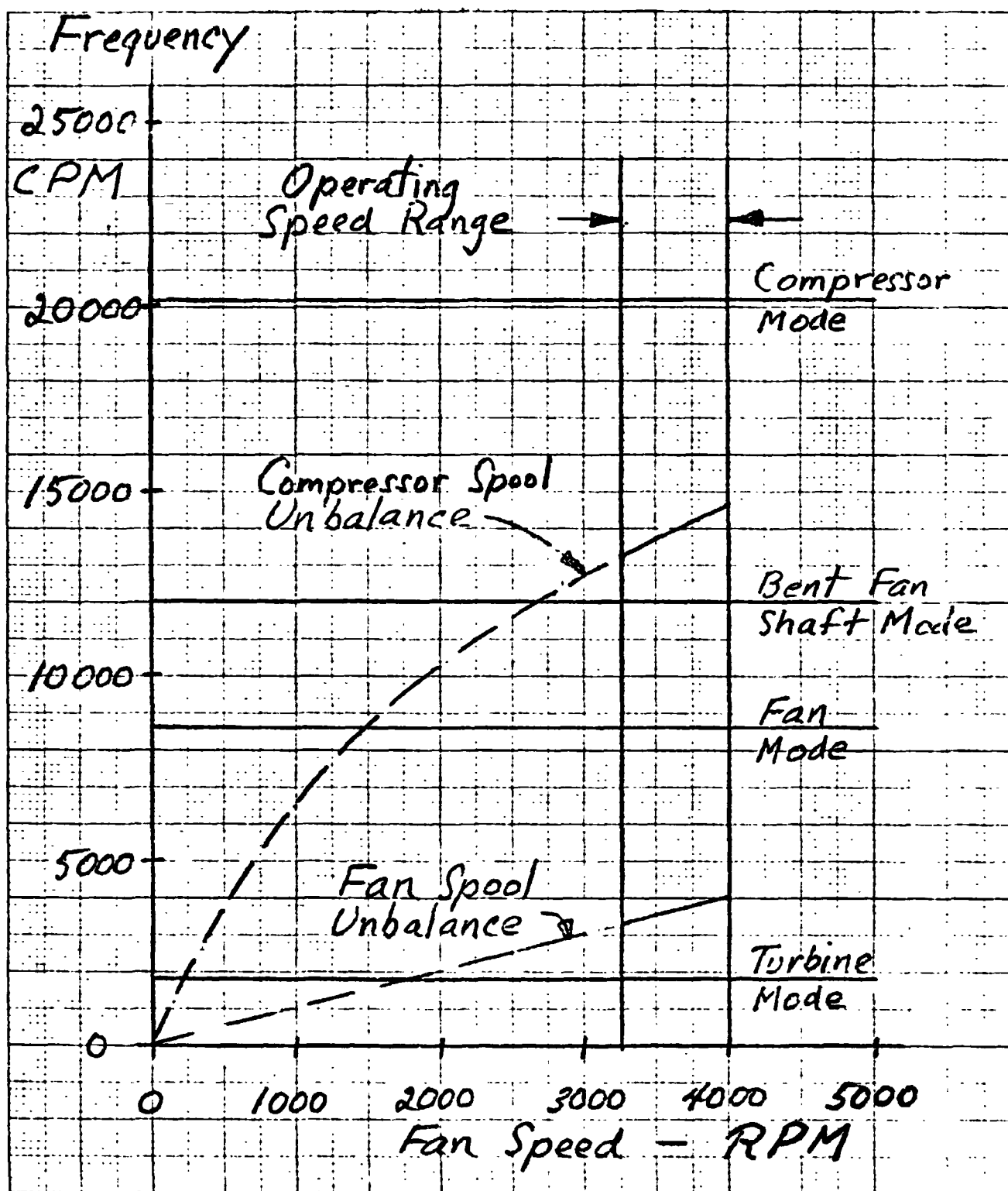


Figure 50

ENGINE RESISTANCE TORQUE

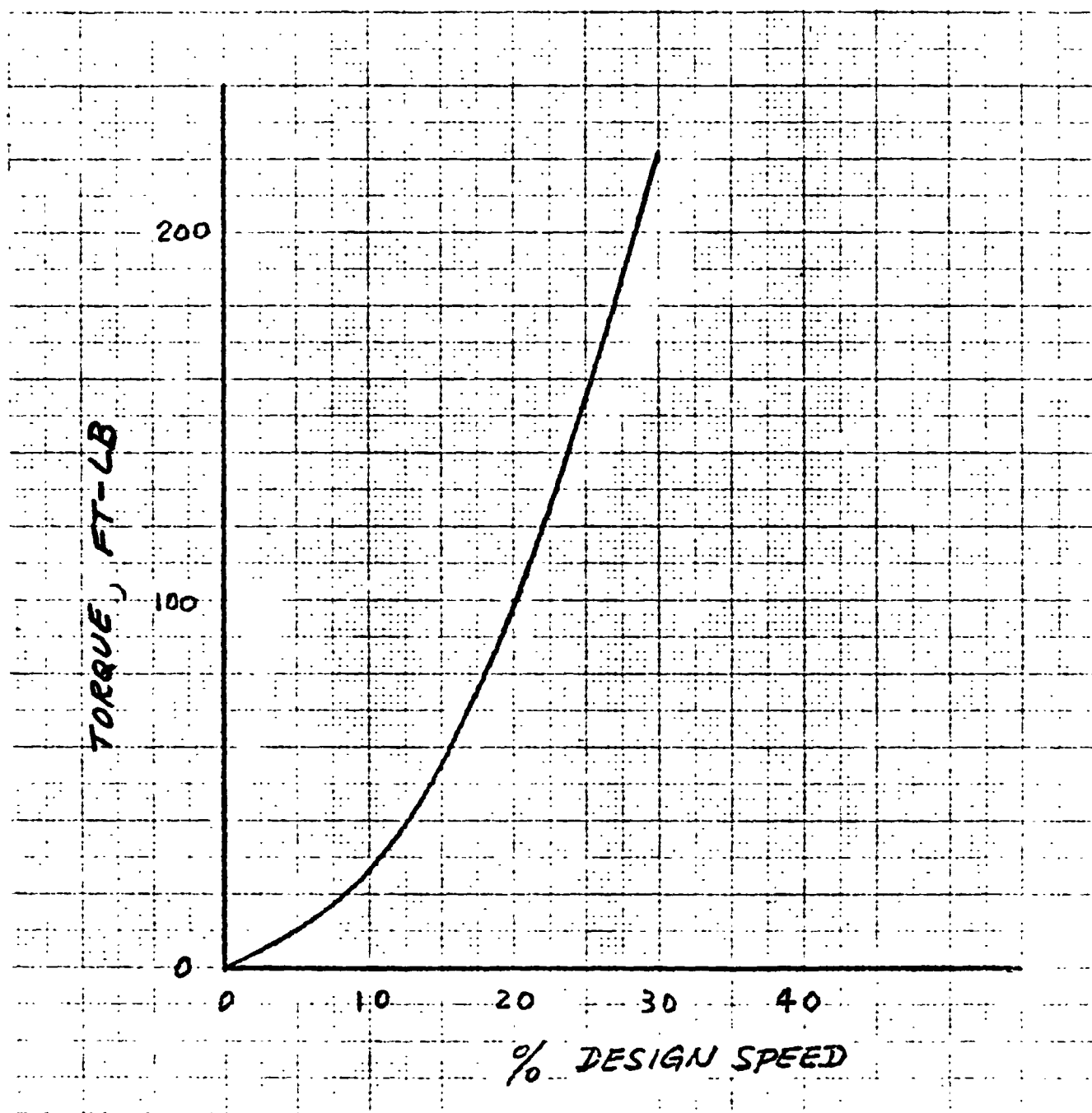


Figure 51

ENGINE STARTING ACCELERATION CHARACTERISTICS

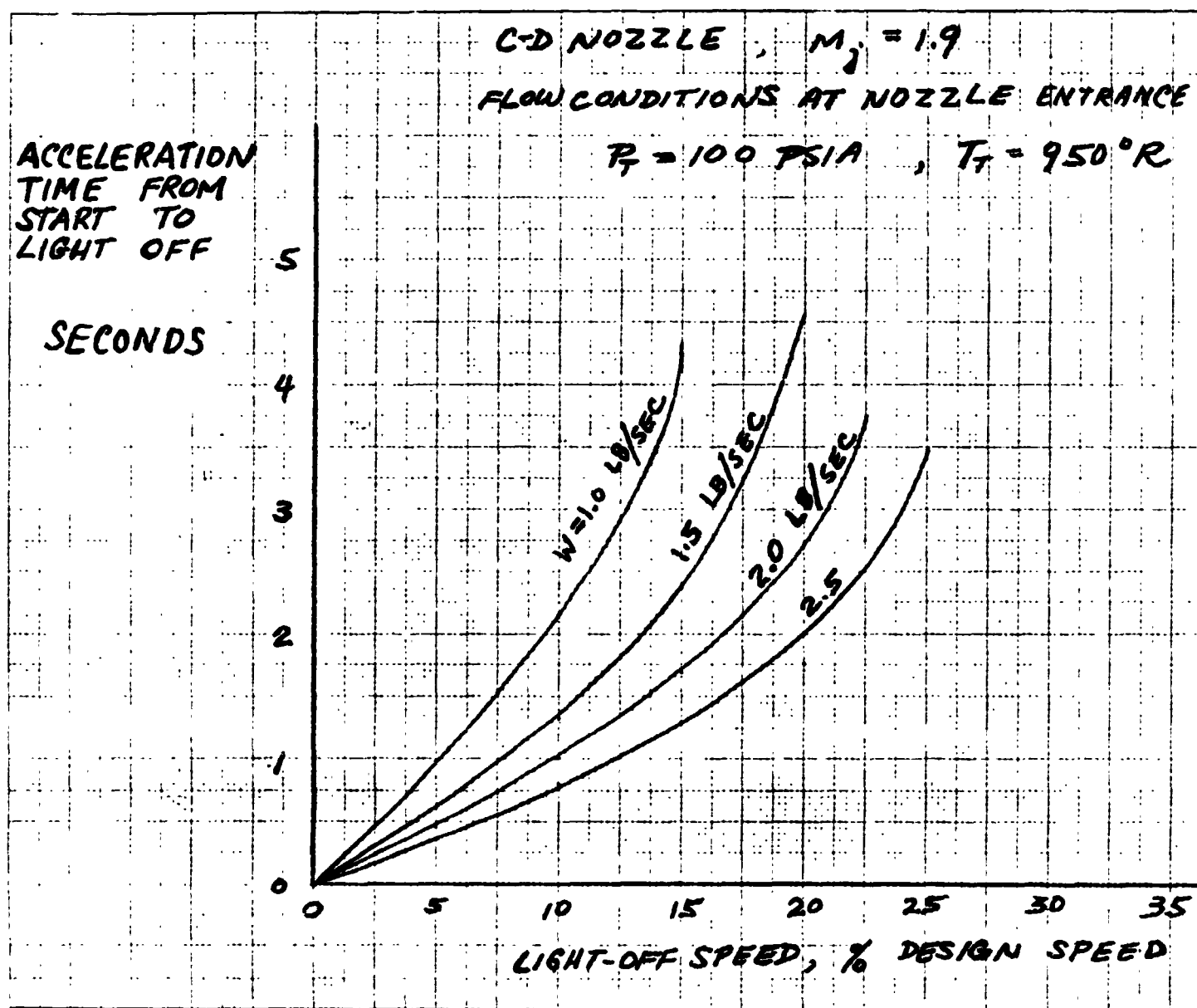


Figure 52

STARTER NOZZLE SIZING

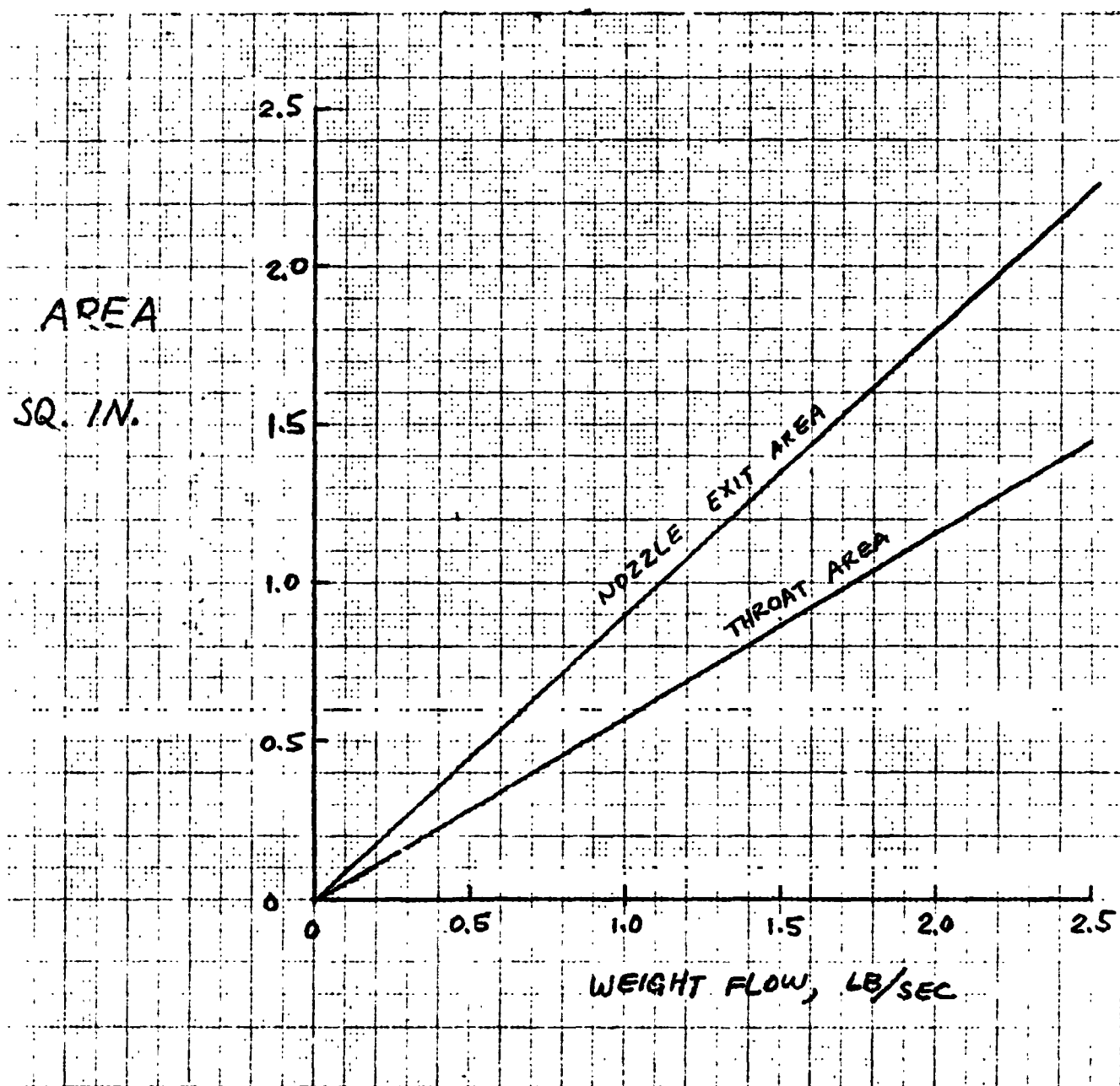


Figure 53

<u>ENGINE WEIGHT</u>		
<u>FAN SECTION</u>	<u>Configuration</u>	
	<u>1</u>	<u>2</u>
Rotor	63.1 lb.	66.7 lb.
Stator Housing	104.0	104.0
Exit Duct	48.0	48.0
	215.1	218.7
<u>COMPRESSOR SECTION</u>		
Rotor	71.0	72.6
Stator Housing	39.1	41.3
Actuation	27.5	27.5
	137.6	141.4
<u>COMBUSTOR SECTION</u>		
Combustor Liner	23.2	23.2
Casing	56.4	56.4
Impingement Starter	3.8	3.8
	83.4	83.4
<u>HP TURBINE SECTION</u>		
Rotor	49.5	65.4
Stator	29.7	29.7
Compressor Exit Diffuser	13.2	13.2
	92.4	108.3
<u>LP TURBINE SECTION</u>		
Rotor	119.4	130.2
First Stator and Bearing Support	53.6	53.6
Stator Housing	146.0	146.0
	319.0	329.8
<u>BEARING AND SHAFT SECTION</u>		
Fan Shaft	37.0	37.0
Bearings and Seals, Etc.	27.5	27.5
	64.5	64.5
<u>ACCESSORIES</u>		
Fuel and Lub. Systems	<u>65.6</u>	<u>65.6</u>
TOTAL	977.6	1011.7

Figure 54